



**Formulation Optimization and Characterization of Colistin Using  
Sodium Deoxycholate Sulfate for Intravenous Administration**

**Muhammad Ali Khumaini Mudhar Bintang**

**A Thesis Submitted in Partial Fulfillment of the Requirements for the  
Degree of Doctor of Philosophy in Pharmaceutical Sciences**

**Prince of Songkla University**

**2023**

**Copyright of Prince of Songkla University**



**Formulation Optimization and Characterization of Colistin Using  
Sodium Deoxycholate Sulfate for Intravenous Administration**

**Muhammad Ali Khumaini Mudhar Bintang**

**A Thesis Submitted in Partial Fulfillment of the Requirements for the  
Degree of Doctor of Philosophy in Pharmaceutical Sciences**

**Prince of Songkla University**

**2023**

**Copyright of Prince of Songkla University**

**Thesis Title** Formulation Optimization and Characterization of Colistin Using Sodium Deoxycholate Sulfate for Intravenous Administration

**Author** Mr. Muhammad Ali Khumaini Mudhar Bintang

**Major Program** Pharmaceutical Sciences

---

**Major Advisor**

.....  
(Prof. Dr. Teerapol Srichana)

**Examining Committee :**

.....Chairperson  
(Assoc. Prof. Dr. Somchai Sawatdee)

.....Committee  
(Prof. Dr. Teerapol Srichana)

.....Committee  
(Asst. Prof. Dr. Bhutorn Canaryuk)

.....Committee  
(Assoc. Prof. Dr. Varomyalin Tipmanee)

The Graduate School, Prince of Songkla University, has approved this thesis as partial fulfillment of the requirements for the Doctor of Philosophy Degree in Pharmaceutical Sciences

.....  
(Asst. Prof. Dr. Thakerng Wongsirichot)  
Acting Dean of Graduate School

This is to certify that the work here submitted is the result of the candidate's own investigations. Due acknowledgement has been made of any assistance received.

.....Signature  
(Prof. Dr. Teerapol Srichana)  
Major Advisor

.....Signature  
(Mr. Muhammad Ali Khumaini Mudhar Bintang)  
Candidate

I hereby certify that this work has not been accepted in substance for any degree, and is not being currently submitted in candidature for any degree.

.....Signature  
(Muhammad Ali Khumaini Mudhar Bintang)  
Candidate

<b>Thesis Title</b>	Formulation Optimization and Characterization of Colistin Using Sodium Deoxycholate Sulfate for Intravenous Administration
<b>Author</b>	Mr. Muhammad Ali Khumaini Mudhar Bintang
<b>Major Program</b>	Pharmaceutical Sciences
<b>Academic Year</b>	2023

### **Abstract**

Colistin is still used in multidrug-resistant gram-negative bacteria (MDR-GNB) therapy but the nephrotoxicity and neurotoxicity still become a major setback for its clinical use. Sodium deoxycholate sulfate (SDCS) carrier is used in micelle formulation with colistin to mitigate the known toxicity of colistin. The surface property of colistin and SDCS were evaluated before formulation with the lyophilisation technique. Several physicochemical parameters were evaluated like particle size, zeta potential, morphology, encapsulation efficiency (EE) and release profile. The chemical interactions were analysed using FTIR, NMR and molecular docking. The cytotoxicity of formulations was tested with different kidney cell lines. The in vivo toxicity was carried out in male mice C57BL/6 with colistin and colistin formulation for 7 consecutive days. The physiological changes were observed and measured after treatment. The serum biomarkers were measured including blood urea nitrogen (BUN), creatinine (Cr), superoxide dismutase (SOD), and catalase (CAT). Histopathological alterations in mice organs were analysed. The hydrodynamic diameters of the formulation were in the range of 140 to 170 nm with a spherical shape and negative zeta potential between  $-35.3$  and  $-22.8$  mV. The EE of formulations were between 70 and 76.4% with slower release measured compared to colistin. Molecular interactions were determined from FTIR and NMR spectra. Molecular docking simulation showed that multiple hydrogen bonds were present between the hydrophilic ring of colistin and SDCS. The colistin:SDCS formulations improved the thermal sensitivity of the mice compared to the control group. The BUN and Cr results showed no significant kidney dysfunction; however, the oxidative stress biomarkers decreased in the colistin with a lesser decrease in colistin-SDCS treated mice. Several histological

alterations were observed in the kidney, liver, spleen, and sciatic nerve tissues following colistin treatment, whereas less evidence of toxicity with colistin-SDCS. The overall results indicated that micelle formulations with SDCS showed safer for kidney and nerve cells while maintaining the antibacterial activity of colistin. This study revealed the potential for colistin development with SDCS for safer clinical use against MDR-GNB.

Keywords: Colistin, Sodium deoxycholate sulfate, Micelles, Nephrotoxicity, Neurotoxicity, Molecular docking, Histopathology.

## ACKNOWLEDGEMENT

All praise to Allah the Most Merciful, the Most Compassionate, for His guidance, blessings, and unwavering presence in my life. His infinite mercy and wisdom have been the source of my strength, and I am forever indebted for His boundless love and guidance. Additionally, I extend my utmost gratitude and reverence to the Prophet Muhammad (peace be upon him), the Messenger of Allah, whose teachings and example continue to inspire and guide humanity. His profound wisdom, compassion, and unwavering dedication to spreading the message of Islam have had an immeasurable impact on my life. I am truly blessed to have the opportunity to follow in the footsteps of the Prophet Muhammad (peace be upon him) and strive to embody the values he exemplified.

I am extremely grateful for the guidance and support provided by my advisor Prof. Dr. Teerapol Srichana, Faculty of Pharmaceutical Sciences, Prince of Songkla University, throughout the entire process of my study. I am truly fortunate to have had such a dedicated and knowledgeable advisor, whose guidance and encouragement have been invaluable to me. I extend my deepest appreciation for the patience, guidance, and mentorship, which have been crucial in helping me complete my PhD.

I would like to extend my heartfelt appreciation to Assoc. Prof. Dr. Somchai Sawatdee and Asst. Prof. Dr. Bhutorn Canyuk as the examining committee for their input and guidance in improving the thesis quality. I am thankful to Assoc. Prof. Dr. Varomyalin Tipmanee, Department of Biomedical Sciences, Faculty of Medicine, Prince of Songkla University, for the guidance and expertise in molecular docking studies and also for the overall quality of the thesis. I am truly thankful to Asst. Prof. Dr. Jongdee Nopparat, Division of Health and Applied Sciences, Faculty of Science, Prince of Songkla University, For the help with the animal studies.

I am sincerely grateful to the Graduate Scholarship and Conference Scholarship from the Faculty of Pharmaceutical Sciences, Prince of Songkla University, and the Thesis Grant from Graduated School, Prince of Songkla University



that has financially supported my academic journey. Additionally, I extend my appreciation to all faculty members, especially Ms. Panisara Boonsanong, and Ms. Sasipa Intharueangrugh who support and coordinate all the administration required for me as a student.

I deeply appreciate the support and contributions of all the staff of the Drug Delivery System Excellence Center and Pharmaceutical Laboratory Service Center, Faculty of Pharmaceutical Sciences, Prince of Songkla University and Medical Sciences Research and Innovation Institute, Research and Development Office, Prince of Songkla University for the facility and help provided. I am grateful to Ms. Titpawan Nakpheng, Ms. Kornkamon Petyord, Ms. Wilaiporn Buatong, Mr. Ekawat Thawitong, Ms. Kittiya Tinpun, and Dr. Pornvichai Tempoot for their support, lab expertise, and collaboration which have been crucial in shaping the success of my research.

I deeply appreciate my fellow PhD friends especially Ms. Sunisa Kaewpaiboon, Ms. Krittawan Tongkanarak, Ms. Nattanit Aekwattanaphol, Dr. Sukanjana Kamlungmak and Dr. Charisopon Chunhachaichana for their invaluable support and companionship throughout this challenging journey. Their encouragement, insights, and camaraderie have made this experience more fulfilling and enjoyable.

I am deeply thankful to all my friends and fellow Indonesian students from Indonesian Students Association in Thailand (PERMITHA) especially Ms. Nanda Safira, Mr. Hasriadi, and Mr. Mustakim Masnur for your unwavering support and cherished moments together.

Lastly, I would like to express my heartfelt appreciation to my parents, sibling, and family, their guidance, support, and belief in me have been the foundation of my success. Special thanks to Ms. Marsya Fadhia Akmal, your unwavering love, encouragement, and belief in me have been a constant source of inspiration and strength. I am truly grateful for each of their unique contributions, and I cherish the love and support they have shown me.

**Muhammad Ali Khumaini Mudhar Bintang**

**CONTENTS**

<b>Contents</b>	<b>Page</b>
Approval page	ii
Certificate of original work	iii
Certificate of thesis for submit PhD degree	iv
Abstract	v
Acknowledgement	vii
Contents	ix
List of tables	x
List of figures	xi
List of abbreviations and symbols	xiii
List of publications and proceedings	xvii
Reprints were made permission from the publishers	xviii
General introduction	1
Objectives	15
Significant results and discussion	16
Concluding remarks	36
References	37
Appendices	50
Reprint of papers and manuscript	51
Paper 1	52
Paper 2	59
Paper 3	73
Ethical committee approval	84
Vitae	87

**LIST OF TABLES**

<b>Table</b>		<b>Page</b>
Table 1	Particle size and zeta potential of colistin micelle formulations, colistin, and SDCS from dynamic light scattering measurements	18
Table 2	<sup>1</sup> HNMR chemical shifts of colistin, colistin:SDCS 1:1 (F1), and colistin:SDCS 1:2 (F2) multiplets	22
Table 3	Percent encapsulation efficiency of colistin in different ratios of colistin to SDCS formulations	25
Table 4	Effect of colistin-SDCS formulations on body weight gain and paw thermal threshold after seven days of treatment	31

## LIST OF FIGURES

<b>Figure</b>		<b>Page</b>
Figure 1	The bacterial cell envelope illustration of gram-positive and gram-negative bacteria	1
Figure 2	Chemical structure difference of (a) Colistin, (b) Colistin sulfate, and (c) Colistin methanesulfonate	6
Figure 3	Colistin mechanism on the outer membrane of gram-negative bacteria	7
Figure 4	The biochemical pathway involved in colistin renal uptake and colistin-induced apoptosis	11
Figure 5	Sodium deoxycholate sulfate (SDCS) structure	13
Figure 6	The surface tension versus concentration of the (A) colistin and (B) SDCS at 25 °C	16
Figure 7	(A) zeta potential and (B) size average of colistin association into SDCS micelle via titration at 25 °C	17
Figure 8	FTIR spectra of (A) colistin, (B) SDCS, and (C) colistin-SDCS micelle	19
Figure 9	<sup>1</sup> H NMR spectra of (A) colistin, (B) SDCS, (C) colistin-SDCS 1:1 ratio formulation, and (D) colistin-SDCS 1:2 ratio formulation. Also, <sup>13</sup> C NMR spectra of (E) colistin, (F) colistin-SDCS 1:1 ratio formulation, and (G) colistin-SDCS 1:2 ratio formulation	21
Figure 10	Molecular docking structure and plausible interaction of colistin and SDCS in (A) 3D structure that shows colistin as the green stick and SDCS as a cyan and red stick. Also, the illustration of interaction in (B) 2D structure where hydrogen bonding is shown as a red dashed line	24
Figure 11	The colistin release profile from colistin standard and colistin-SDCS formulations at 37°C in (A) water and (B) dextrose 5%	26

### LIST OF FIGURES (CONTINUED)

<b>Figure</b>		<b>Page</b>
Figure 12	Cell viability of (A) human kidney cell line WT9-12, (B) human kidney epithelial cell line 293T/17, and (C) human primary renal proximal tubule epithelial cells PCS-400-010 after 24-h incubation with colistin (■), colistin to SDCS formulation ratios of 1:1 (■) and 1:2 (■) at various concentrations determined by MTT assay	28
Figure 13	Effect of colistin and colistin-SDCS formulations on mice serum biomarkers: <b>A</b> Blood urea nitrogen (BUN), <b>B</b> Creatinine (Cr), <b>C</b> Superoxide dismutase (SOD), and <b>D</b> Catalase (CAT)	32
Figure 14	Histopathological alterations of: - <b>Kidney</b> tissue from (A) Control, (B) Colistin, (C) F1, (D) F2 groups. Deformation of the glomeruli is shown in the yellow circle while congestion of renal blood vessels is shown in the red circle. - <b>Liver</b> tissue from (E) Control, (F) Colistin, (G) F1, (H) F2 groups. Yellow arrows indicate infiltration of monocytes in the tissue. - <b>Spleen</b> tissue from (A) Control, (B) Colistin, (C) F1, (D) F2 groups. The yellow arrow indicates multinucleated giant cells in the tissue. – <b>Sciatic nerve</b> tissue from (A) Control, (B) Colistin, (C) F1, (D) F2 groups. The yellow arrow shows thin and loose fibres	35

**LIST OF ABBREVIATIONS AND SYMBOLS**

°C	degree Celsius
$\alpha$	alpha
$\beta$	beta
$\gamma$	gamma
$\mu\text{g}$	micrograms
$\mu\text{L}$	microliters
$\mu\text{m}$	micrometres
$^{13}\text{C}$	carbon
$^1\text{H}$	proton
293T/17	human kidney epithelial cell line
AMB	amphotericin B
AMP	antimicrobial peptide
AMR	antimicrobial resistant
BUN	blood urea nitrogen
BW	body weight
C	carbon
C57BL6	inbred strain of laboratory mouse
$\text{Ca}^{2+}$	calcium ion
CAT	catalase
$\text{cm}^{-1}$	per centimetre
CMC	critical micelle concentration
CMS	colistin methanesulfonate
COVID-19	coronavirus disease 2019
Cr	creatinine
CRAB	carbapenem-resistant <i>Acinetobacter baumannii</i>
CRE	carbapenem-resistant <i>Enterobacterales</i>
CRPA	carbapenem-resistant <i>Pseudomonas aeruginosa</i> (
Dab	di-aminobutyric acid
dL	decilitres

**LIST OF ABBREVIATIONS AND SYMBOLS (CONTINUED)**

EE	encapsulation efficiency
ESBLs	extended-spectrum $\beta$ -lactamases
F1	mole ratios of SDCS to colistin as 1:1
F2	mole ratios of SDCS to colistin as 2:1
F3	mole ratios of SDCS to colistin as 3:1
F4	mole ratios of SDCS to colistin as 4:1
F5	mole ratios of SDCS to colistin as 5:1
FTIR	Fourier-transform infrared
g	grams
G	g-force
GNB	gram-negative bacteria(l)
h	hour
H	hydrogen
H&E	haematoxylin and eosin
HIP	hydrophobic ion pairing
HPLC	high performance liquid chromatography
ICU	intensive care unit
IL-8	interleukin-8
kcal	kilocalories
Kdo	2-keto-3-deoxyoctonoic acid
Kg	kilograms
Leu	leucine
LPS	lipopolysaccharide
M	Molar
MBC	minimum bactericidal concentration
MDA	malondialdehyde
MDR-GNB	multi-drug resistant gram-negative bacteria
mg	milligrams
Mg <sup>2+</sup>	magnesium ion

**LIST OF ABBREVIATIONS AND SYMBOLS (CONTINUED)**

MIC	minimum inhibitory concentration
min	minutes
mL	millilitres
mm	millimetres
MTT	3-(4,5-dimethylthiazol-2-yl)-2,5-diphenyl-2H-tetrazolium bromide
mV	millivolts
n	number
N	nitrogen
NLC	nanostructured lipid carriers
nm	nanometres
nmol	nanomoles
NMR	nuclear magnetic resonance
O	oxygen
OCTN	organic cation transporter 1
OM	outer membrane
P	p-value
PCS-400-010	human primary renal proximal tubule epithelial cells
PEPT	peptide transporter
Phe	phenylalanine
PMB	polymyxin B
ppm	part per millions
ROS	reactive oxidative stress
s	seconds
SDCS	sodium deoxycholate sulfate
SLN	solid lipid nanoparticles
SOD	superoxide dismutase
tBID	truncated p15 BID
TNF- $\alpha$	tumor necrosis factor alpha



**LIST OF ABBREVIATIONS AND SYMBOLS (CONTINUED)**

U	units
USP	United States Pharmacopeia
UTI	urinary tract infection
WT9-12	human kidney cell line

## LIST OF PUBLICATIONS AND PROCEEDINGS

This thesis is based on the following papers and proceeding, including the experimental design and details of methods. The publications were attached in the appendices part. Reprinted was published with the kindness of permission from the respective journals.

- Paper 1            Bintang MAKM, Srichana T (2022) Antibacterial Activity and In Vitro Cytotoxicity of Colistin in Sodium Deoxycholate Sulfate Formulation. *Adv Sci Technol* 121:25–30. <https://doi.org/10.4028/p-19rsw3>
- Paper 2            Bintang MAKM, Tipmanee V, Srichana T (2023) Colistin sulfate-sodium deoxycholate sulfate micelle formulations; molecular interactions, cell nephrotoxicity and bioactivity. *J Drug Deliv Sci Technol* 79:104091. <https://doi.org/10.1016/j.jddst.2022.104091>
- Paper 3            Bintang MAKM, Nopparat J, Srichana T (2023) In vivo evaluation of nephrotoxicity and neurotoxicity of colistin formulated with sodium deoxycholate sulfate in a mice model. *Naunyn Schmiedebergs Arch Pharmacol*. <https://doi.org/10.1007/s00210-023-02531-4>
- Proceeding 1      Bintang MAKM, Srichana T. Effect of the different molar ratio of colistin on the surface properties of sodium deoxycholate sulfate. The 11th Joint Seminar on Biomedical Sciences: Variety and Controversy to Creativity. 13-15 November 2019. Krabi, Thailand.
- Proceeding 2      Bintang MAKM, Srichana T. Particle size, surface charges and molecular interaction of colistin with sodium deoxycholate sulfate. The 6th CDD International Conference 2020: Natural Medicines. 10-12 November 2020. Hat-Yai, Thailand
- Proceeding 3      Bintang MAKM, Srichana T. Antibacterial Activity and In Vitro Cytotoxicity of Colistin in Sodium Deoxycholate Sulfate Formulation. 5th International Conference and Exhibition on Pharmaceutical Sciences and Technology 2022: Innovations in Pharmaceutical Sciences for Sustainable Development Goals. 23-24 June 2022. Online conference, Thailand.

## PAPER 1

### PERMISSION FROM PUBLISHER

#### Antibacterial Activity and *In Vitro* Cytotoxicity of Colistin in Sodium Deoxycholate Sulfate Formulation

Mudhar Bintang, Muhammad Ali Khumaini; Srichana, Teerapol *5th International Conference and Exhibition on Pharmaceutical Sciences and Technology 2022*, 17 Oct 2022, Vol. 121, pages 25 - 30

DOI: 10.4028/vnc84eg

Language: English

DOI: 10.4028/p-19rsw3

URL: <https://www.scientific.net/AST.121.25>


Publisher: TRANS TECH PUBLICATIONS LTD; Trans Tech Publications Ltd


[Details >](#)

[Request Reprints/ePrints](#) | [Request Permission >>](#)

## PAPER 2

## PERMISSION FROM PUBLISHER

Home Help Live Chat Sign in Create Account



**Colistin sulfate-sodium deoxycholate sulfate micelle formulations; molecular interactions, cell nephrotoxicity and bioactivity**  
Author: Muhammad Ali Khumaini Mudhar Bintang, Varomyalin Tipmanee, Teerapol Srichana  
Publication: Journal of Drug Delivery Science and Technology  
Publisher: Elsevier  
Date: January 2023  
© 2022 Elsevier B.V. All rights reserved.

**Journal Author Rights**

Please note that, as the author of this Elsevier article, you retain the right to include it in a thesis or dissertation, provided it is not published commercially. Permission is not required, but please ensure that you reference the journal as the original source. For more information on this and on your other retained rights, please visit: <https://www.elsevier.com/about/our-business/policies/copyright#Author-rights>

BACK CLOSE WINDOW

### PAPER 3

#### PERMISSION FROM PUBLISHER

**SPRINGER NATURE**

**In vivo evaluation of nephrotoxicity and neurotoxicity of colistin formulated with sodium deoxycholate sulfate in a mice model**

Author: Muhammad Ali Khumaini Mudhar Bintang et al

Publication: Naunyn-Schmiedeberg's Archives of Pharmacology

Publisher: Springer Nature

Date: May 30, 2023

*Copyright © 2023, The Author(s), under exclusive licence to Springer-Verlag GmbH Germany, part of Springer Nature*

## CHAPTER 1

### GENERAL INTRODUCTION

#### 1. Gram-negative bacteria

One of the most critical public health problems faced currently is the infection caused by gram-negative bacteria (GNB). In hospital settings, the clinical importance of GNB infections is significant especially the high risk of morbidity and mortality for the patient in the intensive care unit (ICU) [1]. The main difference between gram-negative and gram-positive bacteria lies in their wall structure composition where the presence of an outer membrane in gram-negative strains gives extra protection against foreign substances. The outer membrane of GNB is responsible for its selective resistance due to the permeability barrier function of the outer membrane [2].

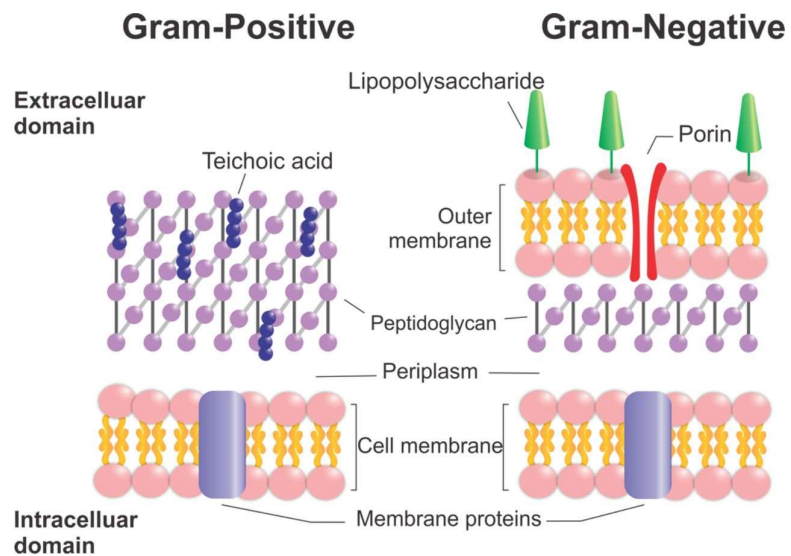


**Figure 1.** The bacterial cell envelope illustration of gram-positive and gram-negative bacteria [3].

The GNB enclose themselves in a three-layer structure which are outer membrane (OM), peptidoglycan, and cytoplasmic membrane (inner membrane) (Figure 1). The OM is a distinguished feature of GNB composed of a lipid bilayer which is not phospholipid like its inner membrane, instead consists of glycolipid and lipopolysaccharide (LPS). LPS has been known as the primary cause of septic shock in GNB infections [4]. LPS function as a barrier for OM which consists of a glucosamine disaccharide with six or seven acyl chains, a polysaccharide centre, and the O-antigen, an elongated polysaccharide chain [5]. Peptidoglycan are polysaccharides which are N-acetylglucosamine and N-acetylmuramic acid linked by pentapeptide side chains where they function as exoskeletons that determine the cell's shape. The inner membrane has many functions such as transport system, structure, and biosynthetic. They consist of phospholipids and inner membrane proteins [4, 6].

The infection caused by GNB could afflict most organs of infected organisms from topical and gastrointestinal to bloodstream and nervous systems. The GNB infections affected millions of people worldwide, especially with the lack of sanitation which is responsible for acquired infections both in the community and hospital environment. Treating nosocomial infections in the respiratory tract also become a huge problem for health professionals with the high resistance of GNB pathogens and the difficulty of drug penetration into the lung parenchyma [7]. Poor sanitation is also responsible for gastroenteritis caused by Enterobacteriaceae (*Salmonella* spp., *E. coli*, *Shigella* spp.) and is responsible for meningitis which can be fatal if not treated in time [8]. Urinary tract infections (UTI) are also prevalent, especially in young women and exacerbated by resistant bacteria. The bloodstream infections like bacteraemia are also important complications which can be acquired from certain wound infections or during iv-catheters [9].

## 2. The multidrug-resistant GNB crisis

With a major shift in healthcare resource allocation due to coronavirus disease 2019 (COVID-19), the antibiotic resistance case continued to increase which is termed "new pandemic" [10, 11]. Multidrug-resistant GNB (MDR-GNB) has been the topic of multiple international health and political summits. Several guidelines have been released by public health executives to increase awareness and contain the danger of antibiotic resistance. There has been no significant improvement in the epidemiology of antibacterial-resistant cases despite the extensive resource allocated [5]. The research toward new antimicrobials for GNB treatments in the past decades has slowed down which further exacerbates the current bacterial resistance. The long discovery process of new antibacterial drugs has kept the pipeline low despite much support from public health organizations and pharmaceutical companies [12].

Asian countries were considered to be hot spots for antimicrobial resistance (AMR) bacteria [13]. The high prevalence of AMR cases for GNB that include extended-spectrum  $\beta$ -lactamases (ESBLs) and carbapenemases exacerbate the public health challenges due to inadequate response of the strain to antimicrobials [14]. Carbapenem resistance GNB has been reported to escalate in South and Southeast Asia. In Thailand itself, it is reported that the number of carbapenem resistance *Acinetobacter spp.* significantly increased from 44.5% in 2015 to 74.3% in 2021 [15]. In the hospital setting, gram-negative strains are the most common cause of nosocomial infection with various resistance mechanisms and increased chance of spreading, with most cases of urinary tract infections and up to 30% of the bloodstream and surgical site infections caused by GNB infections [16].

The treatment option for MDR-GNB cases still provides many challenges for critically-ill patients where the AMR slows down the critical timing to unfavourable adverse events for fast response needed in emergency settings [17]. While the past



decade shows interest in newer antimicrobial drugs for GNB, most of the new compounds are not available for public treatment. Most of the treatment of MDR-GNB, especially for carbapenem-resistant *Enterobacteriales* (CRE), carbapenem-resistant *Pseudomonas aeruginosa* (CRPA); carbapenem-resistant *Acinetobacter baumannii* (CRAB) still rely on its susceptibility toward aminoglycosides, glycolcycline, or polymyxins [18]. The importance of MDR-GNB management in critical settings requires expertise and reasoning for current antimicrobial administration, especially with the currently available drugs can produce adverse effects for the patients due to their known toxicity [14, 19]

### 3. Colistin

Colistin (polymyxin E) have long been used as the last line therapy for resistant gram-negative bacilli infection and was derived from the *Bacillus polymyxa* variant colistinus [20]. Currently, only colistin and polymyxin B are available clinically [21]. First synthesized in 1949 by Japanese researcher Koyama and showed significant activity against GNB, notably *Pseudomonas aeruginosa*, it was begun to be used clinically in 1961 [22, 23]. With the rise of resistant *Pseudomonas aeruginosa* strains, colistin with colistin methanesulfonate (CMS) as its prodrug has been chosen for its good susceptibility [22, 24]. Around the 1970s with the new class of antibiotic discovered and the safety concern of colistin, the clinical use of colistin was mainly replaced by aminoglycosides [25]

Colistin is a cationic decapeptide antibiotic which belongs to the antimicrobial peptide (AMP) classification which consists of cyclic decapeptides with different lengths of fatty acid that present as analogue variation of colistin. Colistin A and B are the majority of analogues found in colistin with some minor analogues present that vary from batch to batch [26]. Colistin and polymyxin B (PMB) are derived from different variants of *Bacillus polymyxa* with structural differences at position 6 in the sequence

with D-Leu for colistin and D-Phe for PMB [22]. Colistin is a hydrophilic drug ( $\log P = -2.4$ ) [27] but with an amphipathic property due to the presence of both lipophilic and hydrophilic groups. Colistin contains five unmasked  $\alpha$ -amino groups from its diaminobutyric acid (Dab), this resulted in the basic properties of colistin with  $pK_a$  around 10. At physiological pH (7.4), colistin is poly-cationic and has a positive surface charge [26]. CMS contain five additional sulfomethyl groups in its Dab residues which increase its molecular weight and polyanionic properties at physiological pH (7.4). [28, 29].

Polymyxin B is administered intravenously in its active form as sulfate salt, while intravenous usage of colistin is in CMS form which is considered to be safer than the active form of colistin (sulfate salt). As a prodrug, CMS undergoes hydrolysis to active colistin *in vivo*, and the degree of conversion can alter the dosage of administered colistin where the antibacterial activity can differ significantly [30, 31]. The concern also comes from the instability of CMS at low concentrations with the conversion of CMS to colistin reported to be faster when the concentration of CMS was below the CMC (60% over 48 h) than when it was above the CMC (1% over 48 h) also the temperature-dependent of hydrolysed CMS where active colistin can present in CMS dosage forms [32, 33].

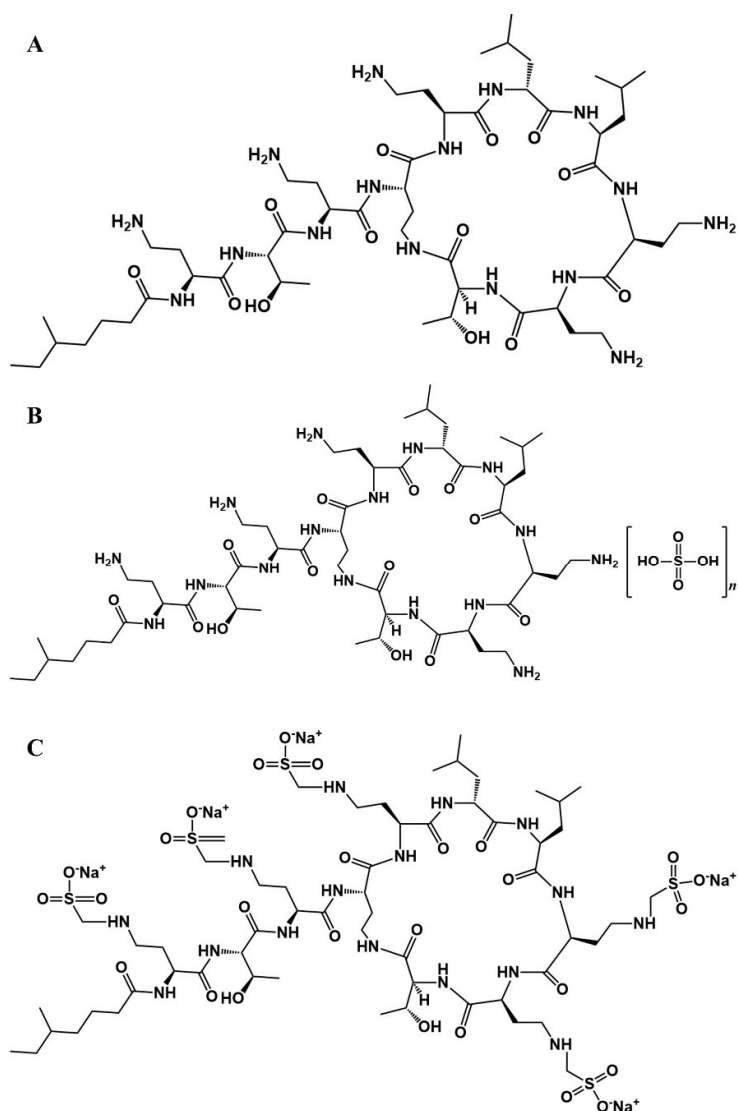


**Figure 2.** Chemical structure difference of (a) Colistin, (b) Colistin sulfate, and (c) Colistin methanesulfonate

#### 4. Mode of action and pharmacokinetic

The evidence suggested polymyxin's antimicrobial actions work by disrupting the membrane permeability of GNB by binding with LPS [30, 34]. The three regions form the LPS with different structures and functions. The first region is a different length of O-antigen consisting of oligosaccharide, the second region linked to lipid A is an inner core oligosaccharide, 2-keto-3-deoxyoctonic acid (Kdo), and the third region is lipid A is glycerophospholipid structure with long fatty acid chains. LPS is

responsible for the membrane integrity of GNB which signifies the permeability barrier against antibacterial compounds and because of the length of its O-chains, it provides protection against complement-mediated lysis [35]. There is still an unclear process for polymyxin's mode of action in disrupting bacterial membranes. LPS is a primary target for colistin which showed in its affinity [36, 37]. The lipid A region of LPS bound with colistin via electrostatic interaction with the di-aminobutyric acid. Colistin competitively displaces the  $Mg^{2+}$  and  $Ca^{2+}$  cations from the outer membrane of GNB which destabilize the membrane, the charged peptide and fatty acid tail are responsible for the membrane disruption via a detergent-like effect. The weakened outer membrane allows further colistin uptake to the cytoplasmic membrane for membrane permeabilization required for bacterial lysis. Therefore, colistin binds to the lipid A component of LPS, causing OM dysfunction [20, 38].

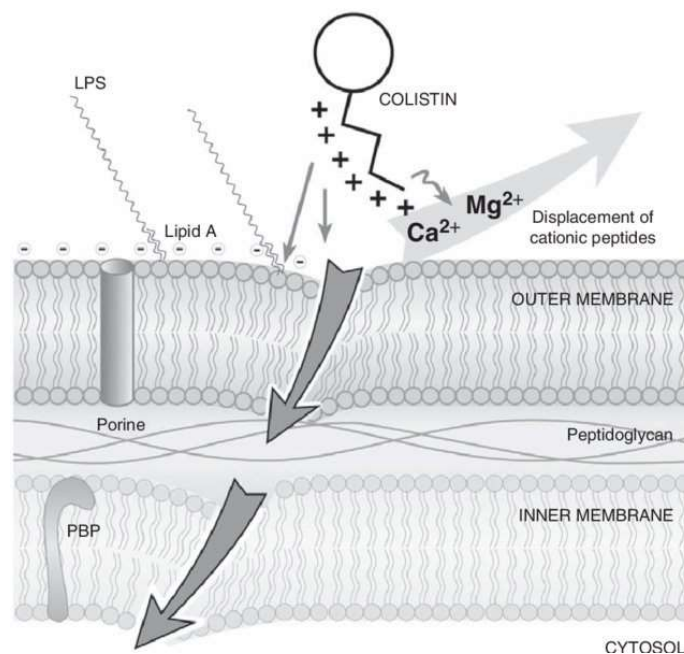


**Figure 3.** Colistin mechanism of action on the cell wall structure of gram-negative bacteria [38]

The neutralization of LPS by colistin resulted in an anti-endotoxic effect on GNB infections. The lipid A region of LPS is an endotoxin that can release the cytokines like tumour necrosis factor-alpha (TNF- $\alpha$ ) and Interleukin 8 (IL-8) [23, 39]. This inflammatory response induces septic shock which should be inhibited by polymyxin which has been shown in *in vivo* models. The mechanism has not yet been studied in clinical studies and the unclear nature of the endotoxin suppression in the plasma where the endotoxin rapid binding to the LPS-binding protein which then bound to cell surface CD14 [40, 41].

The emergence of colistin as the salvage therapy for MDR-GNB infection has increased the number of studies for colistin clinical pharmacodynamics and pharmacokinetics [42]. Most works analysed the CMS for the fact that CMS was mainly used intravenously for the therapy also the conversion of CMS to colistin made the exact dose adjustment complicated [31]. Colistin *in vivo* model demonstrated that the intravenous administration of colistin sulfate (1 mg/kg) resulted in the renal tubular reabsorption of colistin through a process mediated by carriers. This administration exhibited lower renal clearance (5.2 versus 0.01 mL/min.kg) compared to its total clearance, indicating that colistin is primarily eliminated through nonrenal pathway(s). CMS administration *in vivo* showed the renal clearance of CMS was calculated higher at 7.2 mL/min.kg for a total clearance of 11.7 mL/min.kg [42]. The CMS converted to colistin systemically at a low percentage (7%), with the most colistin recovery obtained likely from renal, the bladder or even the sampling container [28, 43]. Therefore, the sufficient amount of CMS dose needed to achieve the plasma concentration suitable for the antibacterial activity paired with the slow rate of conversion can result in resistance during the loading phase when the colistin plasma concentration was still low [34, 42].

## 5. Toxicity of colistin

The emergence of the MDR-GNB epidemic saw the increased usage of polymyxins group and colistin (methanesulfonate) [30]. However, the toxicity of polymyxin drugs still poses a problem, especially for critically ill patients. The most notable adverse event in polymyxin therapy are nephrotoxicity and neurotoxicity where the toxicity is dose-dependent and in-case of nephrotoxicity it can lead to mortality for critically ill patients [44]. The instance of nephrotoxicity is different between trials, with the occurrence between 30 to 60% for patients treated with intravenous polymyxins. The nephrotoxicity occurrence for colistin in high-dose therapy demands strict dose regulation for colistin therapy [45, 46]. Kalin et al. compared the therapy for patients administered with low, normal, and high doses of colistin; the nephrotoxicity occurrence was measured from the creatinine clearance. The results showed that the high doses patients (2.5 mg/kg every 6 h) had a 40% rate, the normal doses (2.5 mg/kg every 12 h) with 35%, and low doses patients (adjusted from creatinine clearance) were 20% [47].

The extensive tubular reabsorption of colistin as mentioned in the previous section is responsible for its nephrotoxicity. Several imaging studies show increased accumulation of colistin in renal tubules preferentially in the renal cortex of studied animals, with a significant amount in the renal proximal tubular cells of the mice treated with colistin where the molecular mechanism of its tubular reabsorption is transporter-mediated [48–50]. It has been shown that the significant accumulation of polymyxins in the proximal involves megalin, the endocytic receptor that is highly expressed in renal tubules [51, 52]. It was reported that colistin competitively inhibited the binding of cytochrome *C* as a megalin substrate. Furthermore, administering colistin on megalin-shed rats resulted in a substantial decrease in kidney accumulation and

increased urinary excretion which showed the dependency of megalin for colistin accumulation in the tubular reabsorption process [51].

Colistin caused acute tubular necrosis in the proximal tubule epithelial cells, which resulted in decreased creatinine clearance and elevated serum urea and creatinine levels, as well as proteinuria, cylindruria, and oliguria. [53]. The mechanism of polymyxin-induced nephrotoxicity has shown multiple biochemical processes involved in renal tubular cells and the kinetics of this biochemical interplay have yet to be deciphered [44]. The amphipathic properties of colistin were responsible for its nephrotoxicity with the structural moiety of Dab and fatty acid colistin to the proximal tubule membrane. The colistin uptake into the proximal tubule alters the membrane permeability that caused cell leakage from ion and water influx which is similar to its antibacterial properties [54]. The biochemical pathway involved in colistin-induced apoptosis is shown in **Figure 4** [55]. The uptake of colistin is mediated by three pathways; through its affinity on megalin-mediated endocytosis, peptide transporter (PEPT), and organic cation transporter 1 (OCTN) which the uptake can be observed from the change in malondialdehyde (MDA), superoxide dismutase (SOD), and catalase (CAT) enzyme. The change in enzyme can increase reactive oxidative stress (ROS) that can cause mitochondrial dysfunction which also can be triggered by the death receptor pathway from truncated p15 BID (tBid) activation that all lead to ROS-mediated damage in renal tubular cells or through caspase activation [51, 55, 56].

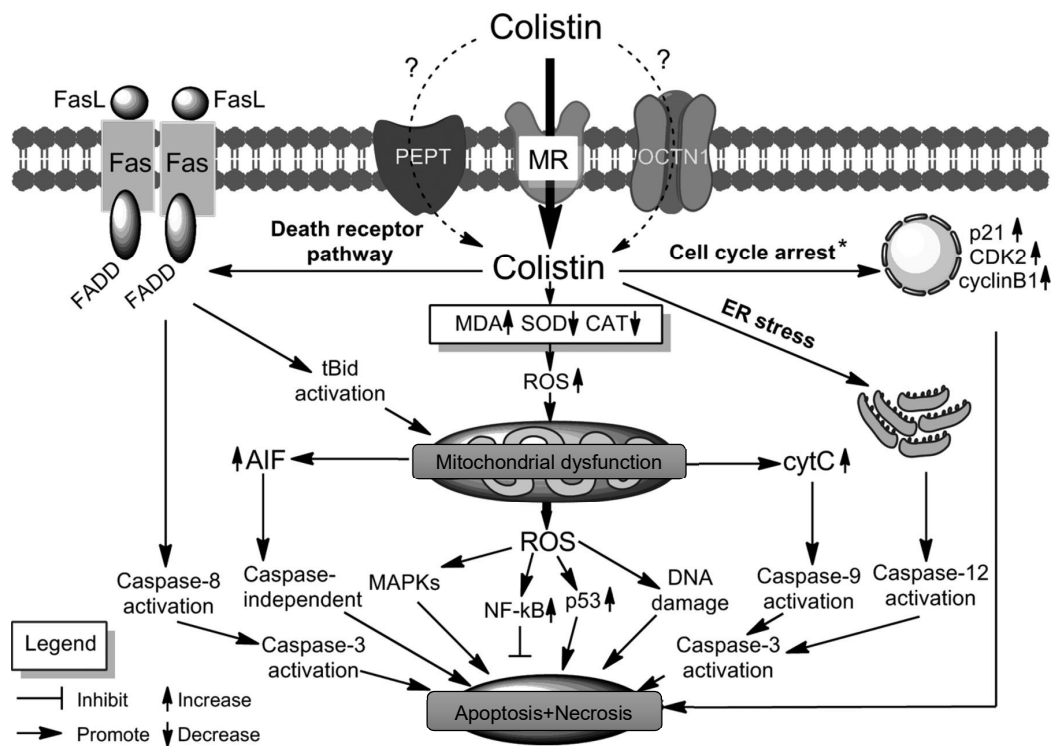


**Figure 4.** The biochemical pathway involved in colistin renal uptake and colistin-induced apoptosis [55].

The second notable adverse event is neurotoxicity which the incidence rate is substantially lower than that of nephrotoxicity [57]. The neurotoxicity of colistin can be manifested with several clinical indications including paraesthesia, myopathy, vertigo, muscle paralysis, nausea, and apnea. The event can be considered mild and reversible with the therapy discontinuation [58]. Colistin neurotoxicity as with its nephrotoxicity is caused by the direct exposure of the drug to neuron cells leading to mitochondrial dysfunction from oxidative stress. Autophagy is responsible for polymyxin-induced neurotoxicity which is shown in *in vitro* and *in vivo* results [59, 60].



## 6. State of the art in colistin delivery system

The development of new antimicrobial agents is a very long and complicated process, where the need for agents to combat multi-drug resistant bacteria is continue rising. Colistin development as an old antibacterial drug still shows high potency for MDR-GNB yet colistin has disadvantages in clinical therapy. Some studies have incorporated colistin in several different delivery systems with lipid carriers. The suitable nano-carrier can improve the properties of the drug and control the residence time when in systemic circulation. The increased bioavailability and high penetrating effect into the biofilm of bacteria can reduce the required dose, therefore, reducing the toxicity.

Nanoparticles based on solid lipids (SLN, NLC) have been used to deliver antibiotics due to their ability to interact with the biofilm of bacteria. The controlled release aspect of solid lipid delivery is a very attractive offering, especially direct lung delivery for cystic fibrosis cases. In the study from Sans-Serramitjana et al., the use of SLN and NLC for the delivery of colistin has shown similar antimicrobial activity (MIC and MBC) as a free drug with more efficient biofilm eradication measures which are crucial for cystic fibrosis patient [61]. Another lipid delivery used is liposome where the liposome-loaded colistin exhibited synergistic activity but the need to increase the electrostatic attraction of colistin toward the lipid bilayer of liposomes is necessary to increase the retention of colistin in liposomes due to amphipathic properties of colistin that can lead to colloidal instability [62, 63]. The other nanoparticle design of colistin involves hydrophobic ion-pairing complexation (HIP) nanoparticles. The formation of the HIP complex occurred through the electrostatic interaction between ionizable peptide groups and the hydrophobic counterion with opposite charge. As a result, the complex demonstrates increased hydrophobicity without any alterations to its chemical composition. During the process of encapsulation, the complex can easily distribute

itself within a polymer matrix.. Therefore, HIP complexation significantly increases the encapsulation efficiency of colistin in the matrix of the polymer. The advantage of HIP complex is the reversible nature of the polymer due to dissociation of oppositely charged ions [64].

### 7. Colistin incorporated into SDCS micelles

Deoxycholic compounds are bile salts and acids which consist of a steroid backbone, a five- or eight-carbon side-chain with a carboxylic chain, and several hydroxyl groups, the number and orientation of which varies depending on the kind of bile acid or salt. [65]. Bile salts are natural steroids with surface-active and detergent-like properties capable of forming micellar aggregates and solubilizing many compounds in water [66], some of which are important from a biological and physiological point of view (for instance, bilirubin, cholesterol, fatty acids, phospholipids, and proteins). The structures of bile salt micellar aggregates are crucial for comprehending their physicochemical and biomedical properties. The ability of bile salts to solubilize other lipids is of crucial importance in intestinal absorption of the products of fat digestion such as fatty acids, monoglycerides, sterols and vitamins [65].

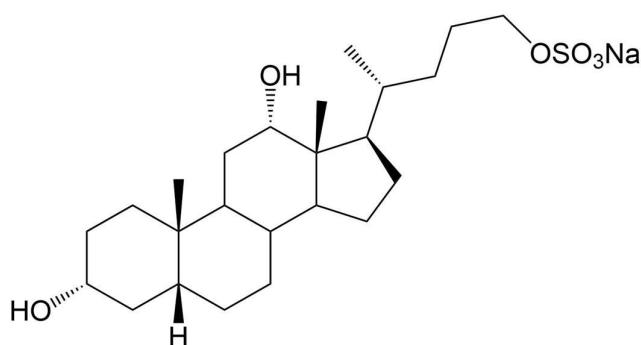


**Figure 5.** Sodium deoxycholate sulfate (SDCS) structure

Sodium deoxycholate sulfate (SDCS) or Sodium 3 $\alpha$ ,12 $\alpha$ -dihydroxy-5 $\beta$ -cholan-24-ol sulfate (Fig. 5) first biosynthesized by Burns *et al.*, by involving sulfation with

the help of sulfur trioxide-pyridine complex at its primary hydroxyl groups after undergoing esterification and reduction to its corresponding alcohol [67, 68]. The first comparison to its micellar properties was by incorporating amphotericin B (AMB), an antifungal drug used for the treatment of pulmonary fungal infections. The commercial formulation of AMB, which is a lipid formulation that used sodium deoxycholate as its carrier (Fungizone<sup>®</sup>), proven to have a weak micelle and has poor stability after reconstitution [68]. The results showed that SDCS produced more stable micelle formation with less toxicity compared to pure drug and its commercial formulation [68, 69]. Furthermore, the formulations of SDCS with PMB in the presence of LPS significantly reduced the surface tension compared to SDCS and commercial PMB alone [70, 71].

Colistin toxicity remains a major concern for the use of colistin in MDR-GNB therapy, and the need for a delivery system that can increase the activity or lower the exposure of colistin in renal tubular cells to reduce its uptake [72]. Currently, the lipid-based formulation of colistin is incorporated to improve the properties of colistin. The dose regulation problem of colistin also needs to be addressed by using colistin sulfate in the therapy instead of CMS which has a slow conversion rate and needs loading dose in its administration. By incorporating colistin in SDCS micelles the toxicity of colistin should be attenuated as demonstrated in the previous study.

## CHAPTER 2

### OBJECTIVES

1. To prepare colistin with synthesized SDCS carriers by the lyophilization process as dry powder formulations for intravenous administration.
2. To investigate the surface properties and CMC of the colistin and SDCS to optimize the formulation.
3. To evaluate the entrapment and release of colistin sulfate in SDCS formulation.
4. To examine the interaction of colistin-SDCS by FTIR, NMR, and docking simulation.
5. To examine the *in vitro* toxicity of colistin-SDCS formulations in kidney cells.
6. To investigate the nephrotoxicity and neurotoxicity of colistin-SDCS formulations in mice models.
7. To measure the mice biomarker changes after colistin-SDCS administration.

## CHAPTER 3

### SIGNIFICANT RESULTS AND DISCUSSION

#### 1. Surface properties of colistin and SDCS formulation

Colistin and SDCS formulations were prepared according to surface properties. Some parameters like surface and micellar properties of mixed micelles were commonly investigated by the surface tension of the solution. Surface tension at the air-water interface will gradually decrease from the surfactant addition. The critical micelle concentration (CMC) is the concentration where the micelles form due to saturation of surfactant at air-water interface with visibly constant surface tension changes. **Figure 6** shows the CMC of colistin and SDCS plotted from the surface tension of the water-air interface against concentration. Colistin as an amphipathic peptide has CMC at 25mg/L, while SDCS as a stronger surfactant has CMC around 8 mg/L. The ability of colistin and SDCS to form micelles resulting from mixed micelles of both components was lower than the CMC of the one-component system.

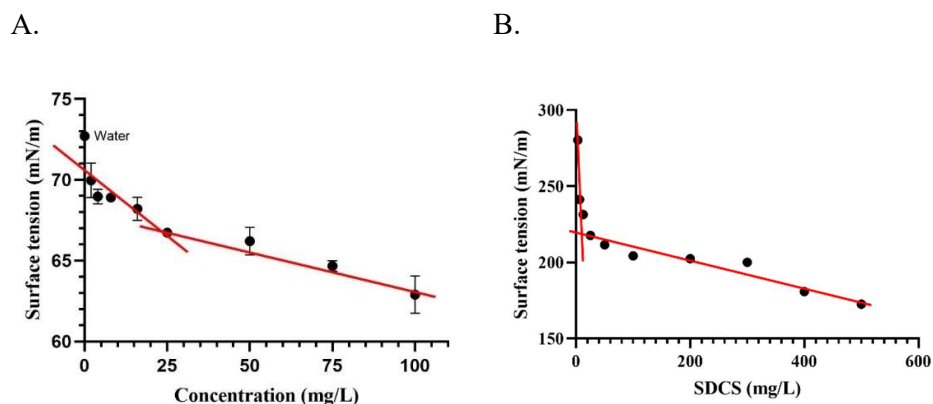


**Figure 6.** The surface tension versus concentration of the (A) colistin and (B) SDCS at 25 °C.

Colistin was associated with SDCS micelles via titration using the above CMC SDCS concentration. The results from titrated colistin against SDCS are shown the increase in particle size (766.87 nm) in the first addition (**Figure 7**). The system was stable around 367 nm with more colistin added during titration. The mixed micelles formed with colistin addition were stable after 5 minutes of titration. The ability of colistin to self-assemble aggregation showed a large particle size (766.87 and 411.03 nm) on the initial titration (0.01 and 0.02 molar ratio) [33]. The zeta potential of the titrated colistin to SDCS starts at -35 mV, the colistin as a cationic drug increased the zeta potential of the system with each addition. The stable charge can be observed from a ratio of 0.13 to 0.2 of colistin to SDCS.

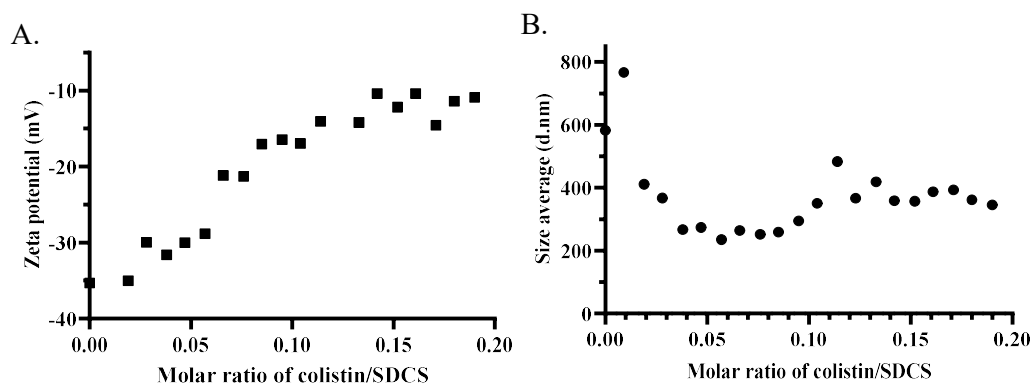


**Figure 7.** (A) zeta potential and (B) size average of colistin association into SDCS micelle via titration at 25 °C (mean,  $n = 3$ ).

## 2. Hydrodynamical properties of the formulation

The lyophilized colistin-SDCS were stable and easily reconstituted in water. The dry powder produced was light and free-flowing with white colour. The hydrodynamical size and charge of colistin-SDCS measured from dynamic-light scattering are shown in **Table 1**. The mean particle sizes of the reconstituted colistin formulations were  $141.9 \pm 1.9$  and  $140.9 \pm 1.2$  nm for F1 and F2, respectively. The

colistin exhibited a larger particle size at  $162.6 \pm 1.4$  nm in comparison with F1 and F2, which could be due to the colistin associated with SDCS micelles. The zeta potentials colistin-SDCS F1 and F2 were  $-22.8 \pm 0.15$  and  $-23.4 \pm 0.62$  mV respectively, compared to  $5.21 \pm 0.15$  mV for colistin sulfate. The significant difference between the hydrodynamic charge of colistin and colistin-SDCS micelles increased the stability of the formulation due to the electrostatic repulsion between the particles.

**Table 1.** Particle size and zeta potential of colistin micelle formulations, colistin, and SDCS from dynamic light scattering measurements (mean  $\pm$  SD,  $n = 3$ ).

Formula	Particle size (nm)	Zeta potential (mV)	Polydispersity index
Colistin:SDCS (1:1)	$141.9 \pm 1.9$	$-22.79 \pm 0.15$	$0.178 \pm 0.015$
Colistin:SDCS (1:2)	$140.9 \pm 1.2$	$-23.37 \pm 0.62$	$0.173 \pm 0.017$
Colistin	$162.6 \pm 1.4$	$5.21 \pm 0.15$	$0.218 \pm 0.04$
SDCS	$142.4 \pm 1.6$	$-33.77 \pm 3.91$	$0.156 \pm 0.02$

### 3. Chemical interaction of colistin and SDCS formulation

The Fourier transform infrared (FTIR) was employed to analyse the functional group shift from SDCS and colistin interaction and the spectra are shown in **Figure 8**. The spectrum of colistin shows high-intensity bands at  $1095 \text{ cm}^{-1}$  for C–O stretching,  $1660 \text{ cm}^{-1}$  for C=O stretching,  $2960$  and  $3060 \text{ cm}^{-1}$  for O–H stretching, and  $3282 \text{ cm}^{-1}$  for N–H stretching. As colistin are polypeptide molecule which consists of several amino acids like Di-aminobutyric acid (Dab) or D-leucine (D-Leu) the characteristics are shown from the well-defined bands. When compared to the spectra of SDCS and colistin SDCS formulation, the shift in C=O bands from  $1644$  to  $1655 \text{ cm}^{-1}$  which

displays the interaction of SDCS and colistin in the C=O function of colistin's amino acid also the O-H stretching from the SDCS which also present from the micelle's spectra interaction from hydroxyl part of SDCS forming hydrogen bond of amide function of amino acids.

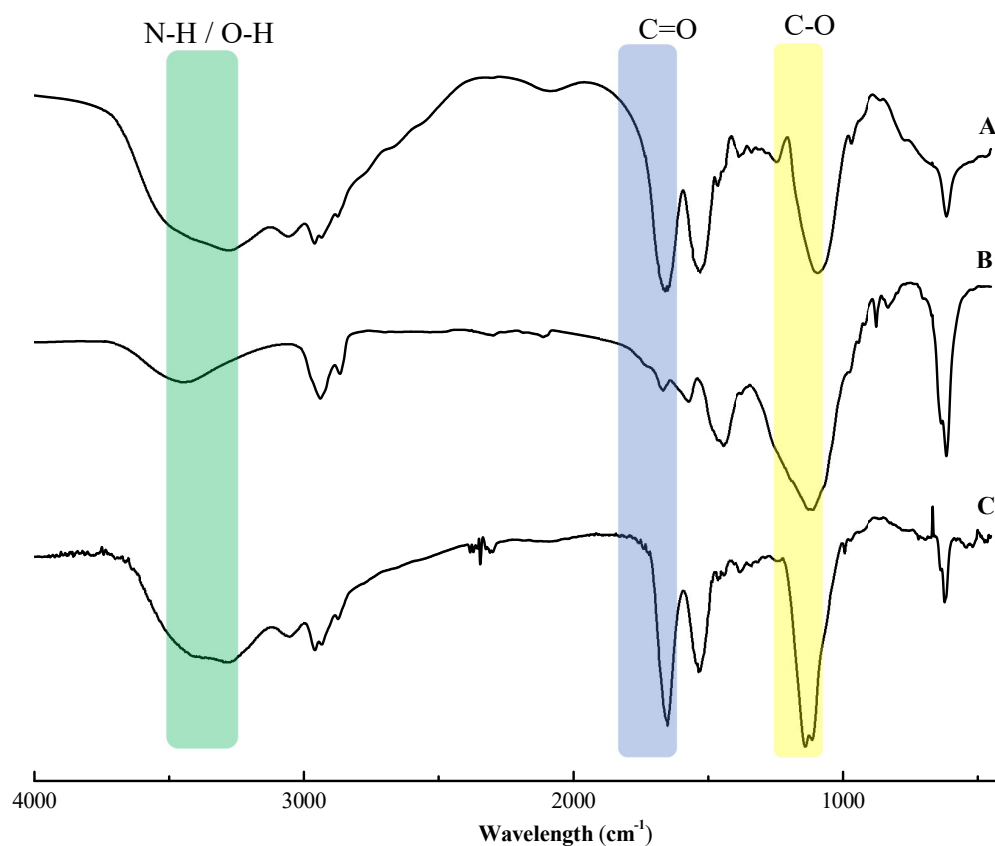


**Figure 8.** FTIR spectra of (A) colistin, (B) SDCS, and (C) colistin-SDCS micelle.

The chemical interaction of colistin and SDCS is also represented by the  $^{13}\text{C}$  and  $^1\text{H}$  NMR spectra shown in **Figure 9**. The NMR spectra from the formulation showed the characteristics of both colistin and SDCS. The shift from 8.4 ppm represents the hydroxyl characteristic of SDCS from **Figure 9B** which appears shifted at colistin-SDCS formulation (**Figure 9C & D**). **Table 2** lists the peak integration of  $^1\text{H}$  NMR spectra of the respective sample along with their chemical shift. The Colistin standard



consists of multiple analogues depending on the length of fatty acid, the mixture of colistin analogues produced several overlapping multiplets in NMR spectra. Several changes in chemical shift displayed from the integration listed for example the methyl function shift at 2.17 to 2.14 and 2.13 ppm, and 3.04 to 3.01 and 3.0 ppm which suggested the interaction from the decapeptide backbone of colistin with SDCS. In another study, it has been suggested that SDCS is bound via hydrogen bonding through its hydroxyl and sulfate function [69, 71]. The chemical shift comparison on colistin and colistin-SDCS formulation showed several peaks shifted from –OH or –NH of the amino acid of colistin interacting with SDCS via hydrogen bond. The interaction can also be observed from the  $^{13}\text{C}$  NMR spectra of colistin-SDCS formulations when compared to the spectra of colistin. The overlapping peaks were shown from the spectra of the colistin-SDCS formulation with the lower number of carbons from integrated peaks when compared to the colistin standard.

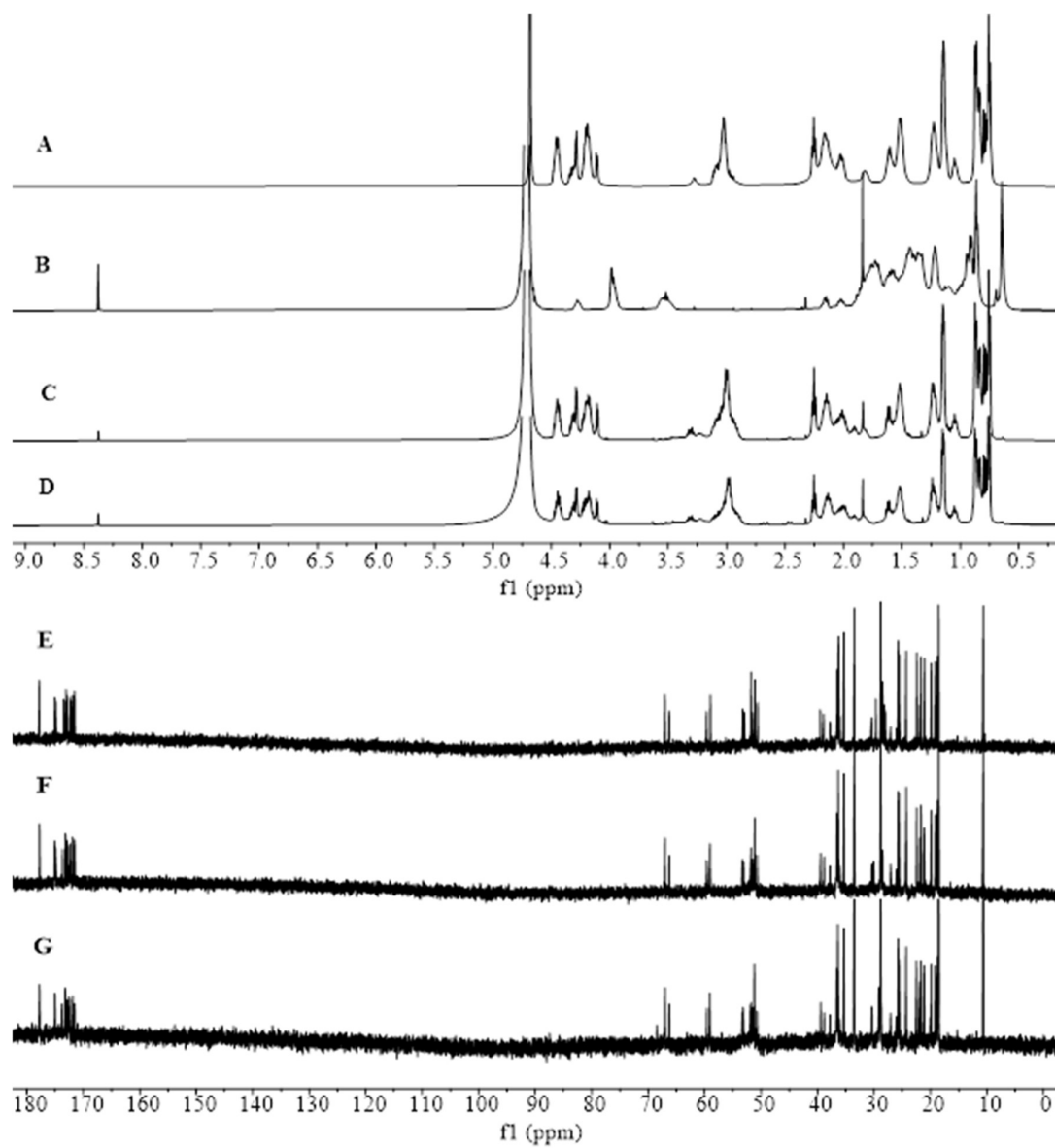


**Figure 9.**  $^1\text{H}$  NMR spectra of (A) colistin, (B) SDCS, (C) colistin-SDCS 1:1 ratio formulation, and (D) colistin-SDCS 1:2 ratio formulation. Also,  $^{13}\text{C}$  NMR spectra of (E) colistin, (F) colistin-SDCS 1:1 ratio formulation, and (G) colistin-SDCS 1:2 ratio formulation.

**Table 2.**  $^1\text{H}$  NMR chemical shifts of colistin, colistin:SDCS 1:1 (F1), and colistin:SDCS 1:2 (F2) multiplets.

Name	Chemical shift (ppm)		
	Colistin	F1	F2
4CH <sub>3</sub> (t)	0.76	0.75	0.75
aliphatic CH <sub>3</sub> (m)	0.79	0.78	0.79
CH <sub>3</sub> (OH) (m)	0.85	0.85	0.86
CH aliphatic (m)	1.05	1.05	1.05
NH <sub>2</sub> (dd)	1.15	1.14	1.15
CH <sub>2</sub> fatty acid (q)	1.22	1.22	1.23
CH ring (s)	1.25	1.25	1.51
OH (m)	1.52	1.51	1.61
CH-(CH <sub>2</sub> )-CH (dt)	1.6	1.61	1.83
-NH- (m)	1.81	1.83	2.01
CH <sub>2</sub> -(CH <sub>2</sub> )-CH (dq)	2.17	2.14	2.13
NH <sub>2</sub> -(CH <sub>2</sub> )-CH <sub>2</sub> (t)	2.25	2.25	2,25
(CH <sub>3</sub> )-CH (dddd)	3.04	3.01	3.0
CH <sub>2</sub> -(CH <sub>2</sub> )-NH (s)	3.28	3.29	3.31
CH <sub>3</sub> -(CH)-OH, beta -CH (m)	4.31	4.30	4.30
R-NH-R aliphatic (ddd)	4.46	4.44	4.44

t, triplet; m, multiplet; dd, doublet of doublets; q, quartet; s, singlet; dt, doublet of triplets; dq, doublet of quartet; dddd, doublet of doublet of doublet of doublets; ddd, doublet of doublet of doublets.

#### 4. Molecular interaction via molecular docking

In-silico modelling or molecular docking can be used to investigate the interaction between drugs and surfactants. The interaction between colistin and SDCS was simulated in a vacuum using docking methods and the docking results with 1 and 2 molecules of colistin as shown in **Figure 10A**. Several conformation and binding sites are shown from the docking results, the SDCS was found to be bound to the L-Dab of colistin in the heptapeptide ring. The side chain of amino acid colistin interacted with SDCS through hydrophobic interaction with its steroid nucleus. After docking the colistin with 10 molecules of SDCS by adding molecules one by one it shows colistin can bind to 5 molecules of SDCS with SDCS on each other intermolecularly after the 5<sup>th</sup> molecule. The binding affinity of SDCS was higher at 1 and 2 molecules with binding scores of  $-7.5$  and  $-7.65$  kcal/mol, respectively. This interaction shows in the 2D structure in **Figure 10B** with further addition of SDCS molecules supposedly occupying the remaining L-Dab before binding on each other intermolecularly. The results also show that SDCS was able to bind to colistin via electrostatic interaction. The negatively charged SDCS molecules in water at the concentration above CMC will form micelles with positively charged colistin by binding with the peptide ring through hydrogen bonding and electrostatic interaction.

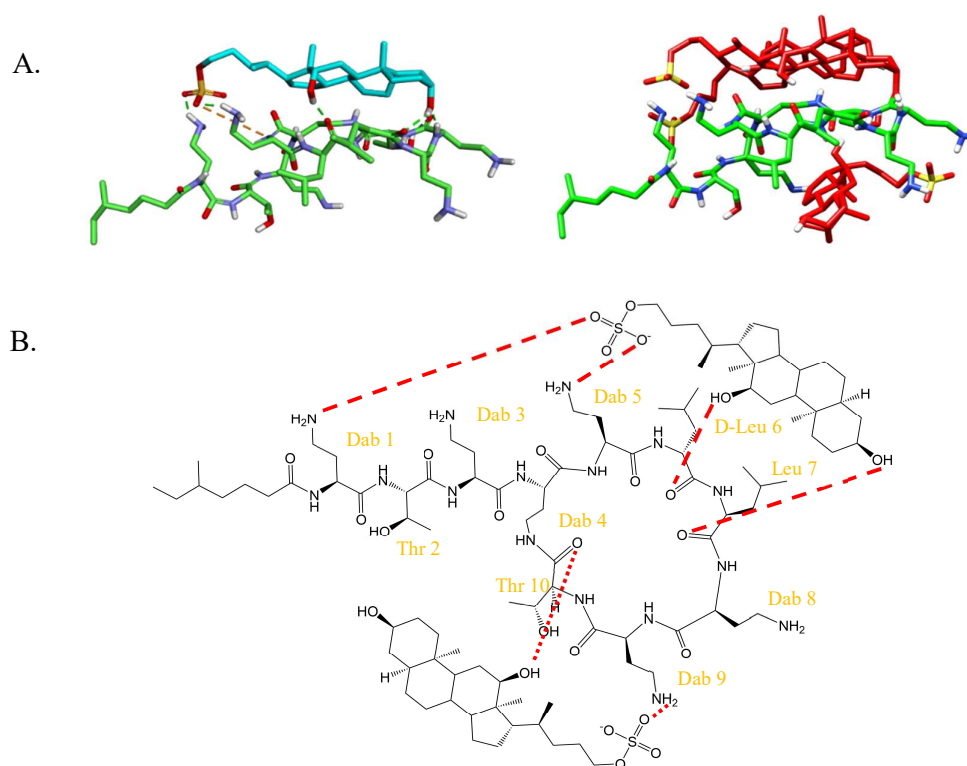


**Figure 10.** Molecular docking structure and plausible interaction of colistin and SDCS in (A) 3D structure that shows colistin as the green stick and SDCS as a cyan and red stick. Also, the illustration of interaction in (B) 2D structure where hydrogen bonding is shown as a red dashed line.

## 5. Encapsulation efficiency and release studies

For the encapsulation efficiency (EE) and release studies of the colistin and SDCS dry-powder micelles, the HPLC was employed to measure the drug content. Colistin standard usually consists of minor analogues with different ratios of analogues per batch, and colistin A (Polymyxin E<sub>1</sub>) was chosen as a standard (66% on the colistin sulfate USP). The EE for the five ratios of the formulation are listed in **Table 3** with the EE of  $70.0 \pm 3.2$ ,  $71.9 \pm 2.4$ ,  $73.4 \pm 3.3$ ,  $75.7 \pm 1.6$ , and  $76.4 \pm 4.1$  % for

colistin:SDCS molar ratio 1:1, 1:2, 1:3, 1:4, and 1:5, respectively. The results indicated that the higher ratio of SDSCS resulted in higher EE from colistin associated with the SDSCS micelles. Colistin nanoparticles entrapped by electrostatic interaction are readily released upon dilution [73].

**Table 3.** Percent encapsulation efficiency of colistin in different ratios of colistin to SDSCS formulations (mean,  $\pm$  SD  $n = 3$ ).

Formulation (molar ratio)	Colistin concentration ( $\mu\text{g/mL}$ )	% Encapsulation efficiency
F1 (1:1)	122.7	70.0 $\pm$ 3.2
F2 (1:2)	81.8	71.9 $\pm$ 2.4
F3 (1:3)	65.4	73.4 $\pm$ 3.3
F4 (1:4)	47.4	75.7 $\pm$ 1.6
F5 (1:5)	41.6	76.4 $\pm$ 4.1

The dosing regulation in antibiotic treatments can dictate the therapeutic effectiveness while lessening the side effects that may occur [74]. When positive clinical outcomes are not achieved in patients with suspected or documented Gram-negative infections, inadequate dosing should be considered as a primary cause [75]. Colistin sulfate has a more desirable conversion rate to colistin which makes the dose adjustment preferable to CMS where the vast majority is renally eliminated before conversion in patients with normal renal function [34, 45]. The colistin cumulative release in water was plotted against time in **Figure 11A**. Colistin standard showed rapid initial release in the medium at 0 min with  $49.95 \pm 4.19\%$  with the concentration plateau reached at 5 min ( $93.8 \pm 3.34$ ). The slower release was observed from colistin-

SDCS formulation with initial release at 0 min with  $29.51 \pm 1.81\%$ ,  $28.78 \pm 3.31\%$ ,  $27.17 \pm 2.1\%$ ,  $27.01 \pm 3.15\%$ , and  $26.13 \pm 0.77\%$  for 1:1, 1:2, 1:3, 1:4, and 1:5, respectively. As for the colistin release in 5% dextrose (**Figure 11B**), the release profile showed similar to that in water but slightly lower release over time. The slower release was observed on the 1:2 formulation in comparison to that in water. The results displayed that higher ratios of SDCS increase the retention of colistin inside the micelles leading to slower release. Colistin-SDCS ratio 1:5 showed the slowest release where the plateau phase was reached at the 20<sup>th</sup> min whereas 1:1, 1:2, 1:3, and 1:4 reached maximum release at the 15<sup>th</sup> min.

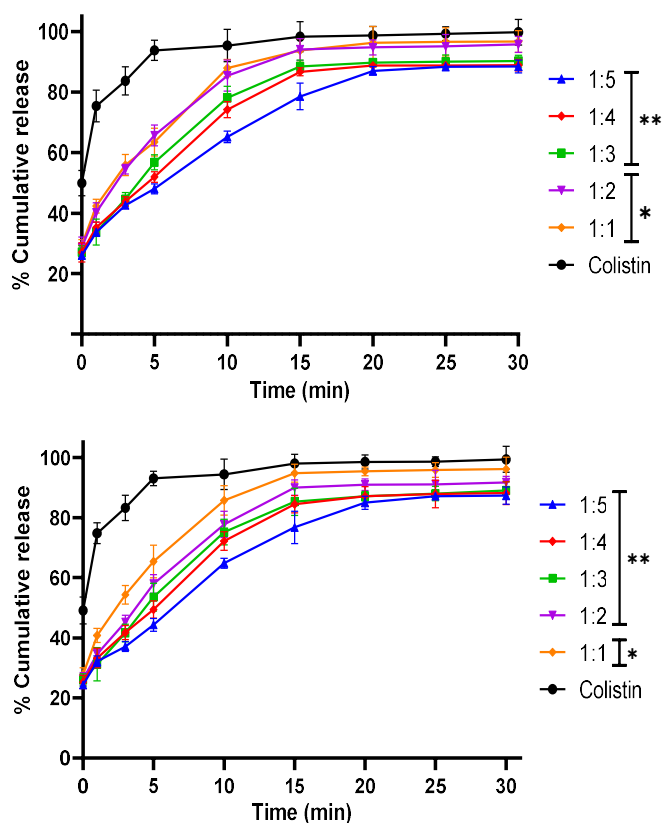


**Figure 11.** The colistin release profile from colistin standard and colistin-SDCS formulations at 37 °C in (A) water and (B) dextrose 5% (mean  $\pm$  S.D., n = 3). The star(s) represent statistical differences compared to colistin (\* = P < 0.05 and \*\* = P < 0.01)

## 6. Cytotoxicity on kidney cells of colistin-SDCS micelles

The cytotoxicity of colistin and colistin-SDCS micelles against human kidney cell line WT9-12, human kidney epithelial cell line 293T/17, and human primary renal proximal tubule epithelial cells PCS-400-010 was investigated in this study. SDCS is nontoxic on human kidney cells in-vitro and has also been shown to reduce the cytotoxicity of AMB on human kidney cells [68, 76]. Colistin potency is still hindered by its nephrotoxicity mainly the result of its increased permeability in tubular epithelial cells due to extensive tubular reabsorption [22, 48]. The percent viability of the human kidney cell lines examined using MTT assay are shown in **Figure 12** when exposed to colistin-free drug and colistin-SDCS micelles. The colistin-SDCS ratio 1:1 and 1:2 overall display a significant decrease in cytotoxicity at high concentrations when compared to a free drug of colistin (<60% cell viability of 293T/17 and <50% cell viability of WT9-12 and PCS-400-010 cells at 1000 µg/mL colistin equivalence). Colistin is shown to have moderate cytotoxicity on the two human kidney epithelial cells (WT9-12 and 293T/12) and the colistin-SDCS formulation displays a significant reduction in cell toxicity in both kidney cells when compared to the colistin standard.



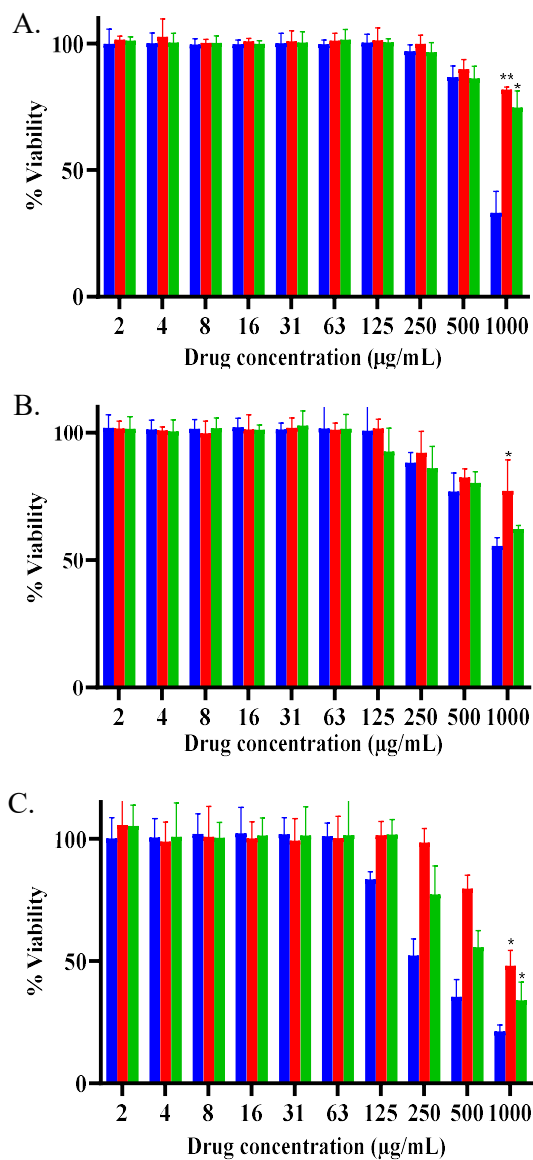


**Figure 12.** Cell viability of (A) human kidney cell line WT9-12, (B) human kidney epithelial cell line 293T/17, and (C) human primary renal proximal tubule epithelial cells PCS-400-010 after 24-h incubation with colistin (■), colistin to SDCS formulation ratios of 1:1 (■) and 1:2 (■) at various concentrations determined by MTT assay. Error bars represent a standard deviation ( $n = 3$ ). The star(s) represent statistical differences from colistin (\* =  $P < 0.05$  and \*\* =  $P < 0.01$ )

Colistin nephrotoxicity can be shown from its cytotoxicity toward human primary renal proximal tubule epithelial cells PCS-400-010 cells based on the dose and length of exposure during extensive tubular reabsorption [77]. Colistin standard showed 52.3% cell viability at 250  $\mu\text{g}/\text{mL}$  with a continual decrease in viability at the added concentration (**Figure 12C**). Significantly lower cytotoxicity was shown from both colistin-SDCS formulations for PCS-400-010 cells compared to the colistin standard which suggested that SDCS lower the colistin exposure immensely toward kidney proximal tubule cell lines. Previous studies have suggested that SDCS minimized the cytotoxicity of AmB and PMB toward kidney cell lines when compared with their free drug [71, 76, 78]. Colistin administered parenterally in micelles form will disassemble when the concentration is lowered by plasma below CMC levels which can result in micelle form that can lower the exposure or in the colistin form with SDCS molecules bound with a negative charge which can result in lower affinity toward megalin that contributed toward colistin nephrotoxicity during tubular reabsorption [51, 79].

## **8. Neurological behaviour and histopathology on mice models**

Sensory neuropathy and histopathology were performed with the approved method from the animal ethics committee, Prince of Songkla University (MHESI 68014/1895, Ref. 81/2021). The experimented mice (*Mus musculus* strain C57BL/6) were divided into four groups (n = 9) at random, and each group was weighed before and after treatment. The typical control group was given a saline solution, which served as the solvent. The colistin group received 15 mg/kg/day of colistin sulfate. Colistin:SDCS ratios of 1:1 and 1:2 were given to the Formulation 1 (F1) and Formulation 2 (F2) groups, respectively, at 15 mg/kg/day colistin equivalent. For seven days, injections were given intraperitoneally, and the dosage was divided into two doses

per day, once in the morning and once in the afternoon. A neurobehavioral evaluation was performed on the mice 12 hours after the last dose. The rodents were then euthanized with a lethal dose of intraperitoneal sodium pentobarbital (90 mg/kg). Blood samples were drawn via cardiac puncture, and serum was separated by centrifugation (3000 G for 15 minutes) and kept at -80 °C until analysis. For histopathological investigations, tissue samples from the kidney, liver, spleen, and sciatic nerve were collected, weighed, and sectioned.

After 7 days of colistin and colistin micelles treatments, there are no severe adverse effects observed from live mice. The initial and final body weight of experimented animals was listed in **Table 4** which showed the normal body weight gain of juvenile rodents from the control group and lower weight was observed from the colistin and colistin micelle group. Significant reduction in percentage body weight gain was measured in the colistin and F2 group, while the F1 showed a lesser reduction. **Table 4** also lists the values of the thermal pain threshold measured after 7 days of treatment where the sign of neurotoxicity can be observed by observing the exhibited sensory neuropathies. The thermal pain threshold of mice subjected to colistin in SDCS micelles show a significant decrease in thermal pain threshold time when compared to colistin. The control group measured 7.32 s for the thermal pain threshold value while F1 and F2 groups were slightly slower at 8.03 and 8.01 s, respectively, while the colistin group showed a significant increase ( $P < 0.01$ ) in the thermal threshold at 10.42 s. The early sign of neurotoxicity is the numbness that can result in a slower reaction time in thermal exposure. The colistin-injected mice showed signs of slower reaction time while the SDCS-incorporated formulation manages to have a significantly faster reaction time compared to the control group.

**Table 4** Effect of colistin-SDCS formulations on body weight gain and paw thermal threshold after seven days of treatment (mean  $\pm$  SD, n = 9)

	Control	Colistin	F1	F2
Initial BW )g(	19.64 $\pm$ 1.11	20.22 $\pm$ 1.15	20.46 $\pm$ 1.26	19.71 $\pm$ 0.61
Final BW )g(	21.00 $\pm$ 1.25	20.81 $\pm$ 0.84	21.34 $\pm$ 1.11	20.35 $\pm$ 0.68
Weight gain )%(	6.95 $\pm$ 1.4	3.06 $\pm$ 2.9 **	4.35 $\pm$ 2.09	3.11 $\pm$ 2.29 **
Thermal threshold )s(	7.35 $\pm$ 0.26	10.42 $\pm$ 0.98 **	8.03 $\pm$ 0.79	8.01 $\pm$ 1.05

*F1* Formulation 1, *F2* Formulation 2, *BW* body weight

\* = P < 0.05, \*\* = P < 0.01, compared with the control group

## 9. Biomarker measurement on the experimented animals

The levels of biomarkers in the serum were measured from 7 days of treated mice and listed in **Figure 13**. No significant changes were observed in the blood urea nitrogen (BUN) levels from the colistin group (21  $\pm$  2.6 mg/dL) and F1 group (21.4  $\pm$  3.4 mg/dL) (**Figure 13A**) with the F2 group showing a lower level of BUN (18.6  $\pm$  1.1 mg/dL) (P < 0.02) when compared to the control group (23.6  $\pm$  2.1 mg/dL). The creatinine (Cr) measurement displays no significant changes in the values of colistin (0.23  $\pm$  0.01 mg/dL), F1 (0.27  $\pm$  0.11 mg/dL), and F2 (0.24  $\pm$  0.05 mg/dL) groups compared to the control group (0.22  $\pm$  0.02 mg/dL) (**Figure 13B**). Acute tubular necrosis can appear as a rise in serum Cr due to a decrease in Cr clearance the same as the urea nitrogen clearance that can indicate kidney dysfunction [80]. The measured results indicate colistin and colistin-SDCS micelles showed no sign of severe damage related to kidney function.

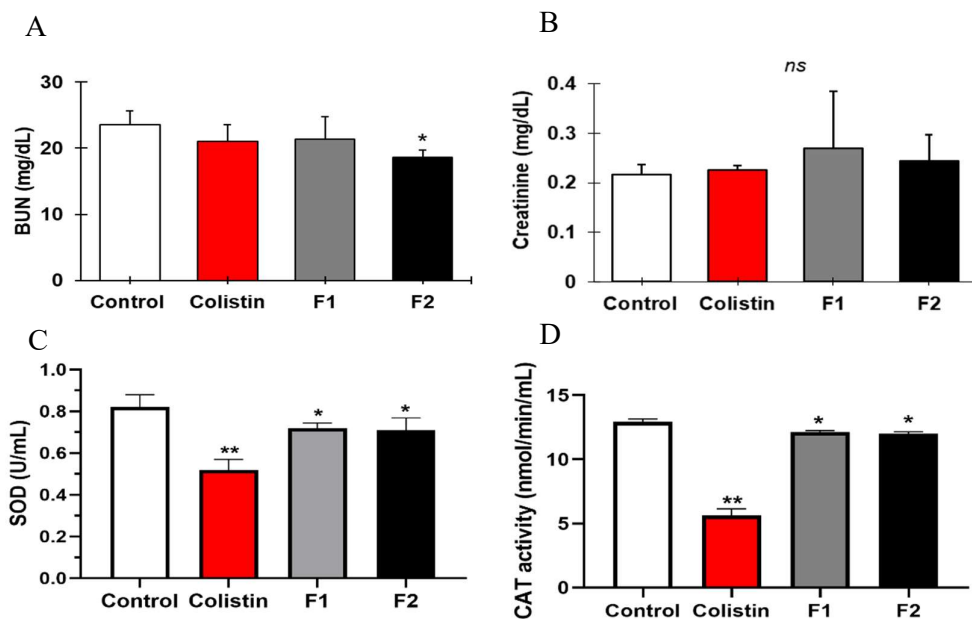


**Figure 13.** Effect of colistin and colistin-SDCS formulations on mice serum biomarkers: **A** Blood urea nitrogen (BUN), **B** Creatinine (Cr), **C** Superoxide dismutase (SOD), and **D** Catalase (CAT) (mean  $\pm$  SD,  $n = 6$ , \* =  $P < 0.05$  and \*\* =  $P < 0.01$ ).

The oxidative stress marker of the 7 days treated mice was measured from the serum levels of Superoxide dismutase (SOD) and Catalase (CAT) biomarkers. Normal levels of serum SOD level were measured from the control group at  $0.82 \pm 0.06$  U/mL, whereas a significantly lower level of SOD was measured from the colistin group ( $0.52 \pm 0.05$  U/mL) (**Figure 13C**). The serum SOD levels from F1 and F2 were shown to be  $0.72 \pm 0.03$  U/mL and  $0.71 \pm 0.06$  U/mL, respectively. Similar trends were displayed from the serum CAT levels where the control group at  $12.92 \pm 0.24$  nmol/min/mL while F1 and F2 groups have significantly lower levels at  $12.12 \pm 0.13$  nmol/min/mL and  $11.99 \pm 0.16$  nmol/min/mL, respectively (**Figure 13D**). Colistin-treated mice showed a

much lower level of CAT ( $5.61 \pm 0.52$  nmol/min/mL) compared to the control. The oxidative stress marker has been shown to have a role in complications of colistin-induced kidney damage with a deficiency that can exacerbate renal dysfunction and tubulointerstitial fibrosis in the kidney [80, 81]. SOD and CAT deficiency were also linked to reactive oxidative stress-induced damage to sciatic nerve tissue [82]. The results from the oxidative stress measurement suggested that SDCS incorporation into the colistin could significantly reduce the kidney damage marked by SOD and CAT.

#### **10. Histopathology of tissue samples from the mice models**

Hematoxylin and eosin (H&E) stains were used to examine the tissue samples of 7 days treated animals. The kidney histopathological results are shown in **Figure 14A-D**. Normal kidney tissue displayed in **Figure 14A** from the control group showed normal glomeruli (white circle). Colistin group kidney tissue showed some deformation of the glomeruli (yellow circle) and congestion of renal blood vessels (red circle) suggesting the kidney damage resulted from colistin treatment (**Figure 14B**). No evidence of renal glomerular injury was found in the F1 and F2 groups (**Figure 14C & D**, respectively) with mild alternation from the blood vessels. The tissue examination suggested that SDCS incorporation manages to lessen the nephrotoxicity of colistin. There was no severe injury observed from the histopathological alteration of the kidney tissues of colistin-treated animals with no sign of necrosis happened across all the tissues alteration as also pointed out by BUN and Cr results.

The liver histology of treated animals is displayed in **Figure 14E-H**, where the normal saline-treated group display the normal central vein surrounded by hepatic cords with no inflammatory infiltration (**Figure 14E**). The inflammation was evident in the

colistin-treated animals with infiltration of monocytes (yellow arrows) and loss of hepatocyte architecture around the blood vessels (**Figure 14F**). Mild inflammations were observed from colistin-SDCS formulation for groups F1 and F2 (**Figure 14G & H**, respectively) with few monocytes shown and no loss of structure observed.

In addition, the spleen histological alterations in the treated animals were shown in **Figure 14I-L**. Spleen function as a blood filter will show normal white pulp composed of lymphatic tissues and red pulp which filters and degrades red blood cells with normal trabeculae surrounding blood vessels as shown from the spleen tissue of the control group (**Figure 14I**). The spleen can show direct or indirect signs of toxicity where the inflammation can be observed from tissue examination. Large numbers of multinucleated giant cells (yellow arrows) were present which indicates inflammation in the spleen tissue of the colistin-treated animals (**Figure 14J**). Fewer numbers of multinucleated giant cells were observed in the spleen of the F1 and F2 groups (**Figure 14K & L**, respectively).

The neurotoxicity results from experimented animals were examined from the histopathology of the sciatic nerve tissue to observe peripheral nerve damage (**Figure 14M-P**). The sciatic nerve histology of the control group shows individual nerve fibres in the section showing central axons and surrounding myelin which appeared dense, and uniform with an ordered lamellar structure with no axonal shrinkage nor swelling (**Figure 14M**). The evidence of neurotoxicity was displayed in the nerve tissue of the colistin-treated group where the myelin sheath of the nerve fibres was thin and loose (**Figure 14N**). The uptake of colistin into the nerve cells of mice is dose-dependent as shown from the SOD and CAT results, the oxidative stress enzyme can be indicative of nerve damage which can also be observed in the increase of withdrawal latency of mice

during hot plate test. The nerve tissues of the F1 and F2 groups (**Figure 14O & P**) display few swollen axons with the appearance of the myelin sheath closely resembling the control group.

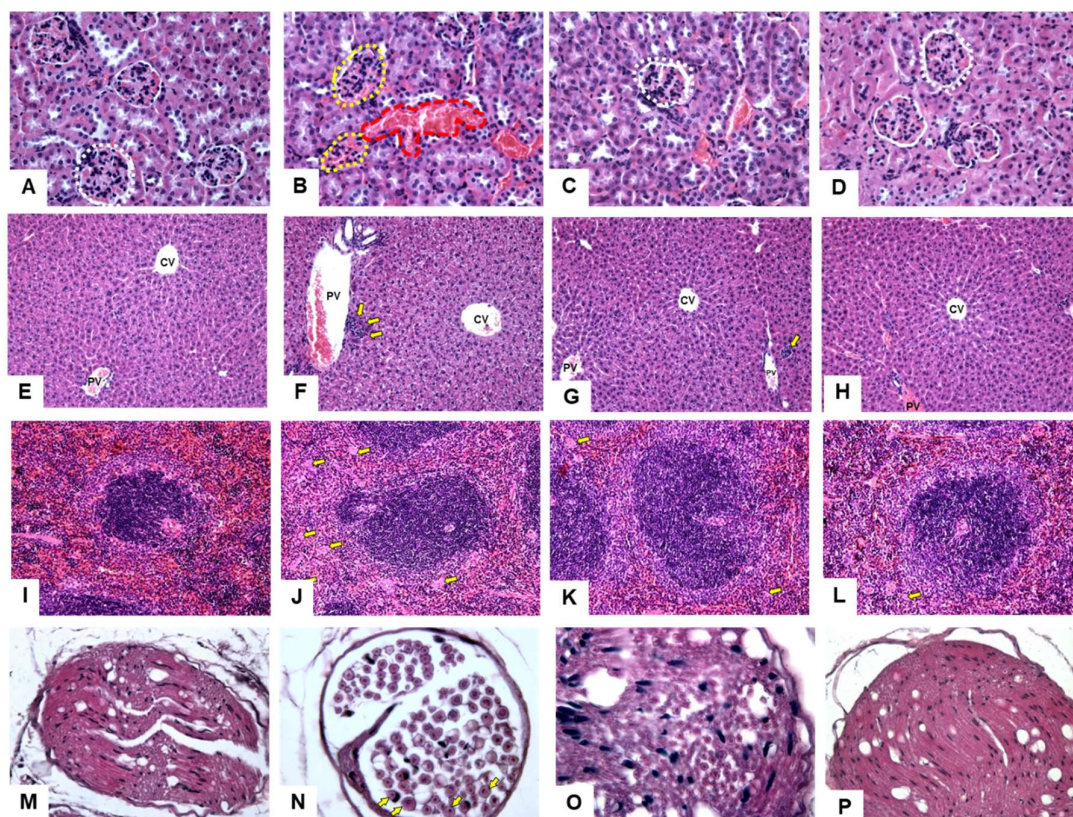


**Figure 14.** Histopathological alterations of: - **Kidney** tissue from (A) Control, (B) Colistin, (C) F1, (D) F2 groups. Visible glomeruli damage (yellow circle) with renal blood vessels congestion (red line). - **Liver** tissue from (E) Control, (F) Colistin, (G) F1, (H) F2 groups. Yellow arrows indicate infiltration of monocytes in the tissue. - **Spleen** tissue from (A) Control, (B) Colistin, (C) F1, (D) F2 groups. The yellow arrow indicates multinucleated giant cells in the tissue. - **Sciatic nerve** tissue from (A) Control, (B) Colistin, (C) F1, (D) F2 groups. The yellow arrow shows thin and loose fibres.



## CHAPTER 4

### CONCLUDING REMARKS

Colistin was formulated with synthesized SDCS as a lyophilized micelle. The surface properties of colistin were measured to optimize the ratio of colistin and SDCS. The different ratios of colistin were prepared and its hydrodynamic size and zeta potential show nanoparticulate size with negative zeta potential. The dry powder has high entrapment efficiency with slower release in the dissolution medium. The chemical interaction shows the colistin mainly binds SDCS through hydrogen bonding from its Dab residues as suggested from FTIR and NMR measurement and docking simulation. SDCS does not hinder the antibacterial activity of colistin against *P. aeruginosa* and the time-kill assay shows better bactericidal efficiency from the colistin-SDCS formulation. SDCS manages to lower the nephrotoxicity of colistin *in vitro* as observed in human kidney cell line WT9-12, human kidney epithelial cell line 293T/17, and human primary renal proximal tubule epithelial cells PCS-400-010. The animal models show a better safety profile from better heat sensitivity and histological alteration with lower signs of nephrotoxicity and neurotoxicity observed. The significantly higher SOD and CAT enzyme was measured from colistin-SDCS treated animals indicative of lesser oxidative stress from the treated animals. The study shows the potential of colistin sulfate as a parenteral formulation to combat MDR-GNB with better properties and safety profiles. There are still many things to further investigate to better understand colistin and SDCS interaction as well as toxicity studies before the formulation can go into clinical trials.

### **Connected publications**

1. Bintang MAKM, Srichana T (2022) Antibacterial Activity and In Vitro Cytotoxicity of Colistin in Sodium Deoxycholate Sulfate Formulation. *Adv Sci Technol* 121:25–30.

**\*\*Study related to in vitro toxicity of colistin-SDCS formulation (Objective 5)**

2. Bintang MAKM, Tipmanee V, Srichana T (2023) Colistin sulfate-sodium deoxycholate sulfate micelle formulations; molecular interactions, cell nephrotoxicity and bioactivity. *J Drug Deliv Sci Technol* 79:104091.

**\*\*Study related to formulation, characterization and molecular interaction of colistin-SDCS micelles formulation (Objective 1-4)**

3. Bintang MAKM, Nopparat J, Srichana T (2023) In vivo evaluation of nephrotoxicity and neurotoxicity of colistin formulated with sodium deoxycholate sulfate in a mice model. *Naunyn Schmiedebergs Arch Pharmacol*.

**\*\*Study related to in vivo nephrotoxicity and neurotoxicity of colistin-SDCS micelles formulation (Objective 6 & 7)**

## References

1. Hormozi SF, Vasei N, Aminianfar M, Darvishi M (2018) Antibiotic resistance in patients suffering from nosocomial infections in Besat Hospital. 28:304–308. <https://doi.org/10.4081/ejtm.2018.7594>
2. Silhavy TJ, Kahne D, Walker S (2010) The bacterial cell envelope. *Cold Spring Harb Perspect Biol* 2:a000414. <https://doi.org/10.1101/cshperspect.a000414>
3. Cremin K, Jones BA, Teahan J, Meloni GN, Perry D, Zerfass C, Asally M, Soyer OS, Unwin PR (2020) Scanning ion conductance microscopy reveals differences in the ionic environments of gram-positive and negative bacteria. *Anal Chem* 92:16024–16032. <https://doi.org/10.1021/acs.analchem.0c03653>
4. Gabarin RS, Li M, Zimmer PA, Marshall JC, Li Y, Zhang H (2021) Intracellular and extracellular lipopolysaccharide signaling in sepsis: Avenues for novel therapeutic strategies. *J Innate Immun* 13:323–332. <https://doi.org/10.1159/000515740>
5. Exner M, Bhattacharya S, Christiansen B, Gebel J, Goroncy-Bermes P, Hartemann P, Heeg P, Ilchner C, Kramer A, Larson E, Merckens W, Mielke M, Oltmanns P, Ross B, Rotter M, Schmithausen RM, Sonntag H-G, Trautmann M (2017) Antibiotic resistance: What is so special about multidrug-resistant Gram-negative bacteria? *GMS Hyg Infect Control* 12:Doc05. <https://doi.org/10.3205/dgkh000290>
6. Mul Fedele ML, Aiello I, Caldart CS, Golombek DA, Marpegan L, Paladino N (2020) Differential thermoregulatory and inflammatory patterns in the circadian response to lps-induced septic shock. *Front Cell Infect Microbiol* 10:1–18. <https://doi.org/10.3389/fcimb.2020.00100>

7. Wenzler E, Fraidenburg DR, Scardina T, Danziger LH (2016) Inhaled antibiotics for gram-negative respiratory infections. *Clin Microbiol Rev* 29:581–632. <https://doi.org/10.1128/CMR.00101-15>
8. Crump JA, Heyderman RS (2015) A perspective on invasive salmonella disease in Africa. *Clin Infect Dis* 61:S235–S240. <https://doi.org/10.1093/cid/civ709>
9. Lee YC, Hsiao CY, Hung MC, Hung SC, Wang HP, Huang YJ, Wang JT (2016) Bacteremic urinary tract infection caused by multidrug-resistant Enterobacteriaceae Are associated with severe sepsis at admission. *Med (United States)* 95:1–7. <https://doi.org/10.1097/MD.00000000000003694>
10. Langford BJ, So M, Raybardhan S, Leung V, Soucy JPR, Westwood D, Daneman N, MacFadden DR (2021) Antibiotic prescribing in patients with COVID-19: Rapid review and meta-analysis. *Clin Microbiol Infect* 27:520–531. <https://doi.org/10.1016/j.cmi.2020.12.018>
11. Brink AJ, Richards G, Tootla H, Prentice E (2022) Epidemiology of gram-negative bacteria during coronavirus disease 2019. What is the real pandemic? *Curr Opin Infect Dis* 35:595–604. <https://doi.org/10.1097/QCO.0000000000000864>
12. Dijkmans AC, Wilms EB, Kamerling IMC, Birkhoff W, Ortiz-Zacarias N V., Van Nieuwkoop C, Verbrugh HA, Touw DJ (2015) Colistin: Revival of an old polymyxin antibiotic. *Ther Drug Monit* 37:419–427. <https://doi.org/10.1097/FTD.0000000000000172>
13. Hsu L-Y, Apisarnthanarak A, Khan E, Suwantararat N, Ghafur A, Tambyah PA (2017) Carbapenem-resistant *Acinetobacter baumannii* and Enterobacteriaceae in South and Southeast Asia. *Asia Clin Microbiol Rev* 30:1–22.

<https://doi.org/https://doi.org/10.1128/CMR.00042-16>

14. Doi Y, Bonomo RA, Hooper DC, Kaye KS, Johnson JR, Clancy CJ, Thaden JT, Stryjewski ME, Van Duin D (2017) Gram-negative bacterial infections: Research priorities, accomplishments, and future directions of the Antibacterial Resistance Leadership Group. *Clin Infect Dis* 64:S30–S35. <https://doi.org/10.1093/cid/ciw829>
15. National Antimicrobial Resistance Surveillance Center Thailand. Antimicrobial Resistance Situation in Thailand Year 2020-2021
16. Mehrad B, Clark NM, Zhanel GG, Lynch JP (2015) Antimicrobial resistance in hospital-acquired gram-negative bacterial infections. *Chest* 147:1413–1421. <https://doi.org/10.1378/chest.14-2171>
17. Bassetti M, Peghin M, Vena A, Giacobbe DR (2019) Treatment of infections due to MDR gram-negative bacteria. *Front Med* 6:74. <https://doi.org/10.3389/fmed.2019.00074>
18. Giacobbe DR, Mikulska M, Viscoli C (2018) Recent advances in the pharmacological management of infections due to multidrug-resistant gram-negative bacteria. *Expert Rev Clin Pharmacol* 11:1219–1236. <https://doi.org/10.1080/17512433.2018.1549487>
19. Uchil RR, Kohli GS, Katekhaye VM, Swami OC (2014) Strategies to combat antimicrobial resistance. *J Clin Diagnostic Res* 8:8–11. <https://doi.org/10.7860/JCDR/2014/8925.4529>
20. Ahmed MAEE, Doi Y, Tian G, Zhong L, Shen C, Yang Y (2020) Colistin and its role in the Era of antibiotic resistance : an extended review. *Emerg Microbes Infect* 9:868–885.

<https://doi.org/https://doi.org/10.1080/22221751.2020.1754133>

21. Yahav D, Farbman L, Leibovici L, Paul M (2012) Colistin: New lessons on an old antibiotic. *Clin Microbiol Infect* 18:18–29. <https://doi.org/10.1111/j.1469-0691.2011.03734.x>
22. Gai Z, Samodelov SL, Kullak-Ublick GA, Visentin M (2019) Molecular mechanisms of colistin-induced nephrotoxicity. *Molecules* 24:653. <https://doi.org/10.3390/molecules24030653>
23. Caniaux I, van Belkum A, Zambardi G, Poirel L, Gros MF (2017) MCR: modern colistin resistance. *Eur J Clin Microbiol Infect Dis* 36:415–420. <https://doi.org/10.1007/s10096-016-2846-y>
24. Bergen PJ, Li J, Rayner CR, Nation RL (2006) Colistin methanesulfonate is an inactive prodrug of colistin against *Pseudomonas aeruginosa*. *Antimicrob Agents Chemother* 50:1953–1958. <https://doi.org/10.1128/AAC.00035-06>
25. Falagas ME, Fragoulis KN, Kasiakou SK, Sermaidis GJ, Michalopoulos A (2005) Nephrotoxicity of intravenous colistin: A prospective evaluation. *Int J Antimicrob Agents* 26:504–507. <https://doi.org/10.1016/j.ijantimicag.2005.09.004>
26. Grégoire N, Aranzana-Climent V, Magréault S, Marchand S, Couet W (2017) Clinical pharmacokinetics and pharmacodynamics of colistin. *Clin Pharmacokinet* 56:1441–1460. <https://doi.org/10.1007/s40262-017-0561-1>
27. Shah SR, Henslee AM, Spicer PP, Yokota S, Petrichenko S, Allahabadi S, Bennett GN, Wong ME, Kasper FK, Mikos AG (2014) Effects of antibiotic physicochemical properties on their release kinetics from biodegradable polymer microparticles. *Pharm Res* 31:3379–3389. <https://doi.org/10.1007/s11095-014->

1427-y

28. Couet W, Grégoire N, Marchand S, Mimos O (2012) Colistin pharmacokinetics: The fog is lifting. *Clin Microbiol Infect* 18:30–39. <https://doi.org/10.1111/j.1469-0691.2011.03667.x>
29. Yapa SWS, Li J, Porter CJH, Nation RL, Patel K, McIntosh MP (2013) Population pharmacokinetics of colistin methanesulfonate in rats: Achieving sustained lung concentrations of colistin for targeting respiratory infections. *Antimicrob Agents Chemother* 57:5087–5095. <https://doi.org/10.1128/AAC.01127-13>
30. Biswas S, Brunel JM, Dubus JC, Reynaud-Gaubert M, Rolain JM (2012) Colistin: An update on the antibiotic of the 21st century. *Expert Rev Anti Infect Ther* 10:917–934. <https://doi.org/10.1586/eri.12.78>
31. Garonzik SM, Li J, Thamlikitkul V, Paterson DL, Shoham S, Jacob J, Silveira FP, Forrest A, Nation RL (2011) Population pharmacokinetics of colistin methanesulfonate and formed colistin in critically ill patients from a multicenter study provide dosing suggestions for various categories of patients. *Antimicrob Agents Chemother* 55:3284–3294. <https://doi.org/10.1128/AAC.01733-10>
32. Wallace SJ, Li J, Rayner CR, Coulthard K, Nation RL (2008) Stability of colistin methanesulfonate in pharmaceutical products and solutions for administration to patients. *Antimicrob Agents Chemother* 52:3047–3051. <https://doi.org/10.1128/AAC.00103-08>
33. Wallace SJ, Li J, Nation RL, Prankerd RJ, Velkov T, Boyd BJ (2010) Self-assembly behavior of colistin and its prodrug colistin methanesulfonate: Implications for solution stability and solubilization. *J Phys Chem B* 114:4836–

4840. <https://doi.org/10.1021/jp100458x>
34. Nation RL, Velkov T, Li J (2014) Colistin and polymyxin B: Peas in a pod, or chalk and cheese? *Clin Infect Dis* 59:88–94. <https://doi.org/10.1093/cid/ciu213>
  35. Caroff M, Novikov A (2020) Lipopolysaccharides: Structure, function and bacterial identification. *OCL* 27:31. <https://doi.org/10.1051/ocl/2020025>
  36. Moubareck CA (2020) Polymyxins and bacterial membranes: A review of antibacterial activity and mechanisms of resistance. *Membranes (Basel)* 10:1–30. <https://doi.org/10.3390/membranes10080181>
  37. Sabnis A, Hagart KL, Klöckner A, Becce M, Evans LE, Furniss RCD, Mavridou DA, Murphy R, Stevens MM, Davies JC, Larrouy-Maumus GJ, Clarke TB, Edwards AM (2021) Colistin kills bacteria by targeting lipopolysaccharide in the cytoplasmic membrane. *Elife* 10:e65836. <https://doi.org/10.7554/eLife.65836>
  38. Bialvaei AZ, Samadi Kafil H (2015) Colistin, mechanisms and prevalence of resistance. *Curr Med Res Opin* 31:707–721. <https://doi.org/10.1185/03007995.2015.1018989>
  39. Yu Z, Qin W, Lin J, Fang S, Qiu J (2015) Antibacterial mechanisms of polymyxin and bacterial resistance. *Biomed Res Int* 2015:679109. <https://doi.org/10.1155/2015/679109>
  40. Şentürk S (2005) Evaluation of the anti-endotoxic effects of polymyxin-E (colistin) in dogs with naturally occurred endotoxic shock. *J Vet Pharmacol Ther* 28:57–63. <https://doi.org/10.1111/j.1365-2885.2004.00634.x>
  41. Baeuerlein A, Ackermann S, Parlesak A (2009) Transepithelial activation of human leukocytes by probiotics and commensal bacteria: Role of Enterobacteriaceae-type endotoxin. *Microbiol Immunol* 53:241–250.



<https://doi.org/10.1111/j.1348-0421.2009.00119.x>

42. Bergen PJ, Landersdorfer CB, Zhang J, Zhao M, Lee HJ, Nation RL, Li J (2012) Pharmacokinetics and pharmacodynamics of “old” polymyxins: What is new? *Diagn Microbiol Infect Dis* 74:213–223. <https://doi.org/10.1016/j.diagmicrobio.2012.07.010>
43. Li J, Milne RW, Nation RL, Turnidge JD, Smeaton TC, Coulthard K (2004) Pharmacokinetics of colistin methanesulphonate and colistin in rats following an intravenous dose of colistin methanesulphonate. *J Antimicrob Chemother* 53:837–840. <https://doi.org/10.1093/jac/dkh167>
44. Nang SC, Azad MAK, Velkov T, Zhou QT, Li J (2021) Rescuing the last-Line polymyxins: Achievements and challenges. *Pharmacol Rev* 73:679–728. <https://doi.org/10.1124/pharmrev.120.000020>
45. Plachouras D, Karvanen M, Friberg LE, Papadomichelakis E, Antoniadou A, Tsangaris I, Karaiskos I, Poulakou G, Kontopidou F, Armaganidis A, Cars O, Giamarellou H (2009) Population pharmacokinetic analysis of colistin methanesulfonate and colistin after intravenous administration in critically ill patients with infections caused by gram-negative bacteria. *Antimicrob Agents Chemother* 53:3430–3436. <https://doi.org/10.1128/AAC.01361-08>
46. Ordooei Javan A, Shokouhi S, Sahraei Z (2015) A review on colistin nephrotoxicity. *Eur J Clin Pharmacol* 71:801–810. <https://doi.org/10.1007/s00228-015-1865-4>
47. Kalin G, Alp E, Akin A, Coskun R, Doganay M (2014) Comparison of colistin and colistin/sulbactam for the treatment of multidrug resistant *Acinetobacter baumannii* ventilator-associated pneumonia. *Infection* 42:37–42.

<https://doi.org/10.1007/s15010-013-0495-y>

48. Yun B, Azad MAK, Wang J, Nation RL, Thompson PE, Roberts KD, Velkov T, Li J (2015) Imaging the distribution of polymyxins in the kidney. *J Antimicrob Chemother* 70:827–829. <https://doi.org/10.1093/jac/dku441>
49. Azad MAK, Yun B, Roberts KD, Nation RL, Thompson PE, Velkov T, Li J (2014) Measuring polymyxin uptake by renal tubular cells: Is bodipy-polymyxin B an appropriate probe? *Antimicrob Agents Chemother* 58:6337–6338. <https://doi.org/10.1128/AAC.03733-14>
50. Sivanesan SS, Azad MAK, Schneider EK, Ahmed MU, Huang J, Wang J, Li J, Nation RL, Velkov T (2017) Gelofusine ameliorates colistin-induced nephrotoxicity. *Antimicrob Agents Chemother* 61:1–7. <https://doi.org/10.1128/AAC.00985-17>
51. Suzuki T, Yamaguchi H, Ogura J, Kobayashi M, Yamada T, Iseki K (2013) Megalin contributes to kidney accumulation and nephrotoxicity of colistin. *Antimicrob Agents Chemother* 57:6319–6324. <https://doi.org/10.1128/AAC.00254-13>
52. Hori Y, Aoki N, Kuwahara S, Hosojima M, Kaseda R, Goto S, Iida T, De S, Kabasawa H, Kaneko R, Aoki H, Tanabe Y, Kagamu H, Narita I, Kikuchi T, Saito A (2017) Megalin blockade with cilastatin suppresses drug-induced nephrotoxicity. *J Am Soc Nephrol* 28:1783–1791. <https://doi.org/10.1681/ASN.2016060606>
53. Cheng CY, Sheng WH, Wang JT, Chen YC, Chang SC (2010) Safety and efficacy of intravenous colistin (colistin methanesulphonate) for severe multidrug-resistant gram-negative bacterial infections. *Int J Antimicrob Agents* 35:297–300.

<https://doi.org/10.1016/j.ijantimicag.2009.11.016>

54. Mendes CAC, Burdmann EA (2010) Polymyxins: review with emphasis on nephrotoxicity. *Rev Assoc Med Bras* 55:752–758. <https://doi.org/10.1590/s0104-42302009000600023>
55. Dai C, Li J, Tang S, Li J (2014) Colistin-induced nephrotoxicity in mice involves the mitochondrial , death receptor , and endoplasmic reticulum pathways. *Antimicrob Agents Chemother* 58:4075–4085. <https://doi.org/10.1128/AAC.00070-14>
56. Ma Z, Wang J, Nation RL, Li J, Turnidge JD, Coulthard K, Milne RW (2009) Renal disposition of colistin in the isolated perfused rat kidney. *Antimicrob Agents Chemother* 53:2857–2864. <https://doi.org/10.1128/AAC.00030-09>
57. Pogue JM, Ortwine JK, Kaye KS (2017) Clinical considerations for optimal use of the polymyxins: A focus on agent selection and dosing. *Clin Microbiol Infect* 23:229–233. <https://doi.org/10.1016/j.cmi.2017.02.023>
58. Claus BOM, Snauwaert S, Haerynck F, Van Daele S, De Baets F, Schelstraete P (2015) Colistin and neurotoxicity: recommendations for optimal use in cystic fibrosis patients. *Int J Clin Pharm* 37:555–558. <https://doi.org/10.1007/s11096-015-0077-4>
59. Dai C, Li J, Li J (2013) New insight in colistin induced neurotoxicity with the mitochondrial dysfunction in mice central nervous tissues. *Exp Toxicol Pathol* 65:941–948. <https://doi.org/10.1016/j.etp.2013.01.008>
60. Dai C, Tang S, Li J, Wang J, Xiao X (2014) Effects of colistin on the sensory nerve conduction velocity and F-wave in mice. *Basic Clin Pharmacol Toxicol* 115:577–580. <https://doi.org/10.1111/bcpt.12272>
61. Sans-Serramitjana E, Fusté E, Martínez-Garriga B, Merlos A, Pastor M, Pedraz

- JL, Esquisabel A, Bachiller D, Vinuesa T, Viñas M (2016) Killing effect of nanoencapsulated colistin sulfate on *Pseudomonas aeruginosa* from cystic fibrosis patients. *J Cyst Fibros* 15:611–618. <https://doi.org/10.1016/j.jcf.2015.12.005>
62. Wallace SJ, Li J, Nation RL, Prankerd RJ, Boyd BJ (2012) Interaction of colistin and colistin methanesulfonate with liposomes: Colloidal aspects and implications for formulation. *J Pharm Sci* 101:3347–3359. <https://doi.org/doi:10.1002/jps.23203>
63. Li Y, Tang C, Zhang E, Yang L (2017) Electrostatically entrapped colistin liposomes for the treatment of *Pseudomonas aeruginosa* infection. *Pharm Dev Technol* 22:436–444. <https://doi.org/10.1080/10837450.2016.1228666>
64. Tang C, Zhang E, Li Y, Yang L (2017) An innovative method for preparation of hydrophobic ion-pairing colistin entrapped poly(lactic acid) nanoparticles: Loading and release mechanism study. *Eur J Pharm Sci* 102:63–70. <https://doi.org/10.1016/j.ejps.2017.02.036>
65. Rub MA, Sheikh MS, Khan F, Khan SB, Asiri AM (2014) Bile salts aggregation behavior at various temperatures under the influence of amphiphilic drug imipramine hydrochloride in aqueous medium. *Zeitschrift fur Phys Chemie* 228:747–767. <https://doi.org/10.1515/zpch-2013-0495>
66. Šarenac TM, Mikov M (2018) Bile acid synthesis: From nature to the chemical modification and synthesis and their applications as drugs and nutrients. *Front Pharmacol* 9:1–22. <https://doi.org/10.3389/fphar.2018.00939>
67. Burns AC, Sorensen PW, Hoye TR (2011) Synthesis and olfactory activity of unnatural, sulfated 5 $\beta$ -bile acid derivatives in the sea lamprey (*Petromyzon*

- marinus). *Steroids* 76:291–300. <https://doi.org/10.1016/j.steroids.2010.11.010>
68. Gangadhar KN, Adhikari K, Srichana T (2014) Synthesis and evaluation of sodium deoxycholate sulfate as a lipid drug carrier to enhance the solubility, stability and safety of an amphotericin B inhalation formulation. *Int J Pharm* 471:430–438. <https://doi.org/10.1016/j.ijpharm.2014.05.066>
69. Usman F, Ul-Haq Z, Khalil R, Tinpun K, Srichana T (2017) Pharmacologically safe nanomicelles of amphotericin B with lipids: Nuclear magnetic resonance and molecular docking approach. *J Pharm Sci* 106:3574–3582. <https://doi.org/10.1016/j.xphs.2017.08.013>
70. Madhumanchi S, Suedee R, Nakpheng T, Tinpun K, Temboot P, Srichana T (2019) Binding interactions of bacterial lipopolysaccharides to polymyxin B in an amphiphilic carrier ‘sodium deoxycholate sulfate.’ *Colloids Surfaces B Biointerfaces* 182:110374. <https://doi.org/10.1016/j.colsurfb.2019.110374>
71. Temboot P, Kaewpaiboon S, Tinpun K, Nakpeng T, Khalil R, Ul-Haq Z, Thamlikitkul V, Tiengrim S, Srichana T (2020) Potential of sodium deoxycholate sulfate as a carrier for polymyxin B: Physicochemical properties, bioactivity and in vitro safety. *J Drug Deliv Sci Technol* 58:101779. <https://doi.org/10.1016/j.jddst.2020.101779>
72. Dubashynskaya N V., Skorik YA (2020) Polymyxin delivery systems: Recent advances and challenges. *Pharmaceuticals* 13:. <https://doi.org/10.3390/ph13050083>
73. Wallace SJ, Li J, Nation RL, Boyd BJ (2012) Drug release from nanomedicines: Selection of appropriate encapsulation and release methodology. *Drug Deliv Transl Res* 2:284–292. <https://doi.org/10.1007/s13346-012-0064-4>

74. de With K, Allerberger F, Amann S, Apfalter P, Brodt HR, Eckmanns T, Fellhauer M, Geiss HK, Janata O, Krause R, Lemmen S, Meyer E, Mittermayer H, Porsche U, Presterl E, Reuter S, Sinha B, Strauß R, Wechsler-Fördös A, Wenisch C, Kern W V. (2016) Strategies to enhance rational use of antibiotics in hospital: a guideline by the German Society for Infectious Diseases. *Infection* 44:395–439. <https://doi.org/10.1007/s15010-016-0885-z>
75. Li J, Nation RL, Milne RW, Turnidge JD, Coulthard K (2005) Evaluation of colistin as an agent against multi-resistant gram-negative bacteria. *Int J Antimicrob Agents* 25:11–25. <https://doi.org/10.1016/j.ijantimicag.2004.10.001>
76. Madhumanchi S, Suedee R, Kaewpiboon S, Srichana T, Khalil R, Ul-Haq Z (2020) Effect of sodium deoxycholate sulfate on outer membrane permeability and neutralization of bacterial lipopolysaccharides by polymyxin B formulations. *Int J Pharm* 581:119265. <https://doi.org/10.1016/j.ijpharm.2020.119265>
77. Zavascki AP, Nation RL (2017) Nephrotoxicity of polymyxins: Is there any difference between colistimethate and polymyxin B? *Antimicrob Agents Chemother* 61:e02319-16. <https://doi.org/10.1128/AAC.02319-16>
78. Usman F, Khalil R, Ul-Haq Z, Nakpheng T, Srichana T (2018) Bioactivity, safety, and efficacy of amphotericin B nanomicellar aerosols using sodium deoxycholate sulfate as the lipid carrier. *AAPS PharmSciTech* 19:2077–2086. <https://doi.org/10.1208/s12249-018-1013-4>
79. Ghezzi M, Pescina S, Padula C, Santi P, Del Favero E, Cantù L, Nicoli S (2021) Polymeric micelles in drug delivery: An insight of the techniques for their characterization and assessment in biorelevant conditions. *J Control Release* 332:312–336. <https://doi.org/10.1016/j.jconrel.2021.02.031>

80. Ozkan G, Ulusoy S, Orem A, Alkanat M, Mungan S, Yulug E, Yucesan FB (2013) How does colistin-induced nephropathy develop and can it be treated? *Antimicrob Agents Chemother* 57:3463–3469. <https://doi.org/10.1128/AAC.00343-13>
81. Keirstead ND, Wagoner MP, Bentley P, Blais M, Brown C, Cheatham L, Ciaccio P, Dragan Y, Ferguson D, Fikes J, Galvin M, Gupta A, Hale M, Johnson N, Luo W, McGrath F, Pietras M, Price S, Sathe AG, Sasaki JC, Snow D, Walsky RL, Kern G (2014) Early prediction of polymyxin-induced nephrotoxicity with next-generation urinary kidney injury biomarkers. *Toxicol Sci* 137:278–291. <https://doi.org/10.1093/toxsci/kft247>
82. Edrees NE, Galal AAA, Abdel Monaem AR, Beheiry RR, Metwally MMM (2018) Curcumin alleviates colistin-induced nephrotoxicity and neurotoxicity in rats via attenuation of oxidative stress, inflammation and apoptosis. *Chem Biol Interact* 294:56–64. <https://doi.org/10.1016/j.cbi.2018.08.012>

**APPENDICES**

Appendix 1 Reprint of papers

Appendix 2 Ethical Committee approval

Appendix 3 Vitae



**Reprints of papers**

**Paper 1**

Antibacterial Activity and In Vitro Cytotoxicity of Colistin in Sodium Deoxycholate  
Sulfate Formulation

## Antibacterial Activity and *In Vitro* Cytotoxicity of Colistin in Sodium Deoxycholate Sulfate Formulation

Muhammad Ali Khumaini Mudhar Bintang<sup>1,a\*</sup> and Teerapol Srichana<sup>2,b</sup>

<sup>1</sup>Faculty of Pharmaceutical Sciences, Prince of Songkhla University, Songkhla, Thailand

<sup>2</sup>Drug Delivery System Excellence Center, Prince of Songkhla University, Songkhla, Thailand

<sup>a</sup>alikhumaini31@gmail.com, <sup>b</sup>teerapol.s@psu.ac.th

**Keywords:** Colistin, sodium deoxycholate sulfate, antibacterial, nephrotoxicity, micelle

**Abstract.** Colistin has its problem with nephrotoxicity despite its capability for combatting multi-drug resistant gram-negative bacteria. Sodium deoxycholate sulfate (SDCS) has been shown to increase the safety profile of nephrotoxic drugs. This study aimed to explore the antimicrobial activity of colistin-SDCS versus free colistin against *P. aeruginosa* and investigate their cytotoxicity on kidney cells. The colistin micelles were formulated with SDCS followed by lyophilization and their properties were analyzed. Minimum inhibitory concentration (MIC) and minimum bactericidal concentration (MBC) of colistin were determined using the broth microdilution method. The static time-kill kinetics were also employed to monitor the bactericidal activity of formulation over time. The cytotoxicity of formulations was analyzed using MTT colorimetric assay against kidney cells. The colistin-SDCS dry-powder was stable after reconstitution and resulted in 240 to 297 nm in particle size with the zeta potential of -22.8 to -23.4 mV. The colistin-SDCS formulations showed similar antibacterial activity against *P. aeruginosa* to pure colistin. MIC and MBC were 7.81 and 15.63 µg/mL, respectively. The static-time kill results displayed slightly better bactericidal activity at 24 h. The viability of kidney cells exposure to colistin-SDCS micelle was higher than that of pure colistin.

### Introduction

Colistin (polymyxin E) is an amphipathic lipopeptide antibiotic that, like polymyxin B, belongs to the polymyxin family of antibiotics. Polymyxin B (PMB) and colistin are non-ribosomal peptides that have a similar structure except for position 6, where D-Phe in PMB is substituted by D-Leu in colistin. As an amphipathic antimicrobial peptide, the polar face will interact with the polar lipid A head groups of bacteria, while the lipophilic face inserts into the hydrophobic fatty acyl layer of the outer bacterial membrane. Colistin not only interacts with the bacterial membrane but also inhibits the toxicity of lipopolysaccharides [1].

Although it has become one of the last lines of defense against the multi-drug resistant epidemic, concerns over its toxicity, particularly nephrotoxicity, which has a 40-60% prevalence, have led to its replacement with a safer alternative. Colistin's nephrotoxicity is primarily due to its d-aminobutyric acid and fatty acid components, and the mechanism of nephrotoxicity is similar to that of its antibacterial effect; in fact, colistin increases tubular epithelial cell membrane permeability, resulting in cations, anions, and water influx, which causes cell swelling and lysis [2].

Sodium deoxycholate sulfate (SDCS) has been synthesized recently to use as a carrier for amphotericin B (AMB) and polymyxin B (PMB) to compare with its more conventional products [3, 4]. The study reported that SDCS formulation showed less toxicity to the alveolar, bronchial epithelium, and primary kidney cell lines compared to the pure drug for either AMB or PMB [4, 5]. The suggested mechanism of SDCS in decreasing renal toxicity is its ability to reduce the exposure of the free drug to the renal cells due to its slower release to the target site which also means a more stable micelle of SDCS and AMB or polymyxins [5, 6]. The promising terms for this novel lipid carrier show the potential for reducing the risk of nephrotoxicity by reducing systemic colistin exposure, and dose-limiting toxicity associated with intravenous polymyxins. The study aimed to

examine the antibacterial activity and cytotoxicity of formulated colistin-SDCS against human kidney cells

### Methods

**Preparation of Colistin-SDCS dry powder formulations.** The preparation was carried out by preparing a mixture of colistin sulfate (70 and 55 mg) and previously synthesized SDCS (26.6 and 41.7 mg) for a 1:1 (F1) and 1:2 (F2) molar ratio in double-distilled water (40 ml) and stirred until dissolved. Sodium dihydrogen phosphate heptahydrate (1.01 g) and sodium hydrogen phosphate monohydrate (169 mg) were added to the solution for phosphate buffer pH 7.4. The final volume of the solution was made to 50 mL by adjusting the volume with double-distilled water. The solution was lyophilized, and the dry powder can be reconstituted with water for further use or studies. The reconstituted formulation particle size and zeta potential were measured by dynamic light scattering (DLS) (Zetasizer NanoZS, Malvern, England).

**Minimum Inhibitory Concentration (MIC) and Minimum Bactericidal Concentration (MBC) determination.** Colistin-SDCS formulation and free colistin sulfate was tested in *P. aeruginosa* (ATCC 27853, Rockville, MD, USA). The MIC was determined using broth microdilution according to Elshikh et. al. [7]. Colistin-SDCS formulations were suspended in Brain Heart Infusion (BHI) and starting from 125 µg/mL of colistin or colistin equivalence of the formulation (containing 75.5 and 58.2% of colistin for F1 and F2, respectively). Decreasing concentrations of formulations were obtained by serial two-fold dilutions in 96-well plates. Bacteria suspension was adjusted to 0.5 McFarland standard ( $1 \times 10^8$  CFU/mL). Bacteria suspension (10 µL) was pipetted into a 96-well plate for the inoculation period of 18 h at 37 °C. Each well has inoculated approximately  $1.0 \times 10^5$  CFU/mL. After the incubation time, 30 µL of 0.02% resazurin sodium salt in phosphate buffer solution was added and incubated for 3 h. The minimum inhibitory concentration (MIC) was determined by the lowest antibiotic concentration that can prevent visible bacterial growth. The minimal bactericidal concentration (MBC) was then determined according to National Committee for Clinical Laboratory Standards [8] by subculturing the samples having a value equal to MIC or higher than MIC. The samples were then transferred from the 96-well plates into freshly prepared tryptic soy agar plates and incubated at 37 °C for 18 h. MBC is the lowest concentration which no single bacterial colony growth.

**Static time-kill experiment.** The static time-kill experiment was conducted to examine the antimicrobial activity of colistin using BHI as the medium. All experiments were performed with an initial inoculum of  $\sim 10^6$  CFU/mL in 20 mL of BHI. Drug concentrations that were tested were the MBC based on the previous results. Samples (50 µL) were collected at 0, 1, 3, 6, and 24 h, centrifuged at  $12000 \times g$  for 10 min, and cell pellets were resuspended in 0.9% saline and diluted accordingly for viable counting on nutrient agar plates. The limit of detection was 20 CFU/mL (equivalent to one colony per plate). A colony counter was used to quantify bacteria after 24 h of incubation at 37 °C.

**Cytotoxicity assay using kidney cells.** The MTT colorimetric assay was used to examine the sample cytotoxicity on human kidney epithelial cell lines WT9-12, 293T/17, and Primary Renal Proximal Tubule Epithelial Cells; PCS-400-010. The kidney cells were distributed in 96-well plates at a density of  $1 \times 10^5$  cells/well in 100 µL of complete DMEM (Dulbecco's Modified Eagle Medium) and allowed to attach overnight at 37°C and 5% CO<sub>2</sub> with 95% relative humidity. After 24 h, the medium (100 µL) was replaced with 100 µL of various concentrations of the sample (1.95 to 1000 µg/mL). After incubation for 24 h, 50 µL of MTT (1.25 mg/mL) was added and further incubated for 4 h. The solutions were removed from the 96-well plates, and 100 µL of DMSO was added to dissolve formazan crystals. The ODs were measured at 570 nm using a microplate reader. The percentage of surviving cells was calculated from the following formula:

$$\% \text{ viability} = (\text{OD}_{\text{treated}} / \text{OD}_{\text{control}}) \times 100. \quad (1)$$

The number of viable cells in the treated wells was compared to those in the untreated wells and estimated as percent viability.

## Results and Discussion

Sodium deoxycholate sulfate has been proven to reduce the toxicity of nephrotoxic drugs. The present work aimed to develop the potential formulation of colistin with an improved biosafety profile. The colistin dry powder formulated using SDCS has a white fluffy powder appearance and can easily be reconstituted in water. The reconstituted micelles were clear and stable (no precipitation occurred). The size of colistin micelles was 240 and 297 nm with zeta potential of -22.8 and -23.4 mV for colistin-SDCS molar ratios of 1:1 and 1:2, respectively. The size distribution is shown in Fig. 1, with the polydispersity index (PDI) of 0.241 and 0.314 for ratios 1:1 and 1:2 respectively. The larger colistin micelles may be contributed from micelle aggregation [9]. The zeta potential of colistin micelles was different from that of colistin sulfate (5.2 mV) implying that the SDCS carrier considerably increased the net negative charge in colistin formulations, hence increasing electrostatic repulsion between nano-particles.

**Antibacterial activity.** The increasing incidence of MDR cases makes the emerging use of polymyxins (PMB and colistin). The values of MIC and MBC of colistin and colistin micelles against *P. aeruginosa* can be seen in Table 1. The concentration of 7.81  $\mu\text{g/mL}$  and 15.63  $\mu\text{g/mL}$  for MIC and MBC respectively were similar to colistin, colistin:SDCS 1:1 (F1) and 1:2 (F2). This suggested that the SDCS molecules did not affect the activity of the colistin, which resulted in a similar spectrum.

The results from the static time-kill experiment showed that the colistin micelles have similar activity in killing *P. aeruginosa* as shown in Fig. 2. The reduction of  $\pm 0.3$  Log CFU/mL per h was achieved within 24 h of observation. The colistin micelles however seem to have slightly better activity with a similar pace at the initial 12 h. These results showed that entrapped colistin in SDCS micelles did not compromise the permeability of colistin through the bacterial membrane.

Table 1. Minimum inhibitory concentration and minimum bactericidal concentration of colistin and colistin:SDCS 1:1 (F1) and 1:2 (F2) equivalent to the pure colistin, against *P. aeruginosa*. The concentration was reported in  $\mu\text{g/mL}$  (n = 3).

Sample test	<i>P. aeruginosa</i>	
	MIC ( $\mu\text{g/mL}$ )	MBC ( $\mu\text{g/mL}$ )
Colistin	7.81	15.63
F1	7.81	15.63
F2	7.81	15.63

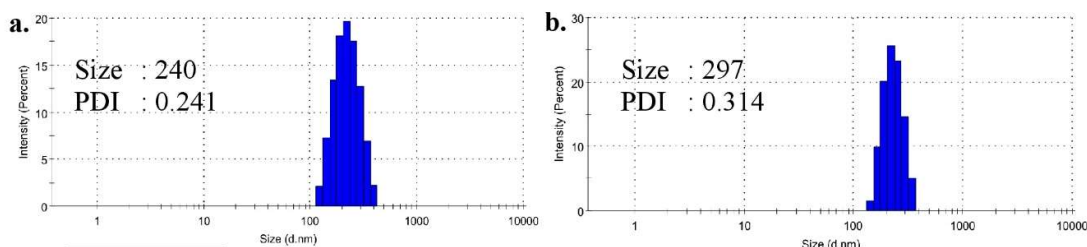


Fig. 1. Particle size and size distribution of colistin-SDCS (a) 1:1 and (b) 1:2, from DLS measurement.

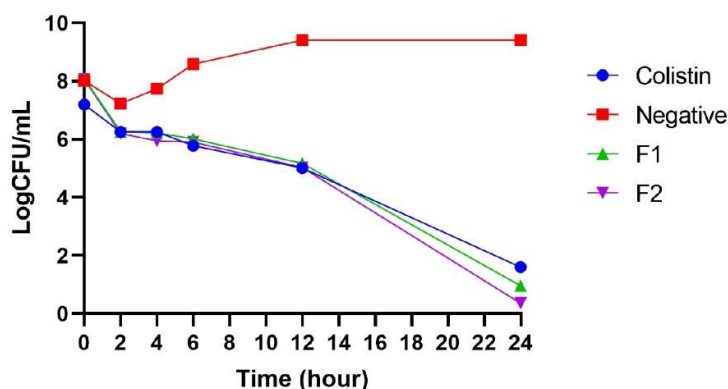


Fig. 2. Bactericidal effects of the colistin and colistin-SDCS 1:1 (F1) and 1:2 (F2) against *Pseudomonas aeruginosa*. The bacteria were subjected to 7.8  $\mu\text{g/ml}$  colistin and colistin micelles, and the number of viable cells was monitored over time. [mean  $\pm$  SD,  $n=3$ ].

**Cytotoxicity on kidney cells.** The evidence pointed out that renal injury developed in patients treated with colistin or PMB which is caused by increased permeability in tubular epithelial cells [10]. In this study, experiments were conducted to investigate the cytotoxicity of the colistin and colistin-SDCS micelles against the human kidney cell line (WT 9-12), the human kidney epithelial cell line (293T/17), and the human primary renal proximal tubule epithelial cells (PCS-400-010). Fig. 3 shows the percent viability of the cells followed by incubation with the colistin micelles and colistin free drug. The colistin SDCS micelles displayed lower toxicity in the concentration range of 1.95-1000  $\mu\text{g/ml}$ .

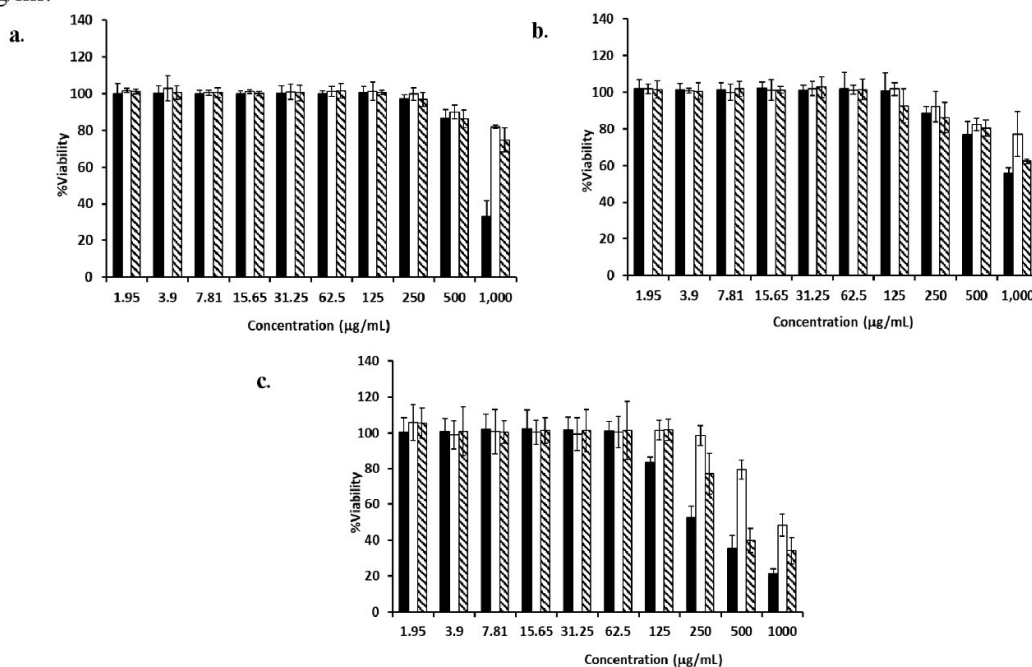


Fig. 3. Cell viability of (a) human kidney cell line WT9-12, (b) human kidney epithelial cell line 293T/17, and (c) human primary renal proximal tubule epithelial cells PCS-400-010 after 24-h incubation with colistin (■), colistin to SDCS formulation ratios of 1:1 (□) and 1:2 (▨) at various concentrations determined by MTT assay. Errors bars represent a standard deviation ( $n = 3$ ).

The F1 and F2 show significantly higher cell viability in all cell lines, while colistin had increased cytotoxicity at this concentration (<60% cell viability of 293T/17, < 50% cell viability of WT 9-12 and PCS-400-010 cells). The two human kidney epithelial cells (WT 9-12 and 293T/12) showed that colistin-SDCS micelles have improved cell viability at higher concentrations (1000 µg/ mL for WT 9-12 and >1000 µg/ mL for 293T/17) compared to pure colistin. The higher cytotoxicity of colistin was observed in human primary renal proximal tubule epithelial cells (PCS- 400-010), at 250 µg/mL colistin showed 52.3% cell viability whereas the micelle formulation has significantly higher cell viability even at higher concentration. The major nephrotoxicity of colistin takes place at the kidney's proximal tubule, that is why the higher cytotoxicity of colistin is observed in PCS- 400-010 [10]. Colistin-SDCS micelles significantly lowered cytotoxicity in the proximal tubule cells. This is in line with the previous studies which suggest SDCS minimized the cytotoxicity of amphotericin B and PMB compared with their free drug counterpart [3, 5, 7]. The work reveals that F1 has significantly higher cell viability compared to F2 with colistin at higher concentrations. The cytotoxicity reduction of colistin micelles indicates that SDCS can overcome the nephrotoxicity of colistin by forming micelles that reduce the exposure of colistin directly to the kidney cells. Also, the SDCS itself is proven to be non-cytotoxic [5]. The potential for an alternative delivery system for colistin in multi-drug resistant gram-negative bacterial infection treatment by employing it in SDCS micelle can help with the prevalent nephrotoxic problem colistin currently suffer.

### Conclusion

The present study represents the ability of SDCS in improving the biosafety profile of colistin. The colistin micelles showed that they can improve the cell viability of various kidney cell lines significantly while not compromising their antibacterial activity. These results showed the promising alternative carrier for colistin in combating its nephrotoxicity.

### References

- [1] I. Karaiskos, M. Souli, I. Galani, and H. Giamarellou, "Colistin: still a lifesaver for the 21st century?," *Expert Opin. Drug Metab. Toxicol.*, vol. 13, no. 1, pp. 59–71, 2017.
- [2] A. Ordooei Javan, S. Shokouhi, and Z. Sahraei, "A review on colistin nephrotoxicity," *Eur. J. Clin. Pharmacol.*, vol. 71, no. 7, pp. 801–810, 2015.
- [3] K. N. Gangadhar, K. Adhikari, and T. Srichana, "Synthesis and evaluation of sodium deoxycholate sulfate as a lipid drug carrier to enhance the solubility, stability and safety of an amphotericin B inhalation formulation," *Int. J. Pharm.*, vol. 471, no. 1–2, pp. 430–438, 2014.
- [4] P. Temboot *et al.*, "Potential of sodium deoxycholate sulfate as a carrier for polymyxin B: Physicochemical properties, bioactivity and in vitro safety," *J. Drug Deliv. Sci. Technol.*, vol. 58, no. May, 2020.
- [5] F. Usman, R. Khalil, Z. Ul-Haq, T. Nakpheng, and T. Srichana, "Bioactivity, Safety, and Efficacy of Amphotericin B Nanomicellar Aerosols Using Sodium Deoxycholate Sulfate as the Lipid Carrier," *AAPS PharmSciTech*, vol. 19, no. 5, pp. 2077–2086, 2018.
- [6] S. Madhumanchi, R. Suedee, T. Nakpheng, K. Tinpun, P. Temboot, and T. Srichana, "Binding interactions of bacterial lipopolysaccharides to polymyxin B in an amphiphilic carrier 'sodium deoxycholate sulfate,'" *Colloids Surfaces B Biointerfaces*, vol. 182, no. May, p. 110374, 2019.
- [7] M. Elshikh *et al.*, "Resazurin-based 96-well plate microdilution method for the determination of minimum inhibitory concentration of biosurfactants," *Biotechnol. Lett.*, vol. 38, no. 6, pp. 1015–1019, 2016.
- [8] A. L. Barry and N. C. for C. L. Standards., *Methods for determining bactericidal activity of antimicrobial agents : approved guideline*, vol. 19, no. 18. 1999.

- [9] S. J. Wallace, J. Li, R. L. Nation, R. J. Pranker, T. Velkov, and B. J. Boyd, "Self-assembly behavior of colistin and its prodrug colistin methanesulfonate: Implications for solution stability and solubilization," *J. Phys. Chem. B*, vol. 114, no. 14, pp. 4836–4840, 2010.
- [10] Z. Gai, S. L. Samodelov, G. A. Kullak-Ublick, and M. Visentin, "Molecular Mechanisms of Colistin-Induced Nephrotoxicity," *Molecules*, vol. 24, no. 3, 2019.
- [11] S. Madhumanchi, R. Suedee, S. Kaewpiboon, T. Srichana, R. Khalil, and Z. Ul-Haq, "Effect of sodium deoxycholate sulfate on outer membrane permeability and neutralization of bacterial lipopolysaccharides by polymyxin B formulations," *Int. J. Pharm.*, vol. 581, no. January, p. 119265, 2020.



**Paper 2**

Colistin Sulfate-Sodium Deoxycholate Sulfate Micelle Formulation; Molecular Interaction,  
Cell Nephrotoxicity and Bioactivity



ELSEVIER

Contents lists available at ScienceDirect

Journal of Drug Delivery Science and Technology

journal homepage: [www.elsevier.com/locate/jddst](http://www.elsevier.com/locate/jddst)

## Colistin sulfate-sodium deoxycholate sulfate micelle formulations; molecular interactions, cell nephrotoxicity and bioactivity

Muhammad Ali Khumaini Mudhar Bintang<sup>a</sup>, Varomyalin Tipmanee<sup>b</sup>, Teerapol Srichana<sup>a,\*</sup>

<sup>a</sup> Drug Delivery System Excellence Center, Faculty of Pharmaceutical Sciences, Prince of Songkla University, Hat Yai, 90110, Songkhla, Thailand

<sup>b</sup> EZ-Mol-Design Laboratory and Department of Biomedical Sciences, Faculty of Medicine, Prince of Songkla University, Hat Yai, 90110, Songkhla, Thailand

### ARTICLE INFO

#### Keywords:

Colistin  
Sodium deoxycholate sulfate  
Antibacterial  
Nephrotoxicity  
Micelles  
Molecular docking

### ABSTRACT

This study aimed to develop a micelle formulation of colistin with several mole ratios of sodium deoxycholate sulfate (SDCS) carrier to reduce its nephrotoxicity. The molar ratio and surface properties of colistin and SDCS were determined. Colistin was incorporated into SDCS micelles followed by lyophilisation. The formulated micelles were evaluated in terms of particle size, zeta potential, morphology, thermal properties, encapsulation efficiency (EE) and release profile. The interactions were analysed with FTIR, NMR and also *in-silico* studies using molecular docking. The MIC and MBC were calculated, while time-kill kinetics were observed. Furthermore, a cytotoxicity study of the formulations against kidney cells was carried out and data were analysed. Particle sizes were in the range of 140.9–162.6 nm with spherical shapes, and the zeta potential values were between –35.3 and –22.8 mV. The EE of colistin was between 17.73 and 40.15%. FTIR and DSC data indicated an interaction between the colistin and SDCS, and the NMR analysis revealed hydrogen bonding and electrostatic interaction as the main interaction. Molecular docking simulation showed that multiple hydrogen bonds were present between the hydrophilic ring of colistin and SDCS. The formulations showed good safety profiles with non-cytotoxic effects against the kidney cell while maintaining antibacterial activity. The overall results indicated that micelle formulations with SDCS can be a good option for the delivery of colistin to reduce its nephrotoxicity with better antibacterial activity, while further studies in the animal model are important.

### 1. Introduction

The emergence of multi-drug resistant (MDR) gram-negative bacteria and the lack of new antibiotics have led to the return and growing worldwide use of colistin [1,2]. Colistin (polymyxin E) is an amphipathic lipopeptide antibiotic that belongs to the polymyxin group along with polymyxin B (PMB). The drug is used as “salvage” therapy for the treatment of MDR gram-negative bacilli. Colistin sulfate and colistin methanesulfonate (CMS) are the two forms of colistin available for clinical application. CMS is synthesized by the addition of a sulfomethyl group to the primary amines of colistin and its drug form is administered parenterally, while colistin sulfate is primarily used topically [3]. However, *in vivo* conversion of CMS, the prodrug of colistin, is required for its antibacterial activity, but the risk of toxicity frequently prevents the use of high doses to achieve the maximum anti-bacterial effect [4]. The general model for the action of colistin involves the interaction of the polar face of the peptide with the polar lipid A head groups of gram-negative bacteria. Colistin selectively binds to lipid A of

lipopolysaccharides (LPS) and displaces the Mg<sup>2+</sup> and Ca<sup>2+</sup> cations on bacteria, leading to an increase in its permeability, leakage of cell contents, and cell death [5,6]. Even though colistin is one of the last lines of effective antibiotics to combat the MDR bacterial epidemic, nephrotoxicity is a particular concern with a prevalence of 33%–60.4%, which has called for safer alternatives as a replacement [7]. Colistin increases tubular epithelial cell membrane permeation, which results in cations, anions and water influx, leading to swelling of the kidney cells and cell lysis [8].

Recently, the nanotechnological approach are proven to be one of the promising techniques to incorporate in antibiotics formulation due to its potential to enhance the effectiveness of existing therapeutics through drug repurposing and other physicochemical properties [9]. Additional advantages of the nano-drug include; sustained drug release, targeted drug delivery with improved efficacy and reduction of systemic side effects compared to its free drug counterpart [10]. The use of micelles as a drug delivery system has been demonstrated to improve antibiotic effectiveness against gram-negative bacteria and reduce the

\* Corresponding author.

E-mail address: [teerapol.s@psu.ac.th](mailto:teerapol.s@psu.ac.th) (T. Srichana).

<https://doi.org/10.1016/j.jddst.2022.104091>

Received 10 August 2022; Received in revised form 25 November 2022; Accepted 17 December 2022

Available online 19 December 2022

1773-2247/© 2022 Elsevier B.V. All rights reserved.

toxicity of antimicrobial peptides [11,12]. In terms of intravenous administration of micelles, the CMC is an important factor in drug stability upon dilution. The combination of two or more distinct amphiphilic compounds to assemble mixed micelles can lower the CMC of the formulation [13]. Micelles-based that present low CMC value may resist to a greater extent from the dilution when administered intravenously. If the micelles disassemble, the drug may release rapidly and toxic effects may occur [14].

Newly synthesized sodium deoxycholate sulfate (SDCS) has been proven to effectively encapsulate and reduce the nephrotoxicity of amphotericin B (AmB) and PMB [15,16]. It has been reported that the AmB incorporated into SDCS when compared to the commercial formulation that used sodium deoxycholate (Fungizone®), showed more stable micelle formation with less toxicity compared to the pure drug [15,17]. The SDCS also enhanced the stability of PMB as a micelle formulation. The formulation showed a sustained release profile and reduced the haemolytic effect on erythrocytes and lowered the toxicity to kidney cells without affecting the antimicrobial activity [18]. Research has shown the effects of SDCS on the LPS. The PMB-SDCS formulations were prone to release PMB for easy penetration into the lipid membrane or micelles and caused disruption of the complex LPS micelles or membrane and neutralized it with minimal toxicity [19]. Considering its ability to reduce nephrotoxicity caused by AmB and PMB, SDCS holds promise to address nephrotoxicity using similar antibiotics. Although colistin is well-known for its potent antimicrobial activity, the drug is also nephrotoxic as mentioned earlier. It is expected that the micellar formulation of colistin-SDCS could modulate the associated nephrotoxicity of colistin. Therefore, this current research aimed to investigate the compatibility of colistin with SDCS toward the development of a safe and effective antimicrobial colistin-SDCS micelle formulation. Against this drawback, the interaction between SDCS and colistin was analysed by examining the surface charge. Furthermore, details of the binding site interactions were elucidated *in silico* via molecular docking. The physicochemical properties of the resulting formulation were evaluated via Fourier transform infrared (FTIR) spectroscopy, and by dynamic light scattering (DLS), zeta potential, <sup>1</sup>H, and <sup>13</sup>C NMR analyses. The antimicrobial properties of the formulation were also analysed and the toxicity against kidney cells was measured.

## 2. Materials and methods

### 2.1. Materials

Colistin sulfate and deoxycholic acid were purchased from Sigma-Aldrich (St. Louis, MO, USA). Sodium deoxycholate sulfate was synthesized in-house [15]. Sodium dihydrogen phosphate and disodium hydrogen phosphate were obtained from Ajax Finechem Pty Ltd, NSW, Australia. Acetonitrile and methanol were purchased from Labscan Asia (Bangkok, Thailand). Dimethylsulfoxide was purchased from Riedel-de Haën, Seelze, Germany. Polyamide membranes with the pore size of 0.22 µm and 0.45 µm were obtained from Sartorius (Göttingen, Germany). All chemicals, except tetrahydrofuran, were used as received without further purification. All other reagents and chemicals were of analytical grade.

### 2.2. Synthesis of sodium deoxycholate sulfate

Sodium deoxycholate was synthesized following the methods used by Ref. [15]; involving esterification, reduction, and sulfation of the base material, i.e. deoxycholic acid. The esterification step was done by reacting deoxycholic acid with sulfuric acid and methanol under reflux for several hours while monitoring the reaction with thin-layer chromatography (TLC) until methyl deoxycholate was produced. The resulting material was then reduced to its corresponding alcohol by using sodium borohydride and tetrahydrofuran under reflux while adding methanol for 8 h. Thereafter, hydrochloric acid was added. This

was followed by column chromatography to separate the pure substance. The last step involved deoxycholic alcohol sulfation by dissolving with dimethylformamide and dichloromethane under reflux, then adding sulphur trioxide pyridine complex and saturated sodium bicarbonate during the reaction. The resulting substance was then purified using column chromatography and TLC. All these steps were controlled using TLC and FTIR to confirm the completion of the reactions.

### 2.3. Surface tension and critical micelle concentration (CMC) determination

The surface tensions of SDCS and colistin in an aqueous solution and phosphate buffer (pH 7.4) were measured with a pendant drop tensiometer (OCA 15 EC; DataPhysics Instruments, Filderstadt, Germany). The dropped image acquired by the digital camera was processed by a software module (SCA 22; DataPhysics Instruments, Filderstadt, Germany) to subsequently analyze the image. The surface tension of colistin and SDCS was measured at different concentrations (2–500 mg/L) to determine its critical micelle concentration (CMC) by observing the change in the surface tension.

### 2.4. Size and surface charge of colistin in SDCS via titration

A 10 mL SDCS solution (80 mg/L CMC) was prepared by adding 0.8 mg SDCS and 10 mL of injection water in a small Erlenmeyer flask. The mixture was stirred with a magnetic stirrer at 250 rpm for 10 min to dissolve the solids into a solution. The size and zeta potential of the lipid solution were then measured using DLS (Zetasizer, Malvern, UK) by sampling 1 mL of the solution and transferring it to a suitable cuvette for measurement. The aqueous solution of colistin (2 mg/mL) was filtered through a 0.45 µm membrane filter and transferred into a titration burette. The colistin solution was then titrated 1 mL at a time to the SDCS solution while it was stirred continuously with a magnetic stirrer (250 rpm). The same measurements were also carried out with each 1 mL of colistin added to the SDCS solution. The measurements were carried out until 20 mL of colistin was added to the SDCS. By recording the zeta potential and particle size for each addition of colistin, the optimum ratio for colistin-SDCS micelle formulation was determined by monitoring the trend of the graph that showed better stability in terms of size and zeta potential.

### 2.5. Preparation of colistin-SDCS dry powder formulations

The formulations were prepared using a mixture of colistin sulfate and SDCS at a 1:1 to 1:5 molar ratio (selected from pre-formulation done in section 2.4.) in Milli-Q water (30 mL). The mixture was stirred until complete dissolution. To this solution, sodium hydroxide solution (2.7 mL, 0.2 M) was added slowly, dropwise, at room temperature to obtain a clear solution. The pH of the solution was about 9.5, which was adjusted to 7.4 using phosphoric acid (0.2 M) for an *in-situ* phosphate buffer. The final volume of the solution was made to 50 mL by adding deionized water. The solution was lyophilised, and the dry powder was subsequently reconstituted in water for further studies.

### 2.6. Particle size and zeta potential

The mean diameter and zeta potential of the colistin formulation were measured using DLS (Zetasizer NanoZS, Malvern, England). The colistin sample was prepared in double-distilled water at a final concentration of 1 mg/mL then the sample was centrifuged for 5 min at 10000 rpm before being pipetted into a cuvette. The cuvette used for particle size was a standard cell, and for zeta potential, the folded capillary cell was employed. The measurement was carried out at a fixed angle of 173° at 25 °C.

## 2.7. Transmission Electron Microscopy

**Transmission Electron Microscopy (TEM, JEM-2100, JEOL Japan)** was employed to examine the morphology of the reconstituted colistin formulation. Colistin and SDCS (2 mg) at molar ratios of 1:1 and 1:2 were reconstituted with 2 mL of filtered milliQ water. The obtained solution (10 µL) was dropped on a copper grid, stained with phosphotungstic acid and dried at room temperature for 30 min before observation under the TEM. The data and image produced were used to directly measure nanoparticle size and morphology.

## 2.8. Differential scanning calorimetry (DSC)

A differential scanning calorimeter (DSC, PerkinElmer) was used to obtain the thermal properties of the samples. Approximately 4–5 mg of the sample was accurately weighed and placed into standard aluminium pans, which were hermetically sealed. An empty pan was used as a reference. The sample was heated from 25 to 200 °C at a constant heating rate of 10 °C/min and then cooled to 25 °C.

## 2.9. Fourier transform infrared (FTIR) spectroscopy

The FTIR spectra of colistin and SDCS-colistin dry powders were recorded on a PerkinElmer FTIR spectrometer (USA) in the range of 400–4000 cm<sup>-1</sup> by 120 scans with a resolution of 4 cm<sup>-1</sup>. KBr powder which was used as the carrier for the samples. Each sample was pressed with hydraulic pressure to produce a thin film before the measurement at ambient temperature. All formulations were scanned as well as SDCS and colistin for comparison.

## 2.10. Determination of colistin sulfate by HPLC

The quantification of colistin sulfate was conducted by high-performance liquid chromatography (HPLC) adapted from Cancho Grande et al. [20] and using a Waters 1525 HPLC Binary Pump, Waters 2487 UV-detector, and Waters 717 plus autosampler (Waters Corp., Milford, MA, USA). The system was controlled by the Empower software. The column selected was a Novapak C18 × 150 mm with a 4-µm particle size stationary phase. The mobile phase consisted of an aqueous solution (77%) and acetonitrile (33%). The aqueous phase was prepared by dissolving 7.1 g of sodium sulfate, 0.6 g of acetic acid, and 2.2 g of phosphoric acid, adjusted to pH 2.5 with triethylamine and made up to 1 L with water. The flow rate was set at 1.5 mL/min for isocratic elution and the sample injection volume was 50 µL. The standard curve was prepared using colistin (500–50 µg/mL). The absorption of colistin sulfate was measured at 215 nm and 50 µg/ml polymyxin B sulfate was used as an internal standard. This analytical technique was validated following the European Medicines Agency guide for bio-analytical methods [21].

## 2.11. Encapsulation efficiency

Non-entrapped colistin sulfate was determined from the supernatants collected after centrifugation at 90,000 rpm for 15 min. The amount of non-encapsulated drug was detected using HPLC. The supernatant samples were diluted to 10 mL and compared to a calibration curve (5–80 µg/mL). The encapsulation efficiency (EE) was calculated by the following equation.

$$EE(\%) = 100 \times \left( \frac{\text{initial amount of drug} - \text{non encapsulated drug}}{\text{initial amount of drug}} \right) \quad (1)$$

## 2.12. Colistin formulation release profile

The release profile of colistin formulations was determined within 30 min. The experiment was carried out in the 50 ml glass tube placed in

a 500 ml beaker. The bar magnet was equipped and run at 75 rpm to circulate the dissolution medium and control the dissolution medium temperature at 37 °C in the water bath. The two dissolution medium used were 5 ml of Milli-Q water and 5% dextrose, respectively. The colistin and colistin formulations equal to colistin 1 mg of F1, F2, F3, F4, and F5 were gently tapped into the dissolution medium. At 0, 1, 3, 5, 10, 15, 20, 25, and 30 min, the 200 µl of the sample was collected for colistin analysis and replaced with an equal volume of the fresh medium. The amount of colistin was determined using the previously mentioned HPLC methods. All analytes were filtered with 0.45 µm nylon syringe filters and determined in triplicates. The cumulative release of colistin was calculated and plotted against time.

## 2.13. Nuclear magnetic resonance (NMR) spectroscopy

The <sup>1</sup>H NMR and <sup>13</sup>C NMR spectra were acquired on Varian Unity Inova 500 spectrometer at 500 MHz (Varian, Germany). All the NMR spectra were recorded at 298 K using deuterium oxide (D<sub>2</sub>O) as a solvent. The results were analysed using MestReNova software by analysing every peak and multiplet and comparing it with NMR spectrum prediction from ChemDraw software. Comparisons were performed between the data obtained for colistin and micelle formulations.

## 2.14. Binding interaction by molecular docking

The molecular dockings were carried out to analyze the binding interaction between SDCS and colistin. First, the 3D structure of colistin was obtained from the Chempider site. The "mol" file obtained from the site was then converted to a protein database file (.pdb) using the online SMILES translator site. SDCS was drawn from the deoxycholic acid structure (ChemSpider) taken as a starting point using Arguslab software where the structure's geometry was optimized and saved as a protein database (.pdb) file. The pdb file was converted to pdbqt (a molecule with partial charges and atom type) using the autodock tools script for ligand (SDS and SDCS) and receptor (polymyxins). The ligand and receptor files were then loaded on AutoDockTools software to prepare a grid parameter file (.gpf). This involved setting up a grid box with a size of 60 × 60 × 60 Å around the receptor. The docking parameter file (.dpf) was prepared by setting up the number of samples to 200 (population size) and setting up the number of runs to 50 on the Genetic Algorithm (GA) search parameter and using Lamarckian GA as an output. The docking was then processed in autodock tools using the pdbqt file of receptor and ligand, grid parameter file, and docking parameter file, to produce the docking log file (.dlg). The result files were then analysed and converted into another pdb for further docking with SDCS which then adjust the grid box to produce another binding position for SDCS.

## 2.15. Minimum inhibitory concentration (MIC) and minimum bactericidal concentration (MBC) determinations

Colistin-SDCS formulations and free colistin sulfate were tested against *Pseudomonas aeruginosa* bacteria strains. The colistin-SDCS formulations were resuspended in brain heart infusion (BHI) broth and placed in the first row of 96-well plates. Next, starting from 125 µg/mL of the antimicrobial agent, decreasing concentrations of the formulations were obtained by two-fold serial dilutions. The test bacteria were then cultured on a BHI agar plate at 37 °C for 24 h. The number of bacteria in liquid suspension was estimated by analysing the turbidity in the BHI medium using the 0.5 McFarland standard (1 × 10<sup>8</sup> CFU/mL) by measuring absorbance at 600 nm. An amount of 10 µL of the bacteria suspension was pipetted into a 96-well plate for an inoculation period of 18 h at 37 °C. Each well was inoculated by approximately 1.0 × 10<sup>5</sup> CFU/mL. After the incubation time, 30 µL of 0.02% resazurin sodium salt in phosphate buffer solution was added and incubated for 3 h. The minimum inhibitory concentration (MIC) was defined as the lowest antibiotic concentration that can prevent visible bacterial growth. The

minimal bactericidal concentration (MBC) was then determined by subculturing the samples having a value equal to MIC and higher than MIC. The samples were transferred from the 96-well plates into freshly prepared tryptic soy agar plates and incubated at 37 °C for 18 h. MBC was defined as the lowest concentration at which no single bacterial colony grew.

#### 2.16. Static time-kill experiment

The static time-kill experiment was conducted to examine the killing rate of colistin-SDCS against the test organism using BHI as the medium. All experiments were performed with an initial inoculum of  $10^6$  CFU/mL in 20 mL of BHI. The tested drug concentrations were based on the previous MIC results, which were MIC,  $2 \times$  MIC, and  $4 \times$  MIC. Samples (50  $\mu$ L) were collected at 0, 1, 3, 6, and 24 h, centrifuged at 12000g for 10 min, and cell pellets were resuspended in 0.9% saline and diluted accordingly for viable counting on nutrient agar plates. The limit of detection was 20 CFU/mL (equivalent to one colony per plate). A colony counter was used to quantify bacteria after 24 h of incubation at 37 °C.

#### 2.17. Cytotoxicity assay using kidney cells

The 3-(4,5-dimethylthiazol-2-yl)-2,5-diphenyl-2H-tetrazolium bromide MTT assay was used to examine the sample cytotoxicity on human kidney epithelial cell lines WT9-12 and 293T/17, and primary renal proximal tubule epithelial cells (PCS-400-010). The kidney cells were

passed and distributed in 96-well plates at a density of  $1 \times 10^5$  cells/well in 100  $\mu$ L of complete Dulbecco's Modified Eagle Medium and allowed to attach overnight at 37 °C and 5% CO<sub>2</sub> with 95% relative humidity. After 24 h, the medium (100  $\mu$ L) was replaced with a medium containing various concentrations of the different formulations of colistin-SDCS (1.95–1000  $\mu$ g/mL) and equivalent concentration of colistin. After incubation for 24 h, 50  $\mu$ L (1.25 mg/mL) of MTT was added and further incubated for 4 h at 37 °C in 5% CO<sub>2</sub> and 95% humidity. The solutions were removed from the 96-well plates, and 100  $\mu$ L of DMSO was added to dissolve formazan crystals. The optical density (OD) was measured at 570 nm using a microplate reader. The percentage of surviving cells was calculated from the following formula:

$$\% \text{ Viability} = (\text{OD}_{\text{treated}} / \text{OD}_{\text{control}}) \times 100 \quad (2)$$

The number of viable cells in the treated wells was compared to those in the untreated wells and estimated as % viability.

#### 2.18. Statistical analysis

All experiments were performed in triplicate, and the data were represented as mean  $\pm$  SD. Statistical analysis was done using GraphPad Prism version 6.00 for Windows (GraphPad Software, La Jolla, CA, USA, [www.graphpad.com](http://www.graphpad.com)). One-way analysis of variance (ANOVA) and Dunnett's post-hoc test were used to analyze the statistical significance for multiple groups and Student's t-test was used to analyze the statistical significance between two groups, and a significance level (*p* values)

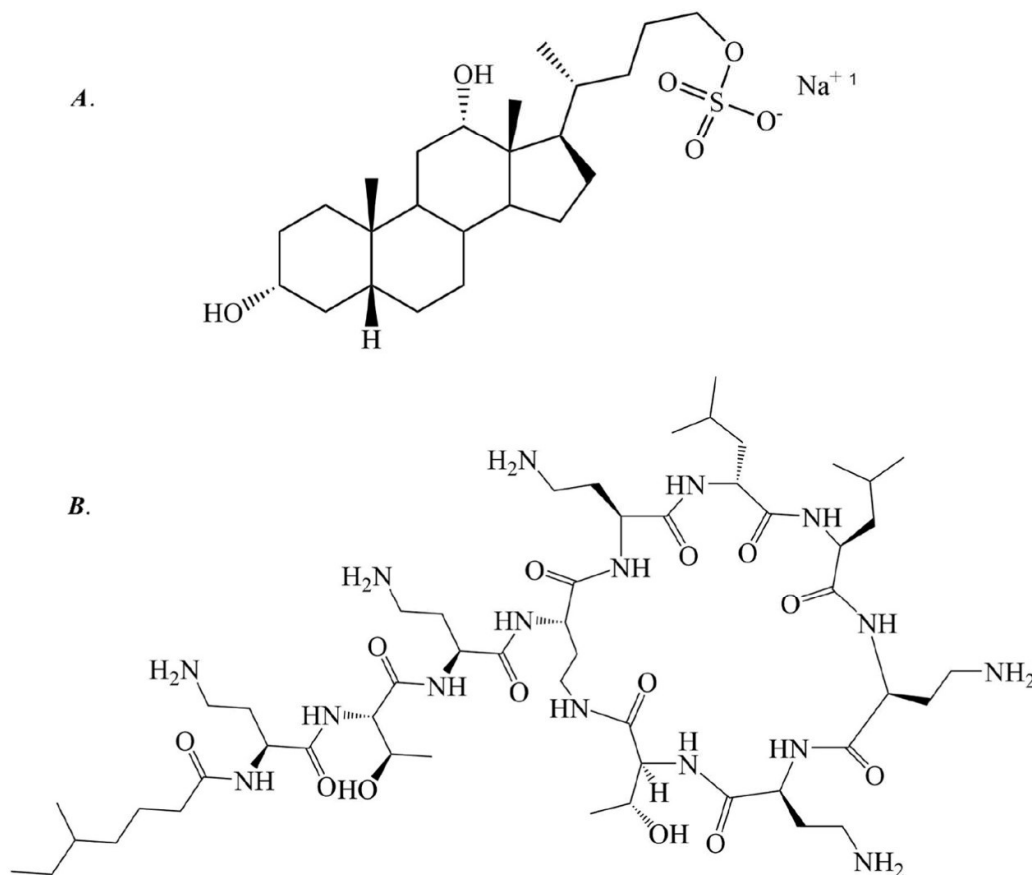


**Fig. 1.** Chemical structures of (A) sodium deoxycholate sulfate and (B) colistin. Colistin A has a 6-methyl-octanoic acid as the fatty acid moiety. In the case of colistin B, the fatty acid is 6-methyl-heptanoic acid.

of  $<0.05$  was considered statistically significant.

### 3. Results and discussion

SDCS consists of a rigid steroid backbone with a hydrophobic and hydrophilic face to which a short and flexible tail is attached in Fig. 1A [22,23]. In this study, the SDCS was synthesized from deoxycholic acid by three-step processes. The surfactant was compared with previously synthesized SDCS in terms of its  $R_f$  value and FTIR spectra [15]. Extensive characterizations were performed to obtain colistin (Fig. 1B) with SDCS as a micelle formulation with desirable attributes.

#### 3.1. Surface properties of SDCS and colistin

Several parameters were carefully considered to determine the optimal ratio for proper formulation development. Amongst these were the CMC value from the surfactant and also colistin considering its self-assembly properties [24]. The surface and micellar properties of a variety of surfactant mixes in bulk aqueous solutions are commonly determined by measuring surface tension at the air-water interface. The addition of surfactant molecules causes the surface tension values to progressively decrease. After saturation at the air-water interface, the surface tension remains virtually constant. Furthermore, they produce micelles in the solution, and the CMC is the concentration at which micelles form. When colistin dissolved in water, colistin lowered the water surface tension from  $72.7 \text{ mN/m}$  to  $69.97 \pm 1.06 \text{ mN/m}$  and dropped to  $66.73 \pm 0.11 \text{ mN/m}$  at saturation point. For colistin, the CMC was formed at  $25 \text{ mg/L}$  in water and phosphate buffer solution acquired from the plots of surface tension ( $\gamma$ ) versus concentration in

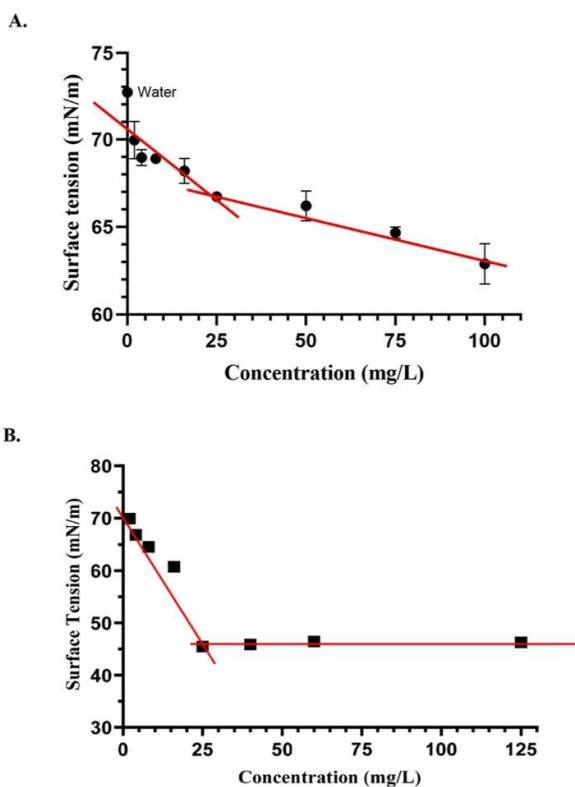


Fig. 2. Surface tension versus concentration of the colistin in (A) water and (B) PBS at  $25^\circ\text{C}$ . Both indicated a critical micelle concentration of around  $25 \text{ mg/L}$  (mean  $\pm$  SD,  $n = 3$ ).

Moreover, SDCS as a surfactant with hydroxyl groups has lower CMC at  $8 \text{ mg/L}$  in water [25]. The mixed micelles produced by the solubilization of two amphiphilic molecules can even produce lower CMC which may affect the formulation stability *in-vitro* or drug safety *in-vivo* [26]. Nonetheless, colistin is a mixture of two major molecules with identical head groups but having fatty acyl tails of different lengths. This unique structural composition is likely to impart slightly different surface properties, making elucidation of a precise CMC necessary from batch to batch [27].

#### 3.2. Size and zeta potential of colistin and SDCS via titration

SDCS was employed to dissolve colistin; after initial titration, there was an increase in particle size ( $766.87 \text{ nm}$ ). Further addition of colistin into the mixture decreased the particle size ( $367.33 \text{ nm}$ ) and this size remained relatively stable without any substantial increase (Fig. 3). This suggests that the interaction of colistin with SDCS does not trigger aggregation. However, the lipid solution required a short period to disperse during mixing which was evidenced by the larger particle size following the initial addition. The initial value of the zeta potential of the SDCS was  $-35.3 \text{ mV}$ . After the addition of  $2 \text{ mL}$  of colistin, the zeta potential continued to increase with further addition of colistin until it was virtually stable at around a colistin/SDCS ratio of  $0.13\text{--}0.2$ . The increase in the zeta potential can be linked to the properties of colistin itself as a cationic drug.

#### 3.3. Particle size, morphology, and zeta potential of colistin and SDCS micelles

Particle size and zeta potential were measured using DLS instrumentation. Table 1 shows the mean particle size and zeta potential of all formulations obtained after reconstitution in distilled water. The mean particle sizes of the reconstituted colistin formulations were  $141.9 \pm 1.9$ ,  $140.9 \pm 1.2$ , and  $162.6 \pm 1.4 \text{ nm}$  for F1, F2, and colistin, respectively. Very similar particle size was observed with F1 and F2. Pristine colistin exhibits a larger particle size in comparison with F1 and F2, which could be due to the association of colistin with SDCS micelles. The size and morphology of colistin-SDCS micelles are presented in Fig. 4 with spherical shape and particle size around  $100\text{--}200 \text{ nm}$ . Several particles are clustered in formation and aggregate form. The F1 showed a smaller size and less uniform shape when compared to F2 which showed a larger size observed. Several studies have shown that the self-assembly of polymyxins (colistin and PMB) in aqueous solutions can result in aggregated forms, which explains higher particle size ( $162 \text{ nm}$ ) and polydispersity index ( $0.218 \pm 0.04$ ) [24]. The zeta potential of colistin sulfate was found to be  $5.21 \pm 0.15 \text{ mV}$ . In contrast, the colistin formulations F1 and F2 showed zeta potentials of  $-22.8 \pm 0.15$  and  $-23.4 \pm 0.62 \text{ mV}$  respectively, suggesting that the SDCS carrier managed to increase significantly, the net negative zeta potential value in the colistin formulations. This, in turn, increases the electrostatic repulsion between the particles, thereby preventing aggregation.

#### 3.4. Differential scanning calorimetry of colistin-SDCS dry powders

DSC analysis represents the change in thermal behaviour pertaining to the interaction between the drug and excipient during formulation. The DSC curves show the thermograms corresponding to colistin, the physical mixture of colistin-SDCS, and colistin-SDCS micelles (Fig. 5). The thermogram of colistin displayed an endothermic peak at  $234^\circ\text{C}$  for both colistin and the physical mixture of colistin-SDCS (Fig. 5A and B). The characteristic of colistin in the physical mixture was lower endothermic peak due to the dilution effect of colistin by SDCS. Whereas the colistin-SDCS micelles showed a broad endothermic peak at  $239^\circ\text{C}$ . The difference in the endothermic peak position of the micelles might indicate colistin interaction with SDCS as well as the more amorphousness of colistin in SDCS micelles after lyophilisation. The hydrogen bonds or

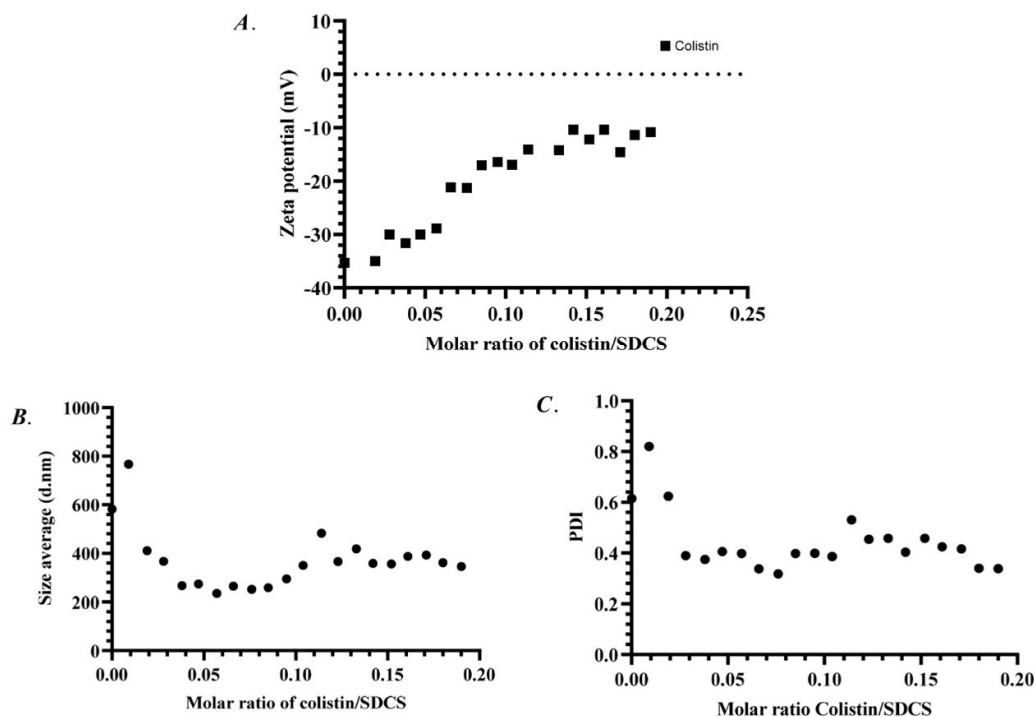


Fig. 3. The molar ratio of colistin/SDCS versus (A) zeta potential, (B) size average, and (C) polydispersity index via titration at 25 °C (mean, n = 3).

Table 1

Particle size and zeta potential of colistin micelle formulations, colistin, and SDCS from dynamic light scattering measurements (mean  $\pm$  SD, n = 3).

Formula	Particle size (nm)	Zeta potential (mV)	Polydispersity index
F1 <sup>a</sup>	141.9 $\pm$ 1.9	-22.79 $\pm$ 0.15	0.178 $\pm$ 0.015
F2 <sup>b</sup>	140.9 $\pm$ 1.2	-23.37 $\pm$ 0.62	0.173 $\pm$ 0.017
Colistin	162.6 $\pm$ 1.4	5.21 $\pm$ 0.15	0.218 $\pm$ 0.04
SDCS	142.4 $\pm$ 1.6	-33.77 $\pm$ 3.91	0.156 $\pm$ 0.02

SDCS, sodium deoxycholate sulfate.

<sup>a</sup> Molar ratio of colistin to SDCS was 1:1.

<sup>b</sup> Molar ratio of colistin to SDCS was 1:2.

electrostatic interactions can be responsible for the difference in endothermic peak due to the SDCS containing hydroxyl and sulfate functionalities that can interact in the aqueous medium [19].

### 3.5. Fourier transform infrared (FTIR) spectroscopy of colistin-SDCS dry powders

The FTIR spectra of colistin formulations are shown in Fig. 6. The characteristic FTIR absorbance peaks were identified for colistin. They were well-defined bands with relatively high intensities at several wave numbers. The FTIR spectrum of colistin featured bands at 3282  $\text{cm}^{-1}$  for N-H stretching, 3060 and 2960  $\text{cm}^{-1}$  for O-H stretching, 1660  $\text{cm}^{-1}$  for C=O stretching, and 1095  $\text{cm}^{-1}$  for C-O stretching. Comparing these data with the colistin-SDCS formulation indicates the existence of a colistin characteristic peak in the spectrum of the formulation, which underscored the successful loading of colistin in the micelles. The remarkable characteristic of the FTIR spectra of the colistin formulations was the shift of C=O stretching from 1644 to 1655  $\text{cm}^{-1}$ . The shift might come from the hydrogen bonding between the hydroxyl group of SDCS and the C=O adjacent to diaminobutyric acid (Dab) or D-leucine (D-Leu). There is also a significant shift of the C-O band of either colistin or SDCS in 1095–1128  $\text{cm}^{-1}$  to 1147  $\text{cm}^{-1}$  which confirms the hydrogen bond through the hydroxyl group of SDCS. The shift in the micelle's

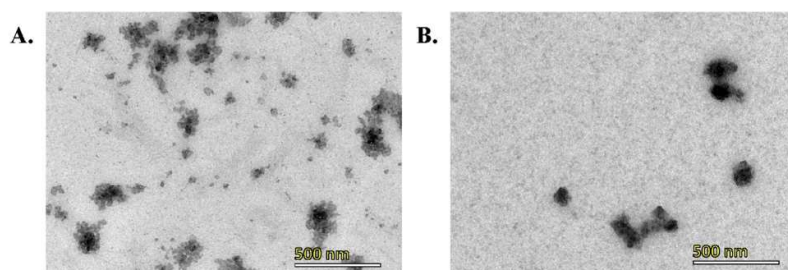


Fig. 4. TEM photograph of colistin-SDCS micelle ratio (A) 1:1 and (B) 1:2.

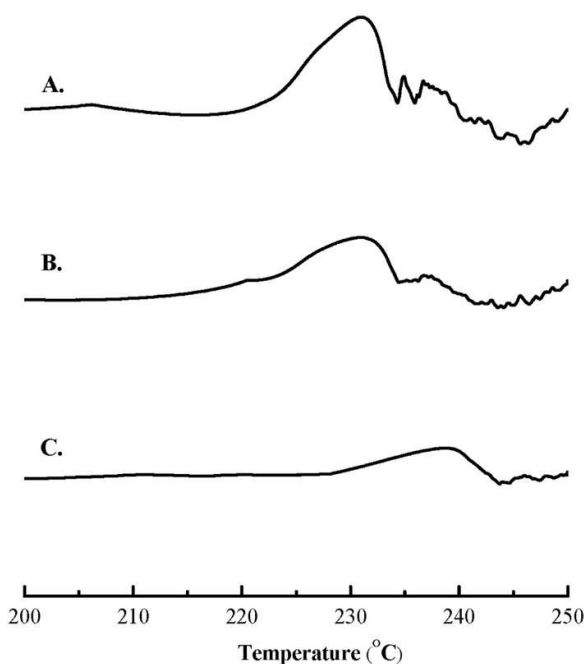


Fig. 5. DSC thermogram of (A) colistin, (B) physical mixture of colistin and SDCS, and (C) freeze-dried colistin-SDCS.

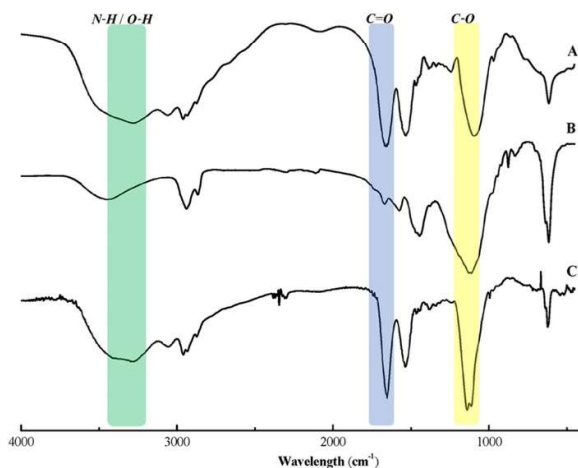


Fig. 6. FTIR spectra of (A) colistin, (B) SDCS, and (C) colistin-SDCS micelle.

formulation spectrum indicated the presence of intermolecular interactions between the amide groups of colistin and the C–O functional group of the SDCS, which presumably was due to the –OH and ether groups, but the interaction did not change the functional group of colistin from the existence of characteristic peak present which also confirmed by our NMR data.

### 3.6. Encapsulation efficiency of colistin in SDCS

HPLC was used for the determination of encapsulation. The selectivity of colistin on HPLC needed to be determined for the colistin content calculation on the micelles. Colistin A (Polymyxin E<sub>1</sub>) was

chosen as a standard for colistin content determination and polymyxin B<sub>1</sub> as an internal standard. The EE values of the colistin-SDCS micelle formulations from five ratios were ascertained. The EE was found to be  $70.0 \pm 3.2$ ,  $71.9 \pm 2.4$ ,  $73.4 \pm 3.3$ ,  $75.7 \pm 1.6$ , and  $76.4 \pm 4.1\%$  for colistin:SDCS molar ratio 1:1, 1:2, 1:3, 1:4, and 1:5, respectively (Table 2). The results correlate with how entrapped colistin driven by electrostatic interaction was readily released upon dilution [27]. The encapsulation efficiency seems to increase with an increase in the amount of SDCS in the formulation. The higher amount of SDCS micelle in the formulation increased the efficiency of colistin to associate with SDCS resulting in a higher %EE.

### 3.7. Release profile of colistin formulation

Colistin undergoes extensive renal tubular reabsorption and its clearance is mostly non-renal mechanisms [28]. The dose and duration of therapy are important factors to take into action to minimize the toxicity associated with colistin [29]. In this study, the colistin cumulative release was plotted against time as shown in Fig. 7. Colistin formulation showed slower release in dissolution medium than colistin standard. Colistin only releases in water exhibited higher initial release at 0 min with  $49.95 \pm 4.19\%$  and continued to increase until the plateau phase reached within 5 min ( $93.8 \pm 3.34$ ). colistin-SDCS showed lower initial release at 0 min with  $29.51 \pm 1.81\%$ ,  $28.78 \pm 3.31\%$ ,  $27.17 \pm 2.1\%$ ,  $27.01 \pm 3.15\%$ , and  $26.13 \pm 0.77\%$  for F1, F2, F3, F4, and F5, respectively. F5 showed the slowest release where the cumulative release reached the plateau phase at 20 min, whereas F1, F2, F3, and F4 reached maximum release at 15 min. At 30 min, the cumulative release for colistin formulations was  $96.75 \pm 3.61\%$ ,  $95.73 \pm 2.66\%$ ,  $90.26 \pm 1.97\%$ ,  $88.91 \pm 1.87\%$ , and  $88.44 \pm 2.11\%$  for F1, F2, F3, F4, and F5, respectively. As high as 88–97% of colistin released in water within 30 min, compared to  $99.79 \pm 4.28\%$  with standard colistin. As for the colistin release in 5% dextrose, the release profile showed similar to that in water but slightly lower release over time. The slower release of F2 formulation was observed in 5% dextrose ( $p$ -value < 0.01) in comparison to that in water ( $p$ -value < 0.05). The higher ratio of SDCS in formulations contributed to slower release of colistin due to the trapped colistin inside the micelles. The slower release can mediate lower exposure to related cell associated with colistin toxicity.

### 3.8. Nuclear magnetic resonance (NMR) spectroscopy of colistin and colistin-SDCS

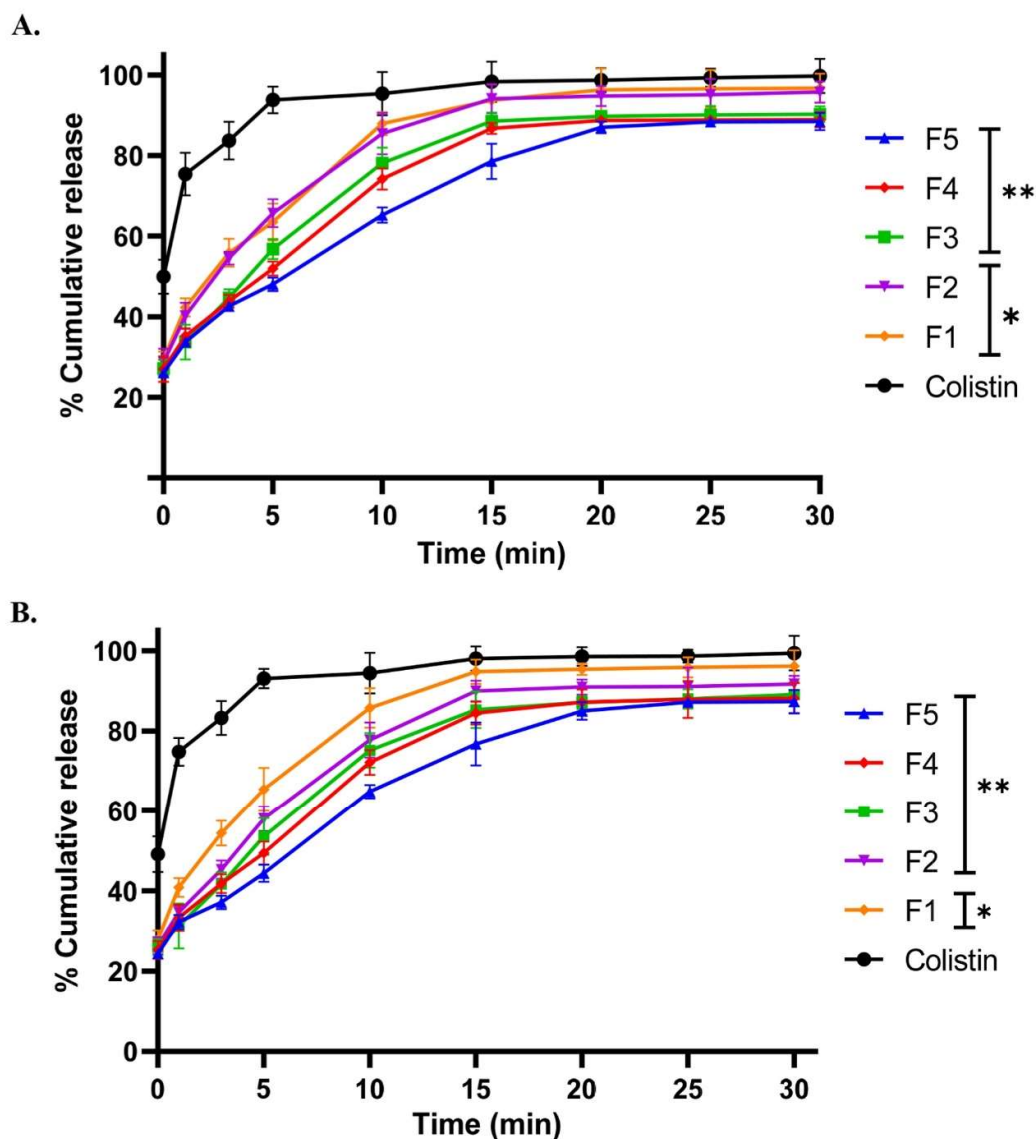
Fig. 8A shows the <sup>1</sup>H-NMR spectrum of colistin, which is a consistent chemical shift according to the spectrum prediction of colistin. Several peaks were observed, many of which were rough in shape, along with multiplets arising from the mixture of colistin A, colistin B, and other minor analogues such as colistin C, D, and E. The spectrum of the colistin-SDCS formulations (Fig. 8C and D) showed a similar pattern of colistin with the SDCS peak (Fig. 8B), and the characteristics are listed in Table 3. A slight decrease in the chemical shift of the formulations, particularly at 1.51 and 1.82 ppm can be attributed to intermolecular hydrogen bonding between –OH or –NH of the peptide ring of colistin, in which the peak of the corresponding functional groups was deshielded

Table 2  
Percent encapsulation efficiency of colistin in different ratios of colistin to SDCS formulations (mean,  $\pm$ SD  $n = 3$ ).

Formulation (molar ratio)	Colistin concentration ( $\mu$ g/mL)	% Encapsulation efficiency
F1 (1:1)	122.7	$70.0 \pm 3.2$
F2 (1:2)	81.8	$71.9 \pm 2.4$
F3 (1:3)	65.4	$73.4 \pm 3.3$
F4 (1:4)	47.4	$75.7 \pm 1.6$
F5 (1:5)	41.6	$76.4 \pm 4.1$

SDCS, sodium deoxycholate sulfate.





**Fig. 7.** The colistin release profile from colistin standard and colistin-SDCS formulations at 37 °C in (A) water and (B) dextrose 5% (mean  $\pm$  S.D.,  $n = 3$ ). The star(s) represent statistical differences from colistin (\* =  $P < 0.05$  and \*\* =  $P < 0.01$ ).

in several multiplets. The  $^{13}\text{C}$  NMR spectrum of colistin is shown in Fig. 8E. It indicates 57 carbon atoms which are also attributed to other analogues of colistin, which have longer fatty acid chains whereas colistin A contains only 53 carbon atoms. The spectra of F1 and F2 (Fig. 8F and G) formulations have only 55 and 53 peaks, respectively, which indicates that the interaction between colistin and SDCS results in overlapping peaks in the spectrum.

### 3.9. Molecular interaction by molecular docking of colistin and SDCS

AutodockTools was used to identify the binding sites of colistin and SDCS. The grid acts as a search space for the binding sites and also as an inert solvent. The docking results showed that SDCS binds to alpha-amino acid at the L-Dab of colistin via hydrogen bonding (Fig. 9A). The results are in line with the fact that the binding sites of colistin

appear to come from its hydrophilic-heptapeptide ring (Fig. 9B). The number of binding sites might be two or more, which are from the L-Dab site on the heptapeptide ring. Molecular docking was done using several SDCS as ligands starting from 1 to 10 molecules docked on colistin. The results show that the binding affinity of SDCS was higher at 1 and 2 molecules with binding scores of  $-7.5 \pm 0.07$  and  $-7.65 \pm 0.03$  kcal/mol, respectively and slowly increased. At the addition of the 7th molecule, the binding score seemed to be constant (Table 4). This was possible because after 6 molecules SDCS tends to bind to other SDCS molecules intermolecularly. The results are in line with the interaction results from NMR and FTIR, which attest to the molecular interaction between colistin and SDCS. SDCS bound to the hydrophilic peptide ring of colistin through hydrogen bonding and electrostatic interaction. At the concentration above CMC, the positive charge colistin and negatively charged SDCS were bound through electrostatic interaction, while

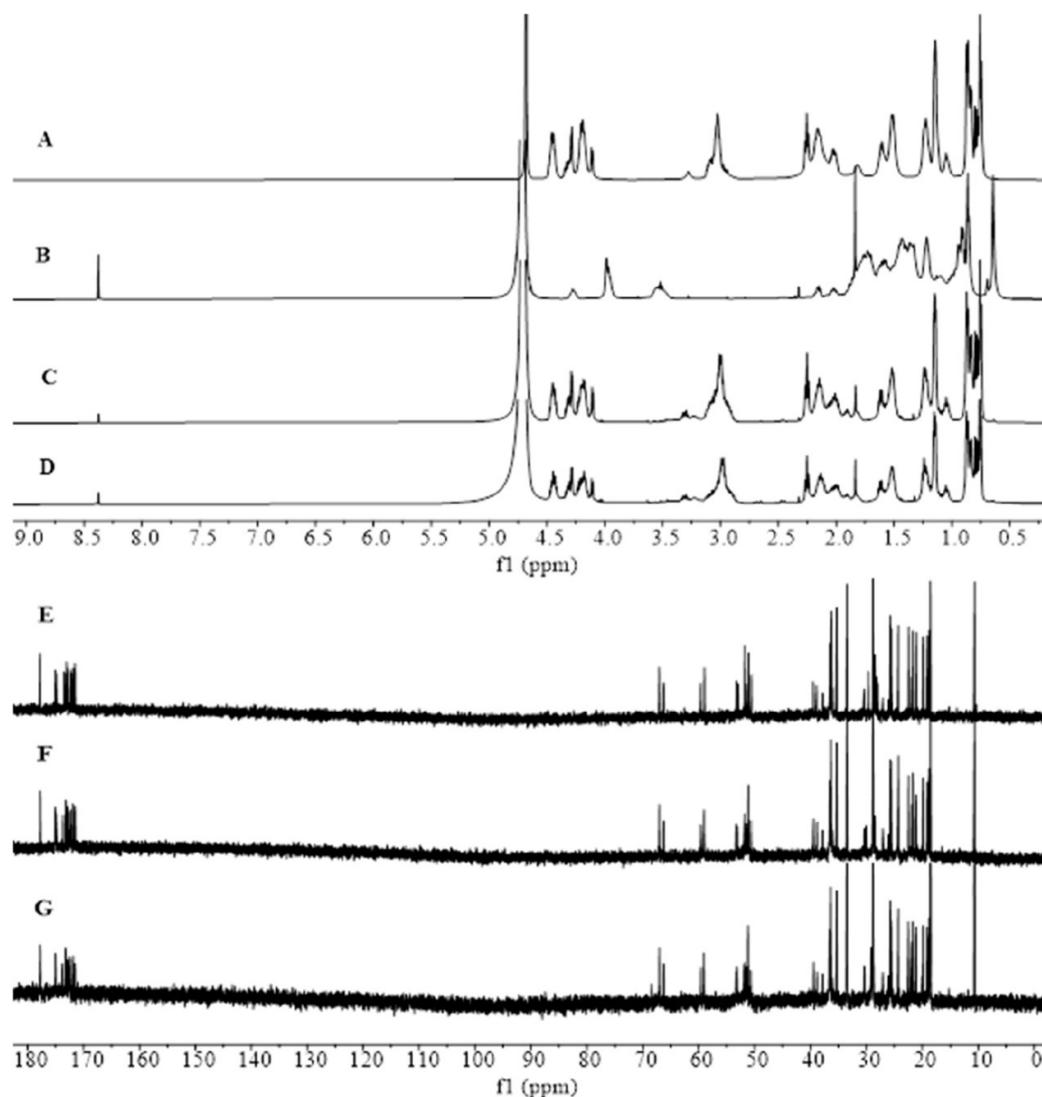


**Fig. 8.**  $^1\text{H}$ NMR spectra of (A) colistin, (B) SDCS, (C) colistin-SDCS 1:1 ratio formulation, and (D) colistin-SDCS 1:2 ratio formulation. Also,  $^{13}\text{C}$ NMR spectra of (E) colistin, (F) colistin-SDCS 1:1 ratio formulation, and (G) colistin-SDCS 1:2 ratio formulation.

the side chain of amino acids of colistin was bound to the SDCS through hydrophobic interaction to form the micelles.

### 3.10. Antibacterial activity of colistin-SDCS micelles

The increasing incidence of MDR cases justifies the emerging use of polymyxins (PMB and colistin). The MIC of colistin and colistin micelles was obtained using the broth microdilution method. Subcultures were performed from broth media that exhibited equal to or higher MIC values to obtain the MBC. The values of MIC and MBC of colistin and colistin micelles against *P. aeruginosa* can be seen in Table 5. The concentrations of 7.81  $\mu\text{g}/\text{mL}$  and 15.63  $\mu\text{g}/\text{mL}$  for MIC and MBC, respectively, were the same for colistin and colistin micelles. The results are in line with another study in which SDCS did not affect the antibacterial activity of polymyxin [18].

The results from the static time-kill experiment showed that the colistin micelles had similar efficiency in killing *P. aeruginosa* when exposed to the same bactericidal concentration (Fig. 10). The reduction

of  $\pm 0.3$  Log CFU/mL per h was achieved within the 24-h observation period. The colistin micelles however seemed to have slightly better efficiency with a similar pace during the initial 12 h. These results showed that entrapping colistin in SDCS micelles did not compromise the permeability of colistin through the bacterial membrane.

### 3.11. Cytotoxicity on kidney cells of colistin-SDCS micelles

Several studies have shown a higher percentage of renal injury developed in patients treated with colistin or PMB which is caused by increased permeability in tubular epithelial cells [30]. Colistin undergoes extensive tubular reabsorption, in the mice and rat models, colistin preferentially accumulates in the renal cortical region. Specifically, substantial accumulation was observed in the renal proximal tubular cells [31,32]. Colistin nephrotoxicity is directly related to its high exposure toward renal proximal tubular cells and the accumulation can be the result of its affinity toward negatively charged megalin that mediates the tubular uptake of several nephrotoxic agents [33]. In this

**Table 3**  
<sup>1</sup>HNMR chemical shifts of colistin, F1, and F2 multiplets.

Name	Chemical shift (ppm)		
	Colistin	F1	F2
4CH <sub>3</sub> (t)	0.76	0.75	0.75
aliphatic CH <sub>3</sub> (m)	0.79	0.78	0.79
CH <sub>3</sub> (OH) (m)	0.85	0.85	0.86
CH aliphatic (m)	1.05	1.05	1.05
NH <sub>2</sub> (dd)	1.15	1.14	1.15
CH <sub>2</sub> fatty acid (q)	1.22	1.22	1.23
CH ring (s)	1.25	1.25	1.51
OH (m)	1.52	1.51	1.61
CH-(CH <sub>2</sub> )-CH (dt)	1.6	1.61	1.83
-NH- (m)	1.81	1.83	2.01
CH <sub>2</sub> -(CH <sub>2</sub> )-CH (dq)	2.17	2.14	2.13
NH <sub>2</sub> -(CH <sub>2</sub> )-CH <sub>2</sub> (t)	2.25	2.25	2.25
(CH <sub>3</sub> )-CH (dddd)	3.04	3.01	3.0
CH <sub>2</sub> -(CH <sub>2</sub> )-NH (s)	3.28	3.29	3.31
HN-(CH)-CH, beta -C=O (dq)	4.19	4.19	4.19
CH <sub>3</sub> -(CH)-OH, beta -CH (m)	4.31	4.30	4.30
R-NH-R aliphatic (ddd)	4.46	4.44	4.44

t, triplet; m, multiplet; dd, doublet of doublets; q, quartet; s, singlet; dt, doublet of triplets; dq, doublet of quartet; dddd, doublet of doublet of doublet of doublets; ddd, doublet of doublet of doublets.

study, experiments were conducted to investigate the cytotoxicity of the colistin and colistin-SDCS micelles against the human kidney cell line WT9-12, human kidney epithelial cell line 293T/17, and human primary renal proximal tubule epithelial cells PCS-400-010. Fig. 11 shows the percent viability of the cells followed by incubation with the colistin

micelles and free drug colistin. The micelles displayed lower toxicity in the concentration range of 1.95–1000 µg/mL. The F1 and F2 showed significant cell viability in all cell lines, while colistin had increased cytotoxicity at this concentration (<60% cell viability of 293T/17 and < 50% cell viability of WT9-12 and PCS-400-010 cells). The two human kidney epithelial cells (WT9-12 and 293T/12) showed a moderate amount of cytotoxicity decrease but the overall cytotoxicity of colistin toward these cell lines was lower where it needed a higher colistin concentration to decrease cell viability to <50% (1000 µg/mL for WT9-12 and > 1000 µg/mL for 293T/17) (Fig. 11A and B). Higher cytotoxicity of colistin was displayed on human primary renal proximal tubule epithelial cells PCS-400-010 (Fig. 11C).

A lower concentration of 250 µg/mL showed 52.3% cell viability as

**Table 4**  
 Binding energy of sodium deoxycholate sulfate molecules docked on colistin (mean ± SD, n = 3).

No. of molecules	Binding energy (kcal/mol)
1	-7.50 ± 0.07
2	-7.65 ± 0.03
3	-6.88 ± 0.19
4	-6.51 ± 0.18
5	-6.03 ± 0.08
6	-5.74 ± 0.11
7	-5.61 ± 0.11
8	-6.00 ± 0.1
9	-5.60 ± 0.03
10	-5.62 ± 0.19

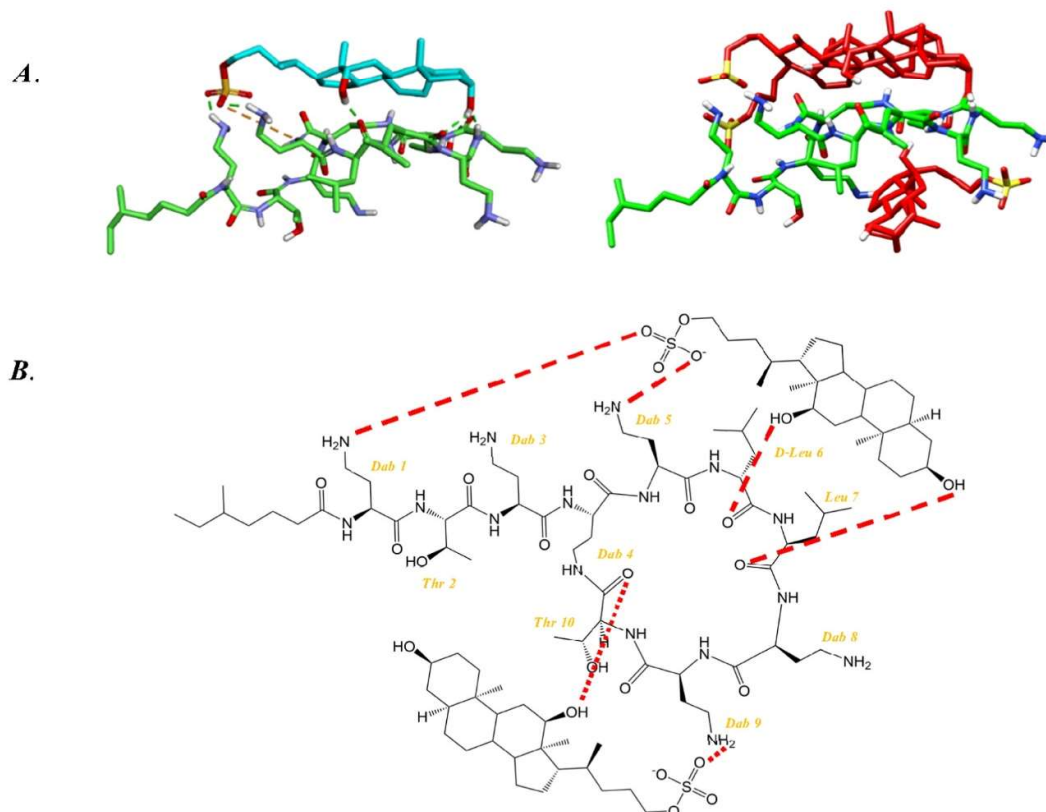


**Fig. 9.** Molecular docking structure and plausible interaction of colistin and SDCS in (A) 3D structure that shows colistin as the green stick and SDCS as cyan and red stick. Also, the illustration of interaction in (B) 2D structure where hydrogen bonding is shown as a red dashed line. (For interpretation of the references to colour in this figure legend, the reader is referred to the Web version of this article.)

**Table 5**  
Minimum inhibitory concentration and minimum bactericidal concentration ( $\mu\text{g/mL}$  of colistin equivalence) of colistin and colistin micelles against *Pseudomonas aeruginosa* ( $n = 3$ ).

Sample test	<i>P. aeruginosa</i>	
	MIC ( $\mu\text{g/mL}$ )	MBC ( $\mu\text{g/mL}$ )
Colistin	7.81	15.63
Colistin-SDCS (1:1)	7.81	15.63
Colistin-SDCS (1:2)	7.81	15.63

MIC, minimum inhibitory concentration; MBC, minimal bactericidal concentration; SDCS, sodium deoxycholate sulfate.

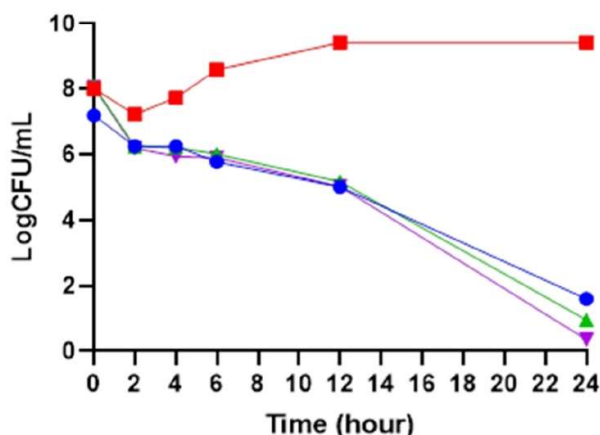


**Fig. 10.** Bactericidal effects of the control negative (■), colistin (●), colistin-SDCS 1:1 (△) and 1:2 (▼) against *Pseudomonas aeruginosa*. The bacteria were subjected to  $7.8 \mu\text{g/mL}$  colistin and colistin micelles, and the number of viable cells was monitored over time (mean,  $n = 3$ ).

in other studies that suggested the nephrotoxicity of colistin (or PMB and AMB) takes place at the kidney proximal tubules [30]. Colistin-SDCS managed to decrease the colistin exposure toward the proximal tubule cell lines, which in turn significantly lowers its cytotoxicity. This is in line with previous studies which suggested that SDCS minimized the cytotoxicity of AmB and PMB compared with their free drug counterparts [15,19,34]. Colistin was released from SDCS when administered and it is expected that the concentration of the colistin formulation went below CMC after dilution in the plasma. While there will be no encapsulated colistin eventually after the micelle disassembles with lowered concentration, the process is not instantaneous and can take hours in a kinetically dominated system [14]. The colistin distributed in the human kidney can still be in micelle form that can lower the exposure or in the colistin form with SDCS molecules bound with a negative charge which can result in lower affinity toward megalin that contributed toward colistin nephrotoxicity [33]. The cytotoxicity reduction of colistin micelles should imply that SDCS can overcome the nephrotoxicity of colistin by forming novel formulations as micelles. The potential for an alternative delivery system for colistin in multi-drug resistant gram-negative bacterial infection treatment by employing it in SDCS micelles can help to prevent the nephrotoxicity that patients suffer from colistin.

#### 4. Conclusions

Colistin has in recent times attracted intense interest for its application in combatting MDR gram-negative bacteria. In this work, colistin was formulated in micelles using SDCS. The SDCS was synthesized and the micelle formulations were prepared by lyophilisation. The results

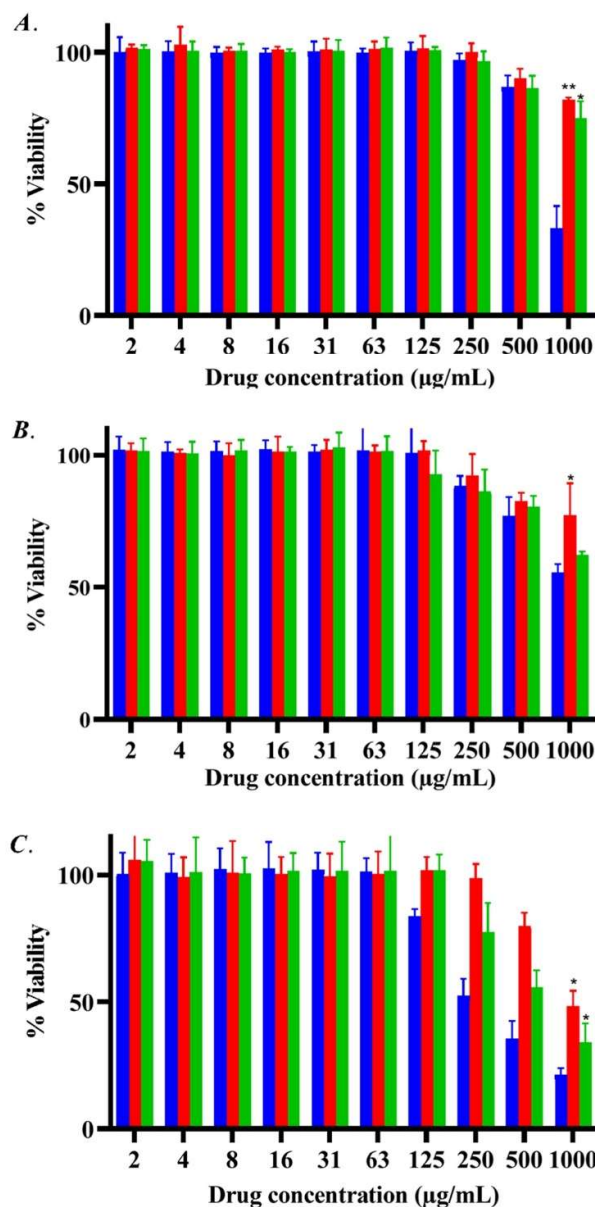


**Fig. 11.** Cell viability of (A) human kidney cell line WT9-12, (B) human kidney epithelial cell line 293T/17, and (C) human primary renal proximal tubule epithelial cells PCS-400-010 after 24-h incubation with colistin (blue), colistin to SDCS formulation ratios of 1:1 (red) and 1:2 (green) at various concentrations determined by MTT assay. Errors bars represent a standard deviation ( $n = 3$ ). The star(s) represent statistical differences from colistin (\* =  $P < 0.05$  and \*\* =  $P < 0.01$ ).

showed that the ratio of colistin to SDCS had significant effects on its particle size, zeta potential, and physicochemical properties of colistin-SDCS micelles. At the optimal ratio, the micelles have high EE. Furthermore, according to data from the NMR and FTIR analyses as well as the docking prediction, it was revealed that SDCS interacted by hydrogen bonding with the hydrophilic ring of colistin. The zeta potential findings suggested that the micellar formulation is stable upon reconstitution. The colistin micelles displayed no compromise of its antibacterial activity and showed a significant reduction in toxicity

toward kidney cell lines. In summary, the data from this investigation showed the potential application of colistin-SDCS as a delivery system for colistin.

#### Authorship statement

##### Category 1.

Conception and design of the study: T. Srichana, V. Tipmanee; Acquisition of data: M.A.K. Mudhar Bintang, V. Tipmanee; Analysis and/ or interpretation of data: T. Srichana, M.A.K. Mudhar Bintang.

##### Category 2.

Drafting the manuscript: M.A.K. Mudhar Bintang; Revising the manuscript critically for important intellectual content: T. Srichana, V. Tipmanee.

##### Category 3.

Approval of the version of the manuscript to be published: M.A.K. Mudhar Bintang, V. Tipmanee, T. Srichana.

#### Declaration of competing interest

On behalf of all the authors, I hereby certify that the work is no conflict of interest with any individual or organization.

#### Data availability

Data will be made available on request.

#### Acknowledgements

This work was supported by the Prince of Songkla University, Songkhla, Thailand (Grant No: PHA6505022M).

#### References

- Anneke C. Dijkmans, B. Erik, Ingrid M.C. Wilms, Kamerling, Willem Birkhoff, V. Natalia, Ortiz-Zacarias, Cees Van Nieuwkoop, Henri A. Verbrugh, Daan J. Touw, Colistin: revival of an old polymyxin antibiotic, *Ther. Drug Monit.* 37 (4) (2015) 419–427, <https://doi.org/10.1097/FTD.0000000000000172>.
- Zakuan Zainy Deris, Suresh Kumar, Rational use of intravenous polymyxin B and colistin: a review, *Med. J. Malaysia* 73 (5) (2018) 351–358.
- Mohamed Abd Ahmed, El-gawad El-sayed, Yohei Doi, Guo-bao Tian, Lan-lan Zhong, Cong Shen, Yongqiang Yang, Colistin and its role in the era of antibiotic resistance: an extended review, *Emerg. Microb. Infect.* 9 (2020).
- Yang Li, Chengcheng Tang, Enbo Zhang, Li Yang, Electrostatically entrapped colistin liposomes for the treatment of *Pseudomonas aeruginosa* infection, *Pharmaceut. Dev. Technol.* 22 (3) (2017) 436–444, <https://doi.org/10.1080/10837450.2016.1228666>.
- L Roger Nation, Jian Li, Colistin in the 21st century, *J. Univ. Pet., China (Ed. Soc. Sci.)* 22 (6) (2009) 535–543, <https://doi.org/10.1097/QCO.0b013e328332e672>.
- Mohan Gurjar, Colistin for lung infection: an update, *Journal of Intensive Care* 3 (1) (2015), <https://doi.org/10.1186/s40560-015-0072-9>.
- Ilias Karaiskos, Maria Souli, Irene Galani, Helen Giamarellou, Colistin: still a lifesaver for the 21st century? *Expet Opin. Drug Metabol. Toxicol.* 13 (1) (2017) 59–71, <https://doi.org/10.1080/17425255.2017.1230200>.
- Carlos Mendes, Alberto Caldeira, A. Emmanuel, Burdmann, Polymyxins: review with emphasis on nephrotoxicity, *Rev. Assoc. Med. Bras.* 55 (6) (2010) 752–758.
- Fadaka, Adewale Oluwaseun, Nicole Remaliah, Samantha Sibuyi, Abram Madimabe Madiehe, Mervin Meyer, Nanotechnology-based delivery systems for antimicrobial peptides, *Pharmaceutics* 13 (11) (2021), <https://doi.org/10.3390/pharmaceutics13111795>.
- Jayanta Kumar Patra, Gitishree Das, Leonardo Fernandes Fraceto, Estefania Vangelie Ramos Campos, Maria Del Pilar Rodriguez-Torres, Laura Susana Acosta-Torres, Luis Armando Diaz-Torres, et al., Nano based drug delivery systems: recent developments and future prospects 10 *Technology 1007 nanotechnology 03 chemical sciences 0306 physical chemistry (incl. Structural) 03 chemical sciences 0303 macromolecular and materials chemistry 11 medical and He, J. Nanobiotechnol.* 16 (1) (2018) 1–33, <https://doi.org/10.1186/s12951-018-0392-8>.
- Morteza Milani, Salehi Roya, Hamishehkar Hamed, Zarebkohan Amir, Akbarzadeh Abolfazl, Synthesis and evaluation of polymeric micelle containing piperacillin/tazobactam for enhanced antibacterial activity, *Drug Deliv.* 26 (1) (2019) 1292–1299, <https://doi.org/10.1080/10717544.2019.1693708>.
- Xingyue Yang, Ren He, Hong Zhang, Gengqi Liu, Zhen Jiang, Qian Qiu, Yu Cui, et al., Antibiotic cross-linked micelles with reduced toxicity for multidrug-resistant bacterial sepsis treatment, *ACS Appl. Mater. Interfaces* 13 (8) (2021) 9630–9642, <https://doi.org/10.1021/acsami.0c21459>.
- Maximiliano Cagel, Fiorella C. Tesan, Ezequiel Bernabeu, Maria J. Salgueiro, Marcela B. Zubillaga, Marcela A. Moreton, Diego A. Chiappetta, Polymeric mixed micelles as nanomedicines: achievements and perspectives, *Eur. J. Pharm. Biopharm.* 113 (2017) 211–228, <https://doi.org/10.1016/j.ejpb.2016.12.019>.
- M. Ghezzi, S. Pescina, C. Padula, P. Santi, E. Del Favero, L. Cantù, S. Nicoli, Polymeric micelles in drug delivery: an insight of the techniques for their characterization and assessment in biorelevant conditions, *J. Contr. Release* 332 (February) (2021) 312–336, <https://doi.org/10.1016/j.jconrel.2021.02.031>.
- Katkam N. Gangadhar, Kajiram Adhikari, Srichana Teerapol, Synthesis and evaluation of sodium deoxycholate sulfate as a lipid drug carrier to enhance the solubility, stability and safety of an amphotericin B inhalation formulation, *Int. J. Pharm.* 471 (1–2) (2014) 430–438, <https://doi.org/10.1016/j.ijpharm.2014.05.066>.
- Sreenu Madhumanchi, Roongnapa Suedee, Titpawan Nakpheng, Kittiya Tinpun, Pornvichai Temboot, Teerapol Srichana, Binding interactions of bacterial lipopolysaccharides to polymyxin B in an amphiphilic carrier 'sodium deoxycholate sulfate, *Colloids Surf. B Biointerfaces* 182 (May) (2019), 110374, <https://doi.org/10.1016/j.colsurfb.2019.110374>.
- Faisal Usman, Zaheer Ul-Haq, Ruqaiya Khalil, Kittiya Tinpun, Teerapol Srichana, Pharmacologically safe nanomicelles of amphotericin B with lipids: nuclear magnetic resonance and molecular docking approach, *J. Pharmaceut. Sci.* 106 (12) (2017) 3574–3582, <https://doi.org/10.1016/j.xphs.2017.08.013>.
- Pornvichai Temboot, Sunisa Kaewpaiboon, Kittiya Tinpun, Titpawan Nakpheng, Ruqaiya Khalil, Zaheer Ul-Haq, Visanu Thamlikitkul, Surapee Tiengrim, Teerapol Srichana, Potential of sodium deoxycholate sulfate as a carrier for polymyxin B: physicochemical properties, bioactivity and in vitro safety, *J. Drug Deliv. Sci. Technol.* 58 (May) (2020), <https://doi.org/10.1016/j.jddst.2020.101779>.
- Sreenu Madhumanchi, Roongnapa Suedee, Sunisa Kaewpaiboon, Teerapol Srichana, Ruqaiya Khalil, Zaheer Ul-Haq, Effect of sodium deoxycholate sulfate on outer membrane permeability and neutralization of bacterial lipopolysaccharides by polymyxin B formulations, *Int. J. Pharm.* 581 (January) (2020), 119265, <https://doi.org/10.1016/j.ijpharm.2020.119265>.
- B. Cancho Grande, M.S. García Falcón, C. Pérez-Lamela, M. Rodríguez Comesaña, J. Simal Gándara, Quantitative analysis of colistin and tiamulin in liquid and solid medicated premixes by HPLC with diode-array detection, *Chromatographia* 53 (2001) 460–463, <https://doi.org/10.1007/bf02490378>.
- Marta Pastor, María Moreno-Sastre, Amaia Esquisabel, Eulalia Sans, Miguel Viñas, Daniel Bachiller, Víctor José Asensio, Ángel Del Pozo, Eusebio Gainza, José Luis Pedraz, Sodium colistimethate loaded lipid nanocarriers for the treatment of *Pseudomonas aeruginosa* infections associated with cystic fibrosis, *Int. J. Pharm.* 477 (1–2) (2014) 485–494, <https://doi.org/10.1016/j.ijpharm.2014.10.048>.
- Aaron C. Burns, Peter W. Sorensen, Thomas R. Hoye, Synthesis and olfactory activity of unnatural, sulfated 5 $\beta$ -bile acid derivatives in the sea lamprey (*Petromyzon marinus*), *Steroids* 76 (3) (2011) 291–300, <https://doi.org/10.1016/j.steroids.2010.11.010>.
- Rub, Abdul Malik, Mohamad Shafi Sheikh, Farah Khan, Sher Bahadur Khan, M. Abdullah, Asiri, Bile salts aggregation behavior at various temperatures under the influence of amphiphilic drug imipramine hydrochloride in aqueous medium, *Zeitschrift Fur Physikalische Chemie* 228 (6–7) (2014) 747–767, <https://doi.org/10.1515/zpch-2013-0495>.
- Stephanie J. Wallace, Jian Li, L. Roger, Richard Nation, J. Frankerd, Tony Velkov, Ben J. Boyd, Self-assembly behavior of colistin and its prodrug colistin methanesulfonate: implications for solution stability and solubilization, *J. Phys. Chem. B* 114 (14) (2010) 4836–4840, <https://doi.org/10.1021/jp100458x>.
- Sunisa Kaewpaiboon, Teerapol Srichana, Formulation optimization and stability of polymyxin B based on sodium deoxycholate sulfate micelles, *J. Pharmaceut. Sci.* (2022) 1–9, <https://doi.org/10.1016/j.xphs.2022.02.011>.
- Anirudh Srivastava, Hiromasa Uchiyama, Yuhei Wada, Yuta Hatanaka, Yoshiyuki Shirakawa, Kazunori Kadota, Yuichi Tozuka, Mixed micelles of the antihistaminic cationic drug diphenhydramine hydrochloride with anionic and non-ionic surfactants show improved solubility, drug release and cytotoxicity of ethenzamide, *J. Mol. Liq.* 277 (2019) 349–359, <https://doi.org/10.1016/j.molliq.2018.12.070>.
- Stepanie J. Wallace, Jian Li, Roger L. Nation, Richard J. Frankerd, Ben J. Boyd, Interaction of colistin and colistin methanesulfonate with liposomes: colloidal aspects and implications for formulation, *J. Pharmaceut. Sci.* 101 (9) (2012) 3347–3359, <https://doi.org/10.1002/jps.23203>.
- S.M. Garonzik, J. Li, V. Thamlikitkul, D.L. Paterson, S. Shoham, J. Jacob, F. P. Silveira, A. Forrest, R.L. Nation, Population pharmacokinetics of colistin methanesulfonate and formed colistin in critically ill patients from a multicenter study provide dosing suggestions for various categories of patients, *Antimicrob. Agents Chemother.* 55 (7) (2011) 3284–3294, <https://doi.org/10.1128/AAC.01733-10>.
- Ordoee Javan, Atefeh, Shervin Shokouhi, Zahra Sahraei, A review on colistin nephrotoxicity, *Eur. J. Clin. Pharmacol.* 71 (7) (2015) 801–810, <https://doi.org/10.1007/s00228-015-1865-4>.
- Zhibo Gai, Sophia L. Samodelov, Gerd A. Kullak-Ublick, Michele Visentin, Molecular mechanisms of colistin-induced nephrotoxicity, *Molecules* 24 (3) (2019), <https://doi.org/10.3390/molecules24030653>.
- Bo Yun, Mohammad A.K. Azad, Jiping Wang, Roger L. Nation, Philip E. Thompson, Kade D. Roberts, Tony Velkov, Jian Li, Imaging the distribution of polymyxins in the kidney, *J. Antimicrob. Chemother.* 70 (3) (2015) 827–829, <https://doi.org/10.1093/jac/dku441>.

- [32] Anna Nilsson, J.A. Richard Goodwin, John G. Swales, Richard Gallagher, Harish Shankaran, Abhishek Sathe, Selvi Pradeepan, et al., Investigating nephrotoxicity of polymyxin derivatives by mapping renal distribution using mass spectrometry imaging, *Chem. Res. Toxicol.* 28 (9) (2015) 1823–1830, <https://doi.org/10.1021/acs.chemrestox.5b00262>.
- [33] Takahiro Suzuki, Hiroaki Yamaguchi, Jiro Ogura, Masaki Kobayashi, Takehiro Yamada, Ken Iseki, Megalin contributes to kidney accumulation and nephrotoxicity of colistin, *Antimicrob. Agents Chemother.* 57 (12) (2013) 6319–6324, <https://doi.org/10.1128/AAC.00254-13>.
- [34] Faisal Usman, Ruqaiya Khalil, Zaheer Ul-Haq, Titpawan Nakpheng, Teerapol Srichana, Bioactivity, safety, and efficacy of amphotericin B nanomicellar aerosols using sodium deoxycholate sulfate as the lipid carrier, *AAPS PharmSciTech* 19 (5) (2018) 2077–2086, <https://doi.org/10.1208/s12249-018-1013-4>.

**Paper 3**

In Vivo Evaluation of Nephrotoxicity and Neurotoxicity of Colistin Formulated with Sodium Deoxycholate Sulfate in Mice Model

RESEARCH



## In vivo evaluation of nephrotoxicity and neurotoxicity of colistin formulated with sodium deoxycholate sulfate in a mice model

Muhammad Ali Khumaini Mudhar Bintang<sup>1</sup> · Jongdee Nopparat<sup>2,3</sup> · Teerapol Srichana<sup>1</sup>

Received: 16 January 2023 / Accepted: 15 May 2023

© The Author(s), under exclusive licence to Springer-Verlag GmbH Germany, part of Springer Nature 2023

### Abstract

Neurotoxicity and nephrotoxicity are the major dose-limiting factors for the clinical use of colistin against multidrug-resistant (MDR) Gram-negative bacteria. This study aimed to investigate the neurotoxic and nephrotoxic effects of colistin formulated with in-house synthesized sodium deoxycholate sulfate (SDCS) in a mouse model. Male mice C57BL/6 were randomly divided into four groups: control (saline solution), colistin (15 mg/kg/day), colistin:SDCS 1:1, and colistin:SDCS 1:2. In the colistin:SDCS treatment groups, the dosage was 15 mg/kg/day colistin equivalent; all mice were treated for 7 successive days. The thermal tolerance, body weight gain and organ weights were measured. The levels of serum blood urea nitrogen (BUN), creatinine (Cr), superoxide dismutase (SOD), and catalase (CAT) were assessed. Histopathological damages were assessed on mice organ. The colistin:SDCS formulations significantly improved thermal pain response of the mice comparable to the control group. The administration did not impair kidney function as evidence from BUN and Cr results; however, the oxidative stress biomarkers decreased in the colistin and colistin-SDCS treated mice. Several abnormalities were observed in the kidney, liver, spleen, and sciatic nerve tissues following colistin treatment, which indicated evidence of toxicity. The colistin-SDCS formulations were associated with less acute toxicity and fewer nephrotoxic and neurotoxic changes compared with the colistin alone group which indicated that SDCS attenuated colistin nephrotoxicity and neurotoxicity. This study highlights the potential application of colistin formulated with SDCS for safer clinical use against MDR Gram-negative bacteria.

**Keywords** Colistin · Sodium deoxycholate sulfate · Nephrotoxicity · Neurotoxicity · Histopathology

### Introduction

Antimicrobial resistance has been marked as one of the top 10 public health crisis to watch with the growing number of mortality-related cases. This situation has become an increasingly serious issue, especially for gram-negative bacteria. Antibiotic resistance among gram-negative bacteria,

which started to rise in the 1970s, is now a serious global concern (Neill 2014; Vardakas and Falagas 2017). Unfortunately, very little has been done in the pharmaceutical sector to address this issue. Since the pipeline for developing new antibiotics against these "superbugs" is running dry, there is renewed interest in reviving older antibiotics that were previously thought to be too toxic for clinical use. In particular, polymyxins, e.g., colistin and polymyxin B, are being revived as "last resort" antimicrobials (Bialvaei and Samadi Kafil 2015; Ahmed et al. 2020).

From a chemical standpoint, colistin and polymyxin B have similar backbones, i.e., cyclic heptapeptide with a tripeptide side chain acylated at the amino terminus by a fatty acid tail. The difference is at position 6 which is occupied by D-phenylalanine in polymyxin B and by D-leucine in colistin (Nation et al. 2014). Colistin's main antibacterial mechanism comes from the disruption of cell membrane integrity of gram-negative bacteria by electrostatic interaction and cationic displacement ( $\text{Ca}^{++}$  and  $\text{Mg}^{++}$ ) of the lipopolysaccharide (LPS), Colistin disrupts the membrane's stability and

✉ Teerapol Srichana  
teerapol.s@psu.ac.th

<sup>1</sup> Drug Delivery System Excellence Center, Department of Pharmaceutical Technology, Faculty of Pharmaceutical Sciences, Prince of Songkla University, Hat Yai, Songkhla 90112, Thailand

<sup>2</sup> Division of Health and Applied Sciences, Faculty of Science, Prince of Songkla University, Hat Yai, Songkhla 90112, Thailand

<sup>3</sup> Center of Excellence for Trace Analysis and Biosensor, Prince of Songkla University, Hat Yai, Songkhla 90110, Thailand



increases its permeability, causing cell contents to leak out and initiate cell death pathways. Other bactericidal mechanisms of colistin may be the neutralization of LPS, which is the endotoxin of gram-negative bacteria, and/or the inhibition of bacterial respiration (Hill et al. 2014; Yu et al. 2015).

The clinical use of colistin was largely abandoned by the mid-1970s due to reported adverse events, primarily nephrotoxicity and neurotoxicity, as well as the discovery and approval of new and effective antibiotics (Grégoire et al. 2017). The most common adverse effect associated with colistin is nephrotoxicity. Almost every clinical study investigating intravenous colistin reported the incidence of renal impairment during treatment (Kalesidis, Theodoros; Falagas 2015; Ortwine et al. 2015). Polymyxin resorption via renal cell receptors such as megalin in conjunction with oxidative stress, may cause kidney toxicity (Suzuki et al. 2013; Perez et al. 2019). Colistin may also disrupt membrane permeability resulting in cell lysis (Zavascki and Nation 2017). Overall, the mechanism of action of polymyxins on the gram-negative cell membrane is similar to that of detergents (Gai et al. 2019). Neurotoxicity is the second most common adverse effect, accounting for approximately 7% of cases and manifesting as peripheral or orofacial paresthesia, vertigo, visual disturbances, confusion, seizures, and the potentially fatal event of neuromuscular blockade leading to respiratory muscle paralysis and apnea (Karaïskos and Giamarellou 2014; Kelesidis and Falagas 2015).

In-vitro and in-vivo studies demonstrated that sodium deoxycholate sulfate (SDCS) effectively attenuated the nephrotoxicity of amphotericin B and polymyxin B (Gangadhar et al. 2014; Madhumanchi et al. 2019; Usman et al. 2020). Drugs incorporated into SDCS showed slower release of the drug resulting in the lower exposure of the nephrotoxic drugs to the kidneys (Gangadhar et al. 2014; Usman et al. 2020). Polymyxin B incorporated into SDCS showed stable micelles and formulations when stored (Temboot et al. 2020; Kaewpaiboon and Srichana 2022). The effect of SDCS on the erythrocytes showed reduced hemolytic properties while still maintaining the antimicrobial properties of polymyxin B (Madhumanchi et al. 2020; Temboot et al. 2020). In our study we have found that colistin in SDCS micelles showed good properties with significantly lower toxicity toward human kidney cells and SDCS have been shown to have no toxicity toward different human cell lines. The nephrotoxic property of colistin can be addressed using SDCS, especially for colistin sulfate that proved to be more toxic toward kidney cells when administered parenterally, while the use of colistin sulfate can release colistin instantly compared to its prodrug, colistin methanesulfonate (Nazer and Anabtawi 2017; Pogue et al. 2017). In the present study, we investigated the effect of colistin-SDCS formulations on mice kidneys in vivo and observed damage to sciatic nerve tissue for potential neurotoxic attenuation.

## Materials and methods

### Chemicals

Colistin sulfate and deoxycholic acid were purchased from Sigma-Aldrich (St. Louis, MO, USA). SDCS was synthesized in-house (Gangadhar et al. 2014). Polyamide membranes with pore sizes of 0.22  $\mu\text{m}$  and 0.45  $\mu\text{m}$  were obtained from Sartorius (Göttingen, Germany). All chemicals, except tetrahydrofuran, were used as received without further purification. All other reagents and chemicals were of analytical grade.

### Animals

Immunocompetent male mice (*Mus musculus* strain C57BL/6) were used in this study. Each mouse weighed 18–22 g and was 6–8 weeks old. They were obtained from Nomura Siam International Co., Ltd., Bangkok, Thailand and supplied with the standard feed protocol by the Southern Laboratory Animal Facility, Faculty of Science, Prince of Songkla University, Hat Yai, Songkhla, Thailand. The mice were inbred and specified as pathogen-free. The animals were put on rest for seven days before the experiment. The mice were kept in stainless steel cages of dimensions 17  $\times$  28.5  $\times$  17 cm with nine mice/cage at  $25 \pm 2$  °C and subjected to alternating 12-h light/dark cycles. The animals were kept at relative humidity (50  $\pm$  10) with no noise disturbance, good ventilation, and continuous electrical power supply. All of the animals were allowed ad libitum access to a standard rodent diet and water. Strict hygienic conditions were maintained throughout the study duration for all of the animals with proper disinfection of the cage floors. All animal experiments were performed with the approval of the animal ethics committee, Prince of Songkla University (MHESI 68014/1895, Ref. 81/2021).

### Preparation of colistin-SDCS dry powder formulations

The formulations were prepared using a mixture of colistin sulfate and SDCS at a 1:1 (70 and 26.6 mg) and 1:2 (55 and 41.7 mg) molar ratio in Milli-Q water (30 mL). The mixtures were stirred until complete dissolution. To these solutions, sodium hydroxide solution (2.7 mL, 0.2 M) was added slowly dropwise at room temperature to obtain a clear solution. The pH of the solution was about 9.5, which was adjusted to 7.4 using phosphoric acid (0.2 M) for an in-situ phosphate buffer. The final volume of the solution was made to 50 mL by adding deionized water. The solution

was lyophilized, and the reconstituted formulation pH was measured.

### Osmolarity of the formulations

The osmolarity of the colistin-SDCS formulations were measured using a freezing point depression osmometer. The measurement was carried out by dissolving 34 mg colistin sulfate equivalent of colistin-SDCS formulation in 7 mL water for injection. The solution was then introduced to the osmometer's cooling chamber, where the instrument

measured the sample's standard freezing curve. The osmolarity of the solution was calculated using the following equation:

$$\Delta T = K_f \times \text{osmolality}$$

$$\Delta T = \text{Temperature change}$$

$$K_f = \text{Cryoscopic constant}(1.86 \text{ K.kg/mol})$$

Moreover, osmolarity can be calculated by the following equation:

$$\text{Osmolarity} = \text{Osmolality} \times (\text{Solution density} - \text{anhydrous solute concentration})$$

The measurement was also carried out using 0.9% NaCl solution as the solvent for the formulations. The ideal osmolality for small volumes (< 100 mL) for an intravenous delivery system is ideally around  $300 \pm 30$  mOsm/kg and preferably < 1000 mOsm/kg for adults (Wang 2015).

### Experimental design

The animals used for this study were randomly divided into four groups (n=9) and each group was weighed before and after treatment. The normal control group was administered a normal saline solution, which was used as the solvent. The colistin group was administered colistin sulfate at 15 mg/kg/day. The Formulation 1 (F1) and Formulation 2 (F2) groups were administered colistin:SDCS at ratios 1:1 and 1:2, respectively, at 15 mg/kg/day colistin equivalent. Injections were administered intraperitoneally, and the dosage was divided into two times a day, once in the morning and once in the afternoon for seven consecutive days. At 12 h following the last dose, the mice were subjected to a neurobehavioral test. Subsequently, the mice were euthanized by a lethal dose of intraperitoneal sodium pentobarbital (90 mg/kg) (Sigma-Aldrich, St Louis, MO, USA). Blood samples were collected by cardiac puncture, and the serum was separated by centrifugation (3000 g for 15 min) and stored at  $-80$  °C until assayed. Kidney, liver, spleen, and sciatic nerve tissue samples were collected, weighed, and sectioned for histopathological studies.

### Hot plate test

A heat sensitivity test was performed using a hot plate at 12 h after the last experimental day. The mice were placed in a plastic cage with a wire mesh floor and allowed to acclimate for 5 min before hind paw thermal thresholds were

measured. A hot plate was preheated and maintained at a temperature of  $40 \pm 0.5$  °C. The time for the first sign of nociception, paw licking, flinching, or a jumping response to avoid the heat was recorded. A cut-off period of 80 s was established to avoid damage to the hind paws.

### Biochemical analysis

Blood samples were centrifuged at 3,000 g for 15 min to obtain serum for biochemical analysis. After the 7-day treatment period, the levels of serum blood urea nitrogen (BUN) and creatinine (Cr) were measured to investigate the effects of the SDCS formulations and colistin treatments on the kidney and liver physiology. The measurements were performed by an autoanalyzer using the standard diagnostic kits.

Also, the serum levels of superoxide dismutase (SOD) and catalase (CAT) were measured after the 7-day treatment period to investigate the oxidative properties of the treatments. The measurements were carried out using commercial kits according to the manufacturer's instructions (Merck KGaA, Darmstadt, Germany). One unit of SOD is defined as the amount of enzyme needed to exhibit a 50% dismutation of the superoxide radical, and one unit of CAT is defined as the amount of enzyme that will cause the formation of 1.0 nmol formaldehyde per min at 25 °C.

The data from each group of treated mice were compared with the control using one-way analysis of variance (ANOVA). The level of significance was defined as  $P < 0.05$ .

### Histopathological examination

Investigations of the histological appearance of the kidney, liver, spleen, and sciatic nerve tissues were undertaken.

The tissues were dissected and trimmed to remove excess fat. All tissues were fixed using 10% buffered formalin for three days. The tissues were then processed in gradually increasing concentrations of ethanol to 100% using a tissue processor (LEICA TP 1020, Leica Microsystems GmbH, Wetzlar, Germany) for 24 h to remove any water. The processed tissues were then embedded in Paraplast blocks using a tissue embedder (LEICA EG 1160, Leica Microsystems GmbH, Wetzlar, Germany). Sections of 5- $\mu$ m thickness were cut from the tissues using an automatic microtome. The tissue slides were stained with Harris hematoxylin and eosin (H&E) and examined using a microscope (Olympus DP73 equipped with cellSens software, version 6.1.4.2).

### Statistical analysis

The data were statistically processed to determine the level of significance. Data are presented as mean  $\pm$  standard deviation (SD) from at least three samples unless indicated. The data were evaluated using ANOVA followed by any other suitable statistical test if required. All statistical comparisons were determined using Minitab (Penn State University, USA) and GraphPad Prism (GraphPad Software, Inc., USA) software. Statistical significance was designated as  $P < 0.05$ .

## Results

The colistin and colistin-SDCS formulations were administered for seven days. The intraperitoneal route was chosen for the safety reason of blood vessel damage and practicality in repetitive treatment for the small size mice used (C57BL/6). The pH of the colistin-SDCS formulation solutions after reconstitution was 7.43. The osmolarities of formulations F1 and F2 were  $23 \pm 1$  and  $31 \pm 2$  mOsm/kg, respectively, while the osmolarity of the colistin sulfate was  $3 \pm 2$  mOsm/kg (Table 1).

### Effect of the treatment on mice body weight gain

After the colistin and colistin:SDCS formulation treatments of 15 mg/kg/day, the weights of the mice in each group were measured and compared with the weights before treatments. The results showed a significant reduction in the percentage of body weight gain ( $P < 0.01$ ) of mice treated with either colistin or the colistin:SDCS formulations (Table 2).

**Table 1** Osmolarities of colistin and the colistin-SDCS formulations measured by osmometry

	0.9% NaCl	F1	F2	Colistin sulfate
Osmolarity (mOsm/kg)	$289 \pm 4$	$23 \pm 1$	$31 \pm 2$	$3 \pm 2$

NaCl, sodium chloride, F1 Formulation 1, F2 Formulation 2.

### Effect of the treatments on sensory neuropathy in the mice

The mice subjected to colistin exhibited sensory neuropathies compared to the control group (Table 2). After seven days of treatment, the SDCS incorporated formulations markedly decreased the thermal pain threshold compared to the colistin group. The values of thermal pain threshold for the F1- and F2-injected mice decreased to 8.03 s and 8.01 s, respectively, compared to the colistin group (10.42 s), which was significantly higher ( $P < 0.01$ ) than the control group (7.32 s).

### Kidney function in the treated mice

The levels of serum BUN and Cr in the mice after seven days of treatment were measured to examine kidney function. The results showed no significant change in the BUN levels after colistin treatment ( $21 \pm 2.6$  mg/dL) and F1 treatment ( $21.4 \pm 3.4$  mg/dL) (Fig. 1A). However, the F2 group had a significant decrease in the BUN level ( $18.6 \pm 1.1$  mg/dL) ( $P < 0.02$ ) compared to the control group ( $23.6 \pm 2.1$  mg/dL). The Cr levels were not significantly different in the colistin ( $0.23 \pm 0.01$  mg/dL), F1 ( $0.27 \pm 0.11$  mg/dL), and F2 ( $0.24 \pm 0.05$  mg/dL) groups compared to the control group ( $0.22 \pm 0.02$  mg/dL) (Fig. 1B).

### Oxidative stress biomarkers of the treated mice

The serum levels of SOD and CAT in the mice were measured to observe and compare oxidative stress from the treatments. The control group had a serum SOD level of  $0.82 \pm 0.06$  U/mL. Significant decreases in the serum SOD were observed in the F1 ( $0.72 \pm 0.03$  U/mL) and F2 ( $0.71 \pm 0.06$  U/mL) groups ( $P < 0.05$ ). A much lower level of SOD was observed in the colistin treated group ( $0.52 \pm 0.05$  U/mL) ( $P < 0.01$ ) compared to the control group (Fig. 1C).

The serum CAT levels of the treated mice had similar trends as the SOD levels. The serum CAT levels in the F1 and F2 groups were  $12.12 \pm 0.13$  nmol/min/mL and  $11.99 \pm 0.16$  nmol/min/mL, respectively ( $P < 0.05$ ). Also, the colistin treated mice had a much lower level of CAT ( $5.61 \pm 0.52$  nmol/min/mL) compared to the control group ( $12.92 \pm 0.24$  nmol/min/mL).

**Table 2** Effect of colistin-SDCS formulations on body weight gain and paw thermal threshold after seven days of treatment (n=9)

	Control	Colistin	F1	F2
Initial BW(g)	19.64 ± 1.11	20.22 ± 1.15	20.46 ± 1.26	19.71 ± 0.61
Final BW(g)	21.00 ± 1.25	20.81 ± 0.84	21.34 ± 1.11	20.35 ± 0.68
Weight gain(%)	6.95 ± 1.4	3.06 ± 2.9**	4.35 ± 2.09	3.11 ± 2.29**
Thermal threshold(s)	7.35 ± 0.26	10.42 ± 0.98**	8.03 ± 0.79	8.01 ± 1.05

Data are presented as mean ± SD.

F1 Formulation 1, F2 Formulation 2, BW body weight.

\* P < 0.05, \*\* P < 0.01 compared with the control group.

### Histopathological examination of the mice tissue samples

An H&E assay was performed on the collected tissues of all animals to evaluate colistin-induced nephrotoxicity and neurotoxicity. Gross examinations of the kidney (Fig. 3A-D), liver (Fig. 4A-D), and spleen (Fig. 5A-D) morphologies showed no abnormal changes for all treatments. The percentages of organ weight/body weight of the kidney, liver, and spleen from colistin and colistin:SDCS treatments revealed no significant differences compared with the control group (Fig. 2A-C). Nevertheless, the percentages of the kidney and liver weights tended to be lower in the F1- and F2-treated mice compared to the colistin-treated group.

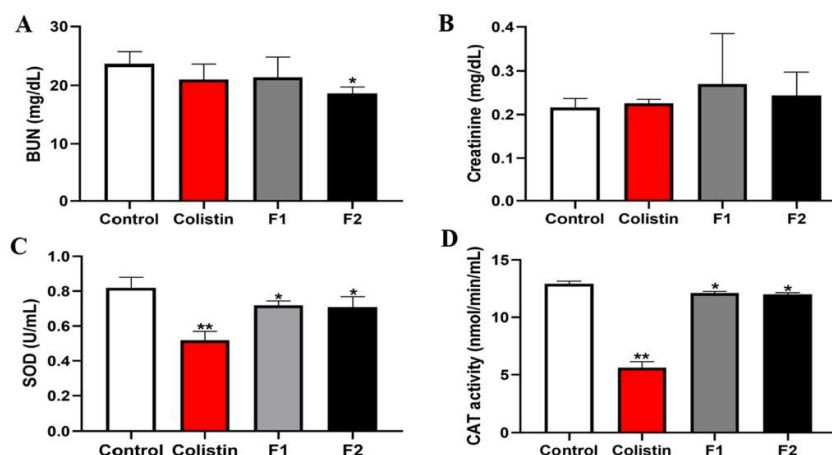
The kidney histopathological results as demonstrated by the H&E assay in the treated animals are shown in Fig. 3. The control group showed normal kidney tissue histopathology (Fig. 3A & E). Deformation of the glomeruli (yellow circle) and congestion of renal blood vessels (red circle) were evident in the colistin-treated-animals (Fig. 3B & F). In contrast, the alternations were mild with no evidence of renal glomerular injury in the F1 (Fig. 3C & G) and F2 (Fig. 3D & H) groups.

Liver histopathological alterations in the treated animals are shown in Fig. 4. The control group showed normal liver

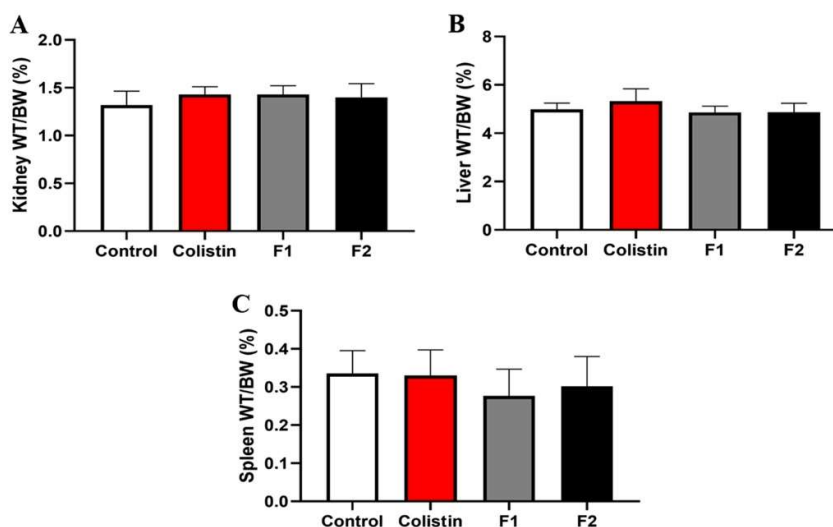
lobular architecture and cell structure, and the hepatocyte cord was neatly arranged with no inflammatory infiltration (Fig. 4A & E). In the colistin-treated animals, infiltration of monocytes (yellow arrows) with loss of hepatocyte architecture around the blood vessels was observed (Fig. 4B & F). The histological changes were less severe with a few monocyte invasions in the F1 (Fig. 4C & G, yellow arrow) and F2 (Fig. 4D & H) treated animals.

We also observed the spleen histopathological alterations in the treated animals (Fig. 5). Normal white and red pulp with predominantly non-activated follicles and unremarkable red pulp were observed in the spleen tissue of the control group (Fig. 5A & E). However, large numbers of multinucleated giant cells (yellow arrows) were present in the spleen tissue of the colistin-treated animals (Fig. 5B & F). Fewer multinucleated giant cells were observed in the spleen of the F1 (Fig. 5C & G, yellow arrows) and F2 (Fig. 5D & H, yellow arrow) treated animals.

We also examined the histopathology of the sciatic nerve tissue to observe peripheral nerve damage of the treated animals (Fig. 6). The myelin in the control group appeared dense, round, and uniform with an ordered lamellar structure that presented neither axonal shrinkage nor swelling (Fig. 6A). In the colistin-treated group, the myelin sheath of the nerve fibers was thin and loose (yellow arrows) (Fig. 6B).

**Fig. 1** Effect of colistin and colistin-SDCS formulations on mice kidney function and serum biomarkers. **A** Blood urea nitrogen (BUN). **B** Creatinine (Cr). **C** Superoxide dismutase (SOD). **D** Catalase (CAT). Data are presented as mean ± SD. n = 6. The star(s) represent statistical differences from the control group. \* P < 0.05 and \*\* P < 0.01

**Fig. 2** Relative wet weights of treated mice organs with respect to body weights. **A** Kidney. **B** Liver. **C** Spleen. Data are presented as mean  $\pm$  SD. n = 9



However, in the F1 (Fig. 6C) and F2 (Fig. 6D) groups only a few swollen axons were detected, and the appearance of the myelin sheath closely resembled the control group.

## Discussion

Antimicrobial resistance continues to be a global public health concern with millions of casualties estimated in the coming decades. The situation is worsened by a shortage in the antibiotic pipeline with no significant developments over the past 20 years. Interest in colistin as a treatment for multi-drug resistant gram-negative bacteria therapy has increased in recent years due to the susceptibility of these "superbugs" to colistin (Dijkmans et al. 2015; Ahmed et al. 2020). Unfortunately, dose-limiting toxicity remains the main concern for effective polymyxin therapy. Accordingly, the development of strategies to attenuate this unwanted side-effects and thereby improve colistin therapy

is of the utmost importance (Ortwine et al. 2015). The most common side effects of colistin therapy are nephrotoxicity and neurotoxicity, which occur in up to 60% of patients (Karaiskos et al. 2017). In the present study, we investigated the potential of SDCS to increase the safety profile of colistin sulfate in an animal model. SDCS has proven to increase the safety profile of nephrotoxic drugs such as amphotericin B and polymyxin B while SDCS itself showed no toxicity toward human cells especially kidney cells in vitro (Gangadhar et al. 2014; Usman et al. 2017; Temboot et al. 2020). The effects of the SDCS on antibacterial activity of polymyxin also have been analyzed where SDCS did not hinder the antibacterial activity of polymyxins (PMB and colistin) against GNB (Temboot et al. 2020; Khumaini Mudhar Bintang et al. 2023).

Although the cellular and molecular causes of colistin nephrotoxicity are still undetermined, some research has revealed a relationship between oxidative stress and complications associated with colistin-induced kidney damage

**Fig. 3** A-D Gross examinations of kidney morphology in treated animals. Representative images of kidney histopathological alterations. **E** Control. **F** Colistin. **G** F1. **H** F2. Deformation of the glomeruli is shown in the yellow circle while congestion of renal blood vessels is shown in the red circle (magnification  $\times 20$ ). Scale bars = 100  $\mu$ m

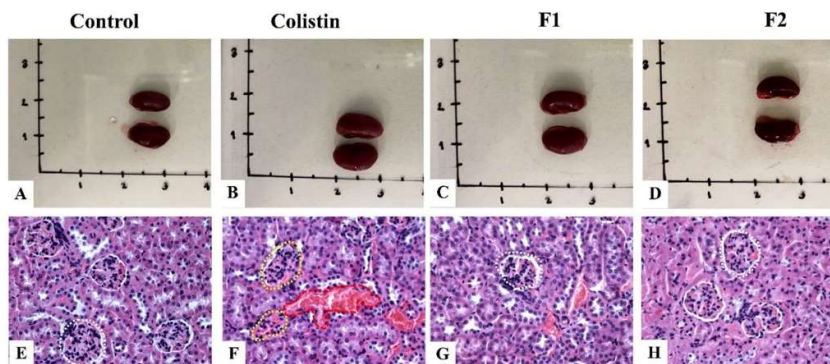
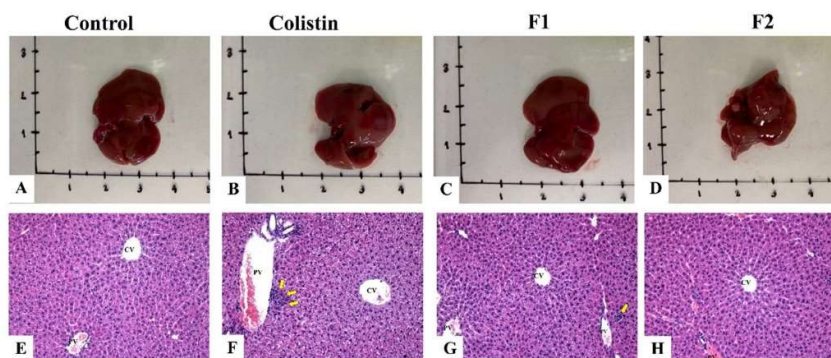


**Fig. 4** A-D Gross examinations of liver morphology in treated animals. Representative images of liver histopathological alterations. **E** Control. **F** Colistin. **G** F1. **H** F2. Yellow arrows indicate infiltration of monocytes in the tissue (magnification  $\times 20$ ). Scale bars = 100  $\mu\text{m}$



(Ozkan et al. 2013). This study showed that after a 7-day administration of colistin in mice, the kidney function still had no signs of severe damage as indicated by the levels of BUN and Cr (Fig. 1A & 1B). A concurrent decrease in the levels of antioxidant enzymes like SOD and CAT was associated with colistin-induced nephrotoxicity (Keirstead et al. 2014). SOD deficiency was reported to exacerbate renal dysfunction, tubulointerstitial fibrosis, inflammation, and apoptosis in the kidney (Kitada et al. 2020). In unilateral ureteral obstruction in mice, CAT deficiency was shown to increase tubulointerstitial fibrosis and lipid peroxidation products of tubulointerstitial lesions (Sunami et al. 2004). Decreases in SOD and CAT were also associated with reactive oxidative stress induced damage on sciatic nerve tissue (Edrees et al. 2018; Dai et al. 2020). Our study revealed a significant decrease in antioxidant enzymes (Fig. 1C & 1D) in the colistin treated group which indicated induced oxidative stress damage. Colistin-induced oxidative stress could play an essential role in the activation of the inflammatory response via the release of pro-inflammatory cytokines (e.g., TNF- $\alpha$  and IL-6) and inflammatory cell migration to the affected tissues, which were demonstrated in histopathological examinations (Dai et al. 2013; Edrees et al. 2018).

Injury can be observed from the histopathological alterations in the kidneys of colistin-treated mice (Fig. 3F). Compared to the control group (Fig. 3E), the kidneys had wider capillaries with more space filled by red blood cells, leading to increased hemolysis. The glomeruli showed hyperemia and widened Bowman's capsule, as evidenced by glomerulus outline deformation. Colistin undergoes extensive renal tubular reabsorption up to 80%. Therefore, most of the filtered colistin is retained in the body and is cleared mainly by non-renal mechanisms (Honoré et al. 2014). Colistin increases the permeability of the tubular epithelial cell membrane, which causes cation, anion, and water influx that leads to cell swelling and cell lysis. The nephrotoxicity of colistin is primarily related to its diaminobutyric acid and fatty acid components. Therefore, colistin causes proteinuria, cylindruria, and oliguria in addition to acute tubular necrosis, which appears as a rise in serum Cr and a decrease in Cr clearance. The concentration and duration of exposure to colistin determine these effects (Dijkmans et al. 2015; Gai et al. 2019). Reduction of the exposure time to kidney cells might lessen the colistin-induced renal damage, which was demonstrated by the colistin-SDCS formulations that showed less damage to the kidney tissue of the treated mice (Fig. 3G & 3H). Our findings from preliminary work

**Fig. 5** A-D Gross examination of spleen morphology in treated animals. Representative images of spleen histopathological alterations. **E** Control. **F** Colistin. **G** F1. **H** F2. The yellow arrow indicates multinucleated giant cells in the tissue (magnification  $\times 20$ ). Scale bars = 100  $\mu\text{m}$

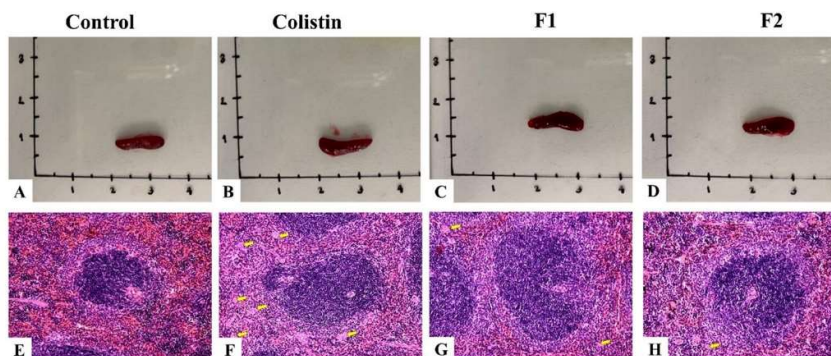
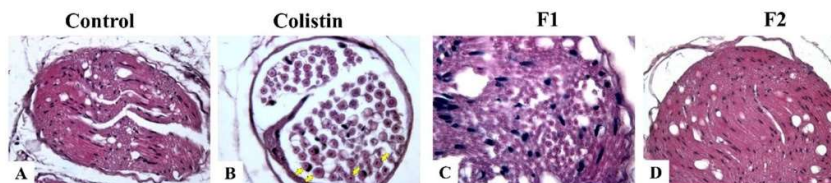


**Fig. 6** Representative images of histopathological alterations of sciatic nerve fibre tissues. **A** Control. **B** Colistin. **C** F1. **D** F2. The yellow arrow shows thin and loose fibres (magnification  $\times 100$ ). Scale bars = 100  $\mu$ m



revealed that SDCS manages to slow the release of colistin. The interaction also suggested that SDCS interacted mainly with colistin through its diaminobutyric acid. The micelles formed through this interaction would prevent fatty acid exposure to the kidney cells, thus lowering its toxicity. It also has been suggested that the high affinity of colistin toward megalin contributes to the high duration of colistin and accumulation in the proximal tubule (Suzuki et al. 2013). Our previous work demonstrated that negatively charged SDCS manages to lower the charge of colistin, which might lower the megalin affinity associated with polybasic drugs such as polymyxins (De et al. 2014).

The neurotoxicity of colistin still causes concerns due to its prevalence in elderly patients during therapy (Claus et al. 2015). According to various studies in mice, colistin therapy results in significant axonal degeneration in sciatic nerve tissue, impairment of the motor and sensory nerve conduction velocity, and loss of heat sensitivity (Dai et al. 2012, 2014). The axonal damage in the sciatic nerve tissue of mice is shown in Fig. 6B with several swollen axons presenting in the colistin-treated mice. Colistin sulfate is made up of hydrophobic fatty acyl chains and positively charged amine groups at a physiological pH. It interacts with the high lipid-containing neurons and causes neurotoxic side effects such as vertigo, generalized muscle weakness, facial and peripheral paresthesia, partial hearing loss, visual abnormalities, disorientation, hallucinations, seizures, ataxia, and neuromuscular blockade (Claus et al. 2015; Dijkmans et al. 2015). Wallace et al. verified that cell apoptosis or necrosis was involved in colistin-induced nephrotoxicity (Wallace et al. 2008). Some authors suggested that the D-amino acid and fatty acid components of colistin, particularly the lipid A of its model structure that interacts with the high lipid content of neurons, cause neurotoxicity in a manner similar to the way colistin induces nephrotoxicity (Falagas and Kasiakou 2006; Ozyilmaz et al. 2011). It is suggested that SDCS reduces the fatty acyl exposure and lowers the charge of colistin, which might contribute to the minimal damage of colistin in the sciatic nerve tissue of treated mice (Fig. 6C & 6D). This was also demonstrated with colistin-treated mice that exhibited sensory neuropathy with the loss of heat sensitivity compared to colistin-SDCS-treated mice (Table 2).

## Conclusions

The data revealed that colistin-SDCS produces less nephrotoxic and neurotoxic products with minimal complications in an animal model. Histopathological and neurobehavioral observations revealed that a colistin-SDCS formulation resulted in less damage, which suggested a colistin-SDCS formulation is potentially a safer formulation. Further studies can confirm the clinical significance of these data.

**Acknowledgements** The authors would like to thank Sunisa Kaewpaiboon and Titpawan Nakpheng for assisting in experimental works.

**Author contributions** MAKMB, JN, and TS contributed to the study conception and design. Material preparation, data collection and analysis were performed by MAKMB, and JN. The first draft of the manuscript was written by MAKMB, and all authors commented on previous versions of the manuscript. All authors read and approved the final manuscript. The authors declare that all data were generated in-house and that no paper mill was used.

**Funding** This work was supported by National Science, Research and Innovation Fund and Prince of Songkla University (PHA6601221S).

**Data availability** The data will be made available upon request.

## Declarations

**Ethics approval** All animal experiments were performed with the approval of the animal ethics committee, Prince of Songkla University (MHESI 68014/1895, Ref. 81/2021).

**Consent for publication** All authors consent to the publication of the manuscript.

**Competing interests** The authors have no competing interests to declare that are relevant to the content of this article.

## References

- Ahmed MAEE, Doi Y, Tian G, et al (2020) Colistin and its role in the Era of antibiotic resistance : an extended review. *Emerg Microbes Infect* 9:868–885. <https://doi.org/10.1080/22221751.2020.1754133>
- Bialvaei AZ, Samadi Kafil H (2015) Colistin, mechanisms and prevalence of resistance. *Curr Med Res Opin* 31:707–721. <https://doi.org/10.1185/03007995.2015.1018989>

- Claus BOM, Snauwaert S, Haerynck F et al (2015) Colistin and neurotoxicity: recommendations for optimal use in cystic fibrosis patients. *Int J Clin Pharm* 37:555–558. <https://doi.org/10.1007/s11096-015-0077-4>
- Dai C, Li J, Lin W et al (2012) Electrophysiology and ultrastructural changes in mouse sciatic nerve associated with colistin sulfate exposure. *Toxicol Mech Methods* 22:592–596. <https://doi.org/10.3109/15376516.2012.704956>
- Dai C, Li J, Li J (2013) New insight in colistin induced neurotoxicity with the mitochondrial dysfunction in mice central nervous tissues. *Exp Toxicol Pathol* 65:941–948. <https://doi.org/10.1016/j.etp.2013.01.008>
- Dai C, Tang S, Li J et al (2014) Effects of Colistin on the Sensory Nerve Conduction Velocity and F-wave in Mice. *Basic Clin Pharmacol Toxicol* 115:577–580. <https://doi.org/10.1111/bcpt.12272>
- Dai C, Xiao X, Zhang Y et al (2020) Curcumin Attenuates Colistin-Induced Peripheral Neurotoxicity in Mice. *ACS Infect Dis* 6:715–724. <https://doi.org/10.1021/acscinfed.9b00341>
- De S, Kuwahara S, Saito A (2014) The endocytic receptor megalin and its associated proteins in proximal tubule epithelial cells. *Membranes (basel)* 4:333–335. <https://doi.org/10.3390/membranes4030333>
- Dijkmans AC, Wilms EB, Kamerling IMC et al (2015) Colistin: Revival of an Old Polymyxin Antibiotic. *Ther Drug Monit* 37:419–427. <https://doi.org/10.1097/FTD.0000000000000172>
- Edrees NE, Galal AAA, Abdel Monaem AR et al (2018) Curcumin alleviates colistin-induced nephrotoxicity and neurotoxicity in rats via attenuation of oxidative stress, inflammation and apoptosis. *Chem Biol Interact* 294:56–64. <https://doi.org/10.1016/j.cbi.2018.08.012>
- Falagas ME, Kasiakou SK (2006) Toxicity of polymyxins: A systematic review of the evidence from old and recent studies. *Crit Care* 10:1–18. <https://doi.org/10.1186/cc3995>
- Gai Z, Samodelov SL, Kullak-Ublick GA, Visentin M (2019) Molecular Mechanisms of Colistin-Induced Nephrotoxicity. *Molecules* 24:653. <https://doi.org/10.3390/molecules24030653>
- Gangadhar KN, Adhikari K, Srichana T (2014) Synthesis and evaluation of sodium deoxycholate sulfate as a lipid drug carrier to enhance the solubility, stability and safety of an amphotericin B inhalation formulation. *Int J Pharm* 471:430–438. <https://doi.org/10.1016/j.ijpharm.2014.05.066>
- Grégoire N, Aranzana-Climent V, Magréault S et al (2017) Clinical Pharmacokinetics and Pharmacodynamics of Colistin. *Clin Pharmacokinet* 56:1441–1460. <https://doi.org/10.1007/s40262-017-0561-1>
- Hill C, Jain A, Takemoto H et al (2014) A secondary mode of action of polymyxins against Gram-negative bacteria involves the inhibition of NADH-quinone oxidoreductase activity. *J Antibiot (tokyo)* 67:147–151. <https://doi.org/10.1038/ja.2013.111.A>
- Honoré PM, Jacobs R, Joannes-Boyau O et al (2014) Continuous renal replacement therapy-related strategies to avoid colistin toxicity: A clinically orientated review. *Blood Purif* 37:291–295. <https://doi.org/10.1159/000363495>
- Kaewpaiboon S, Srichana T (2022) Formulation Optimization and Stability of Polymyxin B Based on Sodium Deoxycholate Sulfate Micelles. *J Pharm Sci* 000:1–9. <https://doi.org/10.1016/j.xphs.2022.02.011>
- Kalesidis T, Falagas ME (2015) The safety of polymyxin antibiotics Theodoros. *Expert Opin Drug Saf* 14:1687–1701. <https://doi.org/10.1517/14740338.2015.1088520>
- Karaiskos I, Giamarellou H (2014) Multidrug-resistant and extensively drug-resistant Gram-negative pathogens: Current and emerging therapeutic approaches. *Expert Opin Pharmacother* 15:1351–1370. <https://doi.org/10.1517/14656566.2014.914172>
- Karaiskos I, Souli M, Galani I, Giamarellou H (2017) Colistin: still a lifesaver for the 21st century? *Expert Opin Drug Metab Toxicol* 13:59–71. <https://doi.org/10.1080/17425255.2017.1230200>
- Keirstead ND, Wagoner MP, Bentley P et al (2014) Early prediction of polymyxin-induced nephrotoxicity with next-generation urinary kidney injury biomarkers. *Toxicol Sci* 137:278–291. <https://doi.org/10.1093/toxsci/kft247>
- Kelesidis T, Falagas ME (2015) The safety of polymyxin antibiotics. *Expert Opin Drug Saf* 14:1687–1701. <https://doi.org/10.1517/14740338.2015.1088520>
- KhumainiMudharBintang MA, Tipmanee V, Srichana T (2023) Colistin sulfate-sodium deoxycholate sulfate micelle formulations; molecular interactions, cell nephrotoxicity and bioactivity. *J Drug Deliv Sci Technol* 79:104091. <https://doi.org/10.1016/j.jddst.2022.104091>
- Kitada M, Xu J, Ogura Y et al (2020) Manganese superoxide dismutase dysfunction and the pathogenesis of kidney disease. *Front Physiol* 11:1–16. <https://doi.org/10.3389/fphys.2020.00755>
- Madhumanchi S, Suedee R, Nakpheng T et al (2019) Binding interactions of bacterial lipopolysaccharides to polymyxin B in an amphiphilic carrier 'sodium deoxycholate sulfate.' *Colloids Surfaces B Biointerfaces* 182:110374. <https://doi.org/10.1016/j.colsurfb.2019.110374>
- Madhumanchi S, Suedee R, Kaewpaiboon S et al (2020) Effect of sodium deoxycholate sulfate on outer membrane permeability and neutralization of bacterial lipopolysaccharides by polymyxin B formulations. *Int J Pharm* 581:119265. <https://doi.org/10.1016/j.ijpharm.2020.119265>
- Nation RL, Velkov T, Li J (2014) Colistin and polymyxin B: Peas in a pod, or chalk and cheese? *Clin Infect Dis* 59:88–94. <https://doi.org/10.1093/cid/ciu213>
- Nazer LH, Anabtawi N (2017) Optimizing colistin dosing: Is a loading dose necessary? *Am J Heal Pharm* 74:e9–e16. <https://doi.org/10.2146/ajhp150876>
- Neill JO\* (2014) Antimicrobial Resistance: Tackling a crisis for the health and wealth of nations The Review on Antimicrobial Resistance Chaired. *Rev Antimicrob Resist* 20:1–16
- Ortwine JK, Sutton JD, Kaye KS, Pogue JM (2015) Strategies for the safe use of colistin. *Expert Rev Anti Infect Ther* 13:1237–1247. <https://doi.org/10.1586/14787210.2015.1070097>
- Ozkan G, Ulusoy S, Orem A et al (2013) How does colistin-induced nephropathy develop and can it be treated? *Antimicrob Agents Chemother* 57:3463–3469. <https://doi.org/10.1128/AAC.00343-13>
- Ozyilmaz E, Ebinc FA, Deric U et al (2011) Could nephrotoxicity due to colistin be ameliorated with the use of N-acetylcysteine? *Intensive Care Med* 37:141–146. <https://doi.org/10.1007/s00134-010-2038-7>
- Perez F, El Chakhtoura NG, Yasmin M, Bonomo RA (2019) Polymyxins: To combine or not to combine? *Antibiotics* 8:1–13. <https://doi.org/10.3390/antibiotics8020038>
- Pogue JM, Ortwine JK, Kaye KS (2017) Clinical considerations for optimal use of the polymyxins: A focus on agent selection and dosing. *Clin Microbiol Infect* 23:229–233. <https://doi.org/10.1016/j.cmi.2017.02.023>
- Sunami R, Sugiyama H, Wang DH et al (2004) Acatalsemia sensitizes renal tubular epithelial cells to apoptosis and exacerbates renal fibrosis after unilateral ureteral obstruction. *Am J Physiol - Ren Physiol* 286:2–5. <https://doi.org/10.1152/ajprenal.00266.2003>
- Suzuki T, Yamaguchi H, Ogura J et al (2013) Megalin contributes to kidney accumulation and nephrotoxicity of colistin. *Antimicrob Agents Chemother* 57:6319–6324. <https://doi.org/10.1128/AAC.00254-13>
- Temboot P, Kaewpaiboon S, Tinpun K, et al (2020) Potential of sodium deoxycholate sulfate as a carrier for polymyxin B:



- Physicochemical properties, bioactivity and in vitro safety. *J Drug Deliv Sci Technol* 58:101779. <https://doi.org/10.1016/j.jddst.2020.101779>
- Usman F, Ul-Haq Z, Khalil R et al (2017) Pharmacologically Safe Nanomicelles of Amphotericin B With Lipids: Nuclear Magnetic Resonance and Molecular Docking Approach. *J Pharm Sci* 106:3574–3582. <https://doi.org/10.1016/j.xphs.2017.08.013>
- Usman F, Nopparat J, Javed I, Srichana T (2020) Biodistribution and histopathology studies of amphotericin B sodium deoxycholate sulfate formulation following intratracheal instillation in rat models. *Drug Deliv Transl Res* 10:59–69. <https://doi.org/10.1007/s13346-019-00662-x>
- Vardakas KZ, Falagas ME (2017) Colistin versus polymyxin B for the treatment of patients with multidrug-resistant Gram-negative infections: a systematic review and meta-analysis. *Int J Antimicrob Agents* 49:233–238. <https://doi.org/10.1016/j.ijantimicag.2016.07.023>
- Wallace SJ, Li J, Nation RL et al (2008) Subacute toxicity of colistin methanesulfonate in rats: Comparison of various intravenous dosage regimens. *Antimicrob Agents Chemother* 52:1159–1161. <https://doi.org/10.1128/AAC.01101-07>
- Wang W (2015) Tolerability of hypertonic injectables. *Int J Pharm* 490:308–315. <https://doi.org/10.1016/j.ijpharm.2015.05.069>
- Yu Z, Qin W, Lin J, et al (2015) Antibacterial mechanisms of polymyxin and bacterial resistance. *Biomed Res Int* 2015:679109. <https://doi.org/10.1155/2015/679109>
- Zavascki AP, Nation RL (2017) Nephrotoxicity of polymyxins: Is there any difference between colistimethate and polymyxin B? *Antimicrob Agents Chemother* 61:e02319–16. <https://doi.org/10.1128/AAC.02319-16>

**Publisher's note** Springer Nature remains neutral with regard to jurisdictional claims in published maps and institutional affiliations.

Springer Nature or its licensor (e.g. a society or other partner) holds exclusive rights to this article under a publishing agreement with the author(s) or other rightsholder(s); author self-archiving of the accepted manuscript version of this article is solely governed by the terms of such publishing agreement and applicable law.

## ETHICAL COMMITTEE APPROVAL



### บันทึกข้อความ

ส่วนงาน สำนักวิจัยและพัฒนา

โทร 6963 E-mail : [sineenart.w@psu.ac.th](mailto:sineenart.w@psu.ac.th)

ที่ มอ 014.4/64 - 1460

วันที่ ๒๑ ตุลาคม 2564

เรื่อง ผลการพิจารณาโครงการวิจัยที่ศึกษาในสัตว์ทดลอง

เรียน ผศ.ดร.จงดี นพรัตน์ คณะวิทยาศาสตร์

ตามที่ท่านได้เสนอโครงการวิจัยที่ศึกษาในสัตว์ทดลอง เรื่อง Formulation optimization and characterization of colistin using sodium deoxycholate sulfate for intravenous administration เพื่อให้คณะกรรมการกำกับดูแลการเลี้ยงและใช้สัตว์ของสถาบัน มหาวิทยาลัยสงขลานครินทร์ พิจารณานั้น คณะกรรมการฯ ได้พิจารณาแล้ว เห็นชอบอนุมัติและได้ส่งหนังสือรับรองมาด้วยแล้ว

จึงเรียนมาเพื่อโปรดทราบ และขอให้จัดส่งแบบรายงานความก้าวหน้าการดำเนินงานที่ใช้สัตว์ มหาวิทยาลัยสงขลานครินทร์ มายังสำนักวิจัยและพัฒนา ทุก 6 เดือน โดยให้รายงานความก้าวหน้าเดือนที่ 3 (ข้อมูล ตุลาคม - มีนาคม) และ เดือนที่ 9 (ข้อมูล เมษายน - กันยายน) ของปี จนเสร็จสิ้นโครงการใช้สัตว์

*ศุภมาสยาม*

(ผู้ช่วยศาสตราจารย์ ดร.วันดี อุดมอักษร)

ประธานคณะกรรมการกำกับดูแลการเลี้ยงและใช้สัตว์ของสถาบัน  
มหาวิทยาลัยสงขลานครินทร์

สำเนาแจ้ง คณะวิทยาศาสตร์



“เป็นองค์กรบริหารจัดการงานวิจัยและนวัตกรรมสู่ความเป็นเลิศ”

สำนักวิจัยและพัฒนา มหาวิทยาลัยสงขลานครินทร์  
Research and Development Office  
โทร. 0-7428-6940 <http://rdo.psu.ac.th>



ที่ อว68014/ ๖๘๖๕

สำนักวิจัยและพัฒนา  
เลขที่ 15 ถนนกาญจนวนิช  
มหาวิทยาลัยสงขลานครินทร์  
อ.หาดใหญ่ จ.สงขลา 90110

Ref. 81/2021

### หนังสือรับรอง

รหัสโครงการ 2564-01-073

โครงการ Formulation optimization and characterization of colistin using sodium deoxycholate sulfate for intravenous administration

นักวิจัย ผศ.ดร.จงดี นพรัตน์  
สังกัด คณะวิทยาศาสตร์

ได้ผ่านการพิจารณาและเห็นชอบจาก คณะกรรมการกำกับดูแลการเลี้ยงและใช้สัตว์ของสถาบัน มหาวิทยาลัยสงขลานครินทร์ โดยขอให้รายงานความก้าวหน้าของโครงการวิจัยทุก 6 เดือน

ให้ไว้ ณ วันที่ 19 ตุลาคม 2564

*อ.จ. อ.จ. อ.จ.*

(ผู้ช่วยศาสตราจารย์ ดร.วันดี อุดมอักษร)  
ประธานคณะกรรมการกำกับดูแลการเลี้ยงและใช้สัตว์ของสถาบัน  
มหาวิทยาลัยสงขลานครินทร์

วันที่รับรอง: 19 ตุลาคม 2564

วันหมดอายุ: 31 ธันวาคม 2565



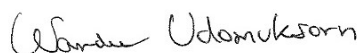
PRINCE OF SONGKLA UNIVERSITY  
15 Karnjanawanij Road, Hat Yai, Songkhla 90110, Thailand  
Tel (66-74) 286940 Fax (66-74) 286961  
Website : [www.psu.ac.th](http://www.psu.ac.th)

MHESI 68014/ 1895

Ref.81/2021

October 20, 2021

This is to certify that the research project entitled "Formulation optimization and characterization of colistin using sodium deoxycholate sulfate for intravenous administration" which was conducted by Asst. Prof. Dr. Jongdee Nopparat, Faculty of Science, Prince of Songkla University, has been approved by Institutional Animal Care and Use Committee, Prince of Songkla University.



Wandee Udomuksorn, Ph.D.

Chairman,

Institutional Animal Care and Use Committee, Prince of Songkla University

## VITAE

**Name** Muhammad Ali Khumaini

**Student ID** 6110730013

### **Educational Attainment**

Degree	Name of Institution	Year of Graduation
Bachelor of Pharmacy	Alauddin State Islamic University	2017

### **Scholarship Awards during Enrolment**

1. Educational fee from Grant of Graduate Student Discipline of Excellence in Pharmacy Project, Faculty of Pharmaceutical Sciences, Prince of Songkla University
2. Thesis Grant by Graduate School, Prince of Songkla University
3. Conference Scholarship Faculty of Pharmaceutical Sciences, Prince of Songkla University

### **List of Publication and Proceeding**

#### **Publications**

1. **Bintang MAKM**, Srichana T (2022) Antibacterial Activity and In Vitro Cytotoxicity of Colistin in Sodium Deoxycholate Sulfate Formulation. *Adv Sci Technol* 121:25–30. <https://doi.org/10.4028/p-19rsw3>.
2. **Bintang MAKM**, Tipmanee V, Srichana T (2023) Colistin sulfate-sodium deoxycholate sulfate micelle formulations; molecular interactions, cell nephrotoxicity and bioactivity. *J Drug Deliv Sci Technol* 79:104091. <https://doi.org/10.1016/j.jddst.2022.104091>.
3. **Bintang MAKM**, Nopparat J, Srichana T (2023) In vivo evaluation of nephrotoxicity and neurotoxicity of colistin formulated with sodium deoxycholate sulfate in a mice model. *Naunyn Schmiedebergs Arch Pharmacol*. <https://doi.org/10.1007/s00210-023-02531-4>
4. Kamlungmak S, Nakpheng T, Kaewpaiboon S, **Bintang MAKM**, Prom-In S, Chunchachaichana C, Suwandecha T, Srichana T (2021) Safety and

biocompatibility of mupirocin nanoparticle-loaded hydrogel on burn wound in rat model. *Biol Pharm Bull* 44:1707–1716. <https://doi.org/10.1248/bpb.b21-00397>.

(Remarks: This paper is not related to Ph.D. thesis)

### Proceedings

1. **Bintang MAKM**, Srichana T. Effect of the different molar ratio of colistin on the surface properties of sodium deoxycholate sulfate. The 11th Joint Seminar on Biomedical Sciences: Variety and Controversy to Creativity. 13-15 November 2019. Krabi, Thailand.
2. **Bintang MAKM**, Srichana T. Particle size, surface charges and molecular interaction of colistin with sodium deoxycholate sulfate. The 6th CDD International Conference 2020: Natural Medicines. 10-12 November 2020. Hat-Yai, Thailand.
3. **Bintang MAKM**, Srichana T. Antibacterial Activity and In Vitro Cytotoxicity of Colistin in Sodium Deoxycholate Sulfate Formulation. 5th International Conference and Exhibition on Pharmaceutical Sciences and Technology 2022: Innovations in Pharmaceutical Sciences for Sustainable Development Goals. 23-24 June 2022. Online conference, Thailand.